Notes on the 1963

Summer Study Program

in

GEOPHYSICAL FLUID DYNAMICS

at

The WOODS HOLE OCEANOGRAPHIC INSTITUTION

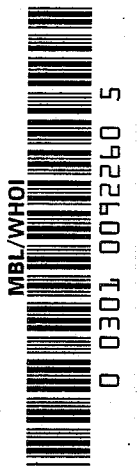

Reference No. 63-34

Contents of the Volumes

Volume I. Student Notes of Lectures by Derek Moore on Rotating Fluids.

Volume II. Lectures by Donald E. Osterbrock on Astrophysics.

Volume III. Participants' Lectures.

Reference No. 63-34

LIST OF PARTICIPANTS

Regular WHOI Staff Members

Alan Faller
Nicholas P. Fofonoff
Melvin E. Stern
George Veronis

Visiting Staff Members

Bernard St.Guily, Lab. of Oceanography, Paris, France
Raymond Hide, Dept. Geophysics, M.I.T., Cambridge, Mass.
Louis N. Howard, Dept. Mathematics, M.I.T., Cambridge, Mass.
Donald E. Osterbrock, Dept. Astronomy, Univ.of Wisconsin, Madison, Wisconsin
Edward A. Spiegel, Inst.Math.Sciences, N.Y.U., New York
Henry Stommel, Harvard University, Cambridge, Mass.
Alar Toomre, Dept. Mathematics, M.I.T., Cambridge, Mass.
Pierre Welander, Univ. Stockholm, Stockholm, Sweden.

Post-doctoral Students

Jai Ding Lin, Univ. Connecticut, Storrs, Conn.
Lorenz Magaard, Kiel University, Kiel, Germany

Pre-doctoral Students

Theodore D. Foster, Scripps Inst.Oceanography, La Jolla, California
Alan Ibbetson, M.I.T., Cambridge, Mass.
Paul H. LeBlond, Inst. Oceanography, Univ.British-Columbia, Vancouver, Canada
Peter B. Rhines, M.I.T., Cambridge, Mass.
Robert Stein, Columbia University, New York, N.Y.
Hendrikus Tinkelenberg, M.I.T., Cambridge, Mass.

Course Listeners

Robert A. Arnoldi, Research Labs., United Aircraft Corporation, East Hartford, Conn.
Victor Barcilon, Div. Appl.Physics, Harvard Univ.,Cambridge, Mass.
Steven Rosencrans, Dept. Mathematics, M.I.T., Cambridge, Mass.
Hans Thomas Rossby, Dept.Geophysics, M.I.T., Cambridge, Mass.

Editors' Preface

This volume contains the manuscripts of the student research lectures as well as research contributions by senior pariticpants in the summer program. The staff guided the selection of the students' topics with several goals in mind. One goal was to isolate that part of a problem which might prove to be tractable in an effort of eight weeks or so. The more important goal was to find "open-ended" problems which would continue to challenge the student after his return to the university.

The degree of direction by the sponsor varied a great deal. In a few cases, there were frequent conferences and discussions about fruitful avenues of approach. In other cases, there was essentially no contact except one of encouragement and interest. The efforts cover a wide spectrum in originality also. Some of the reports represent a more extended study of material presented in the course of lectures - others are original contributions which are being prepared for publication.

Because of time limitations it was not possible for the notes to be edited and reworked. The reports may contain errors the responsibility for which must rest on the shoulders of the participant-author. It must be emphasized that this volume in no way represents a collection of reports of completed and polished work.

All those who took part in the summer program are grateful to the National Science Foundation for its encouragement and financial support of the program.

Mary Thayer
George Veronis

Back Row: (left to right): Veronis, Arnoldi, Stein.
Middle Row: Welander, Lin, Howard, Rosencrans, Thayer, Stommel, Spiegel, Magaard.
Front Row: Foster, LeBlond, Hide, --- , Rhines, Tinkelenberg, Toomre. Reclining: Stern.

The chap with the TIE is a ringer of Hide's and sat in for Ibbetson who was absent. Other absentees were St. Guily, Osterbrock, Rossby, Moore, Barcilon and Kraichnan. There were no other people with ties available as ringers for the remaining absentees.

List of Seminars

1963

June 25	Dr. George Veronis "Wind-driven Ocean Circulation"
June 26	Dr. Pierre Welander "Problems in Thermal Ocean Circulation"
June 27	Dr. Edward A. Spiegel "Waves in the Solar Atmosphere"
June 28	Dr. Melvin E. Stern "What keeps the Salt up in the Sub-tropical Thermocline?"
July 1	Dr. Alan Faller "Instability of Ekman Layers"
July 2	Dr. Stewart Turner "A Laboratory Model of the Tornado Vortex"
July 3	Dr. Nicholas Fofonoff "Current Measurements from Moored Buoys"
July 8	Dr. Bernard St.Guily "Effect of Earth's Rotation on Gravity Waves"
July 9	Dr. Alan Faller: Rotating Tank Demonstration
July 11	Dr. Lorenz Magaard "On Internal Waves in Oceans with Variable Depth"
August 2	Dr. Joseph Pedlosky "Stability of Atmospheric and Oceanic Currents"
August 6	Dr. Louis N. Howard "Time-dependent Ekman Flows"
August 8	Dr. Willem V.R. Malkus "Precessional Torques as the Cause of Geomagnetism
August 12	Dr. Jule G. Charney "Equatorial Flows"
August 20	Dr. Raymond Hide "A Simplified Theory of Thermal Convection in a Rotating Fluid Annulus"
August 26	Dr. Walter Elsasser "Precession in the Core"

Contents of Volume III

Student Lectures

Instability of Geostrophic Shear Flow to Streamwise Vortex Perturbations

by

Robert A. Arnoldi

Instability of Geostrophic Shear Flow to Streamwise Vortex Perturbations

Robert A. Arnoldi

Abstract:

The linearized perturbation equations for geostrophic flow are examined for perturbations of a roll-vortex nature. The steady-flow condition necessary to couple the perturbations into a roll-vortex structure is assumed to be that the primary flow should be perpendicular to the axis of rotation and that the shear of the primary flow should constitute a relative vorticity vector opposite to the rotation vector. The shear magnitude must be sufficient to create an absolute vorticity vector opposed to the rotation. Two such cases are examined and are found to exhibit roll-vortex structure of a particularly simple nature.

Introduction:

The occurrence of stable roll vortices in nature has been largely ascribed to thermal driving forces, except for the Taylor instability of flow between two rotating cylinders and for the spirally banded Ekman boundary layers of rotating discs and basins. It is the purpose of the present study to show the existence of roll-vortex secondary motions in large-scale geostrophic

flows, where great simplicity of the analysis is possible. The iterative technique used to solve the velocity perturbation equations for characteristic structural parameters and for the corresponding distributions of velocity perturbations is a well-known tool of numerical analysis and is easily extended to solve less idealized primary flow distributions with the aid of high-speed computing devices.

A secondary flow structure of roll vortices, their axes aligned with the primary flow velocity, was treated by Taylor (Ref. 1) both theoretically and experimentally for the case of fluid motion in the annulus between two rotating cylinders. H. Boertler (Ref. 2) showed the presence of a similar structure in the laminar boundary layer on a concave, curved wall. K. Kirchgassner (Ref. 3) and G. Hammerlin (Ref. 4) have recently included the effect of heat addition in Boertler's problem (although only abstracts of their papers were available for the present study). Boundary layers of the Ekman type have been shown to exhibit a roll-vortex secondary flow both experimentally and theoretically (Ref. 5, 6, 7, 8). The associated mathematical discussions have been necessarily complicated, and it has been difficult to distinguish the essentials of the physical mechanism leading to the roll vortex.

A possible common bond between these types of flow lies in the observation that in both Taylor and Goertler roll vortices the

axis of rotation is perpendicular to the primary stream and anti-parallel to the vorticity caused by its shear. With this condition in mind, the present study considers analogous problems of a sufficiently large scale to possess geophysical significance, particularly those of an oceanographic nature.

Equations of Motion:

The approach suggested in the introduction leads to the following two problems relating to ocean currents:

Case A: An easterly current near the equator possessing vertical velocity shear, so that the earth's rotation vector is anti-parallel to that of the primary stream vorticity and perpendicular to the primary stream itself.

Case B: A current outside the equatorial regions so that the vertical component of the earth's rotation vector is the important coupling agent, with a transverse velocity shear (the vector of primary stream vorticity is vertical).

Case A corresponds to the equatorial countercurrents which flow in an easterly direction under a westerly surface current. The magnitude of the vorticity in the region overlying the core of these countercurrents is considerably greater than that of the earth's rotation. The perturbation equations for this case are identical with those of Ref. 1 if a linear velocity profile is

assumed, but an iterative method of solution will be employed to facilitate the eventual use of machine calculations for the actual velocity profile observed in the countercurrents.

Case B corresponds to the portions of the Gulf Stream exhibiting maximum transverse variation of current, where the primary stream vorticity opposes and exceeds that of the earth's rotation, but only slightly.

Ignoring the earth's curvature, the equations of motion are:

$$\frac{\partial \bar{u}}{\partial t} + \bar{u}\cdot\nabla\bar{u} + 2\Omega\times\bar{u} = -\frac{1}{\rho}\nabla P + \nu\nabla^2\bar{u} - \bar{k}\rho g \qquad (1)$$

and

$$\nabla\cdot\bar{u} = 0 \qquad (2)$$

where ν is an effective eddy viscosity and will be taken as 10^4 cgs units (see Ref. 5, p.112) for order-of-magnitude calculations. Consider

$$2\bar{\Omega} = (\bar{i}\ell + \bar{j}m + \bar{k}n)f \qquad (3)$$

and a velocity structure

$$\begin{aligned} u &= +u_0(z) + u_1(z)\sin\alpha y\, e^{\beta t} \\ v &= \qquad v_1(z)\cos\alpha y\, e^{\beta t} \\ w &= \qquad w_1(z)\sin\alpha y\, e^{\beta t} \\ P &= P_0(z) + P_1(z)\sin\alpha y\, e^{\beta t} \end{aligned} \qquad (4a)$$

applicable to Case A above. Retaining only the mf component of $2\bar{\Omega}$, the expanded equations (1) and (2) become, after linearization,

$$\begin{aligned} \beta u_1 + u_0' w_1 + mf w_1 &= \nu(u_1'' - \alpha^2 u_1) \\ \beta v_1 &= -\alpha \frac{P_1}{\rho} + \nu(v_1'' - \alpha^2 v_1) \\ \beta w_1 - mf u_1 &= -\frac{1}{\rho} P_1' + \nu(w_1'' - \alpha^2 w_1) \\ -\alpha v_1 + w_1' &= 0 \end{aligned} \tag{5a}$$

These reduce to

$$\nu w_1^{IV} - W_1''(\beta + 2\nu\alpha^2) + \alpha^2(\beta + \nu\alpha^2) W_1 = +\alpha^2 mf u_1 \tag{6a}$$

and

$$\nu u_1'' - (\beta + \nu\alpha^2) u_1 = (u_0' + mf) w_1 \tag{7a}$$

which are closely similar to Goertler's boundary layer equations with mf in equation (6) corresponding to $-2u_0/\mathcal{R}$ where $\mathcal{R}$ is the radius of curvature and $(u_0' + mf)$ in equation (7) corresponding to merely u_0' in the stationary curved flow.

For Case B consider the following velocity structure for a current in the direction of the y-axis, possessing transverse horizontal shear:

$$
\begin{aligned}
u &= u_1(z)\cos\alpha x\, e^{\beta t} \\
v &= v_0(x) + v_1(z)\cos\alpha x\, e^{\beta t} \\
w &= w_1(z)\sin\alpha x\, e^{\beta t} \\
P &= P_0(z) + P_1(z)\sin\alpha x\, e^{\beta t}.
\end{aligned} \tag{4b}
$$

Retaining only the vertical rotation nf, we have

$$
\begin{aligned}
\beta u_1 \qquad - nf v_1 &= -\frac{\alpha}{\rho} P_1 + \nu(u_1'' - \alpha^2 u_1) \\
\beta v_1 + v_0' u_1 + nf u_1 &= \nu(v_1'' - \alpha^2 v_1) \\
\beta w_1 &= -\frac{1}{\rho} P_1' + \nu(w_1'' - \alpha^2 w_1) \\
-\alpha u_1 + w_1' &= 0
\end{aligned} \tag{5b}
$$

which reduce to

$$
\nu w_1^{IV} - (\beta + 2\nu\alpha^2) w_1'' + \alpha^2(\beta + \nu\alpha^2) w_1 = -\alpha nf v_1' \tag{6b}
$$

and

$$
\nu v_1'' - (\beta + \nu\alpha^2) v_1 = (v_0' + nf) w_1'/\alpha \tag{7b}
$$

As shown by the last terms in (6b) and (7b), the coupling in Case B is through the derivatives of the perturbations, v' and w', rather than through the perturbations themselves as in Case A.

Inviscid Approximation:

In the inviscid case, equation (6a) and (7a) give for Case A

$$w_1'' - \alpha^2 \left[\frac{(u_0' + mf)mf}{\beta^2} + 1 \right] w_1 = 0 \qquad (8a)$$

and for Case B,

$$\left[1 + \frac{(v_0' + nf)nf}{\beta^2} \right] w_1'' - \alpha^2 w_1 = 0. \qquad (8b)$$

As neutral stability is approached $(\beta \to 0)$, these equations demand that $-u_0' > mf$ in Case A and $-v_0' > nf$ in Case B if the roll-vortex structure is to exist as a stable perturbation or true secondary flow.

Since the vertical perturbation w_1 must be zero at the ocean bottom $(z = 0)$ and at the surface $(z = \delta)$, equations (8a) and (8b) require (considering u_0' and v_0' as constants and taking the fundamental modes)

$$\alpha \sqrt{-\frac{u_0' + mf}{\beta^2} - 1} = \pi/\delta$$

and $$\alpha \Big/ \sqrt{-1 - \frac{(v_0' + nf)nf}{\beta^2}} = \pi/\delta$$ respectively. The ratio of transverse wavelength $2\pi/\alpha$ to depth δ is therefore

$$2\pi/\alpha\delta = 2\sqrt{-\frac{u_0' + mf}{\beta^2} - 1} \qquad (9a)$$

and

$$2\pi/\alpha\delta = 2\Big/\sqrt{-1 - \frac{(v_0' + nf)nf}{\beta^2}}. \qquad (9b)$$

As $\beta \to 0$, the ratio apparently increases without limit for Case A and decreases to zero for Case B. In either case, it will be necessary to retain the viscous terms to investigate the roll-vortex structure.

An exact solution of equation (8a) is available for a quadratic velocity profile

$$u_0/\bar{u}_0 = 1 - (z/\delta)^2$$

Equation (8a) may be transformed to a special form of Bessel's equation

$$\frac{d^2 w_1}{d\tau^2} + \frac{\beta^2}{\alpha^2}\left(\frac{(mf)^2+\beta^2}{(mf)^2}\right)\tau w_1 = 0$$

(see Jahnke and Emde, p.143), with the general solution

$$w_1 = \sqrt{\tau}\, Z_{\frac{1}{3}}\left(\frac{2}{3}\frac{\beta}{mf}\sqrt{((mf)^2+\beta^2)}\,\tau^3\right)$$

where

$$\tau = \left(\frac{\alpha}{\beta}\right)^{\frac{4}{3}}\left(\frac{\delta^2((mf)^2+\beta^2)}{2\bar{u}_0}\right)^{\frac{2}{3}}\left[\frac{2\bar{u}_0 mf}{\delta^4((mf)^2+\beta^2)}z - 1\right].$$

The problem of matching boundary conditions is difficult however, and requires numerical approximations which make its utility rather doubtful. This exact solution will therefore merely be noted in passing, and iterative numerical methods will be developed which permit inclusion of the effects of eddy viscosity.

The interpretation of the condition of neutral stability $(\beta=0)$ for roll-vortex structure of ocean currents is similar for Cases A and B. Equations (8a) and (8b) show that for a given absolute vorticity $u_0' + mf$ or $v_0' + nf$, there will be a group

of solutions having wavelengths depending on β in the range from $\beta = 0$ to some critical value. All these solutions will be amplified accordingly, leading to a well-mixed condition of the region of flow. When eddy viscosity is included, the existence of such a group of solutions will depend on its value relative to the absolute vorticity and the characteristic length dimension. Hence there will be a limiting condition at which only the roll vortex corresponding to $\beta = 0$ can exist. If conditions become more favorable than this, the resulting confusion of roll-vortex wavelengths with their various amplification factors will merely result in a well-mixed condition, and no vortex structure will be distinguishable.

It is therefore necessary to search for those limiting values of the parameters expressing the absolute vorticity, which permit the existence of neutral stability. These will then constitute the basis for examination of oceanographic data for evidence of a roll-vortex wavelength consistent with the calculations. It is clear that eddy viscosity must be retained during this examination.

Viscous Solution for Neutral Stability - Case A

If a characteristic dimension δ is introduced, the following dimensionless quantities may be formed:

$$\eta \equiv z/\delta , \quad \sigma \equiv \alpha\delta \tag{10}$$

Setting $\beta = 0$, equations (6a) and (7a) may be written as:

$$w^{IV} - 2\sigma^2 w'' + \sigma^4 w = +\sigma^2\left(\frac{\delta^2 m_f}{\nu}\right)u \tag{11a}$$

and

$$u'' - \sigma^2 u = \left(\frac{\delta^2 u_o'}{\nu} + \frac{\delta^2 m_f}{\nu}\right)w \tag{12a}$$

where the subscripts signifying perturbation quantities have been omitted. A linear velocity profile (constant u_o') will again be assumed.

If boundary conditions corresponding to zero shear stress on the free surface are taken,

$$\eta = 0: \; u = v = w = 0 \;\; (\text{hence } w' = 0)$$

$$\eta = 1: \; u' = v' = w = 0 \;\; (\text{hence } w'' = 0)$$

the equations become

$$w(\eta) = -\sigma^2\left(\frac{\delta^2 m_f}{\nu}\right)\left\{\int_0^\eta\int_0^\eta\int_\eta^1\int_0^\eta u\,d\eta^4 - \left(\frac{\eta^2}{2} - \frac{\eta^3}{6}\right)3\int_0^1\int_0^\eta\int_\eta^1\int_0^\eta u\,d\eta^4\right\} \tag{13a}$$

$$+2\sigma^2\left\{\int_0^\eta\int_0^\eta w\,d\eta^2 - \left(\frac{\eta^2}{2} - \frac{\eta^3}{6}\right)3\int_0^1\int_0^\eta w\,d\eta^2\right\}$$

$$+\sigma^4\left\{\int_0^\eta\int_0^\eta\int_\eta^1\int_0^\eta w\,d\eta^4 - \left(\frac{\eta^2}{2} - \frac{\eta^3}{6}\right)3\int_0^1\int_\eta^1\int_0^\eta w\,d\eta^4\right\}$$

$$4(\eta) = -\left(\frac{\delta^2 u_o'}{\nu} + \frac{\delta^2 m_f}{\nu}\right)\int_0^\eta\int_\eta^1 w\,d\eta^2 - \sigma^2\int_0^\eta\int_\eta^1 u\,d\eta^2 \tag{14a}$$

For $O(\delta) = 10^{-5}$, $O(\nu) = 10^{4}$, $O(mf) = 10^{-4}$, $O(u_0') = 10^{-3}$

then $\left(\frac{\delta^2 mf}{\nu}\right) \sim 10^{2}$ and $\left(\frac{\delta^2 u_0'}{\nu}\right) \sim 10^{3}$ (15)

For small σ and large $(\delta^2 mf/\nu)$,

$$\frac{w}{\sigma^2} \approx \left(\frac{\delta^2 mf}{\nu}\right)\left\{\int_0^{\eta}\int_0^{\eta}\int_0^{\eta}\int_0^{1} u\, dy^4 - \left(\frac{\eta^2}{2} - \frac{\eta^3}{6}\right)3\int_0^{1}\int_0^{\eta}\int_0^{\eta}\int_0^{\eta} u\, dy^4\right\} \tag{16a}$$

$$u \approx -\sigma^2\left\{\left(\frac{\delta^2 u_0'}{\nu} - \frac{\delta^2 mf}{\nu}\right)\int_0^{\eta}\int_{\eta}^{1} \frac{w}{\sigma^2}\, d\eta^2 - \int_0^{\eta}\int_{\eta}^{1} u\, d\eta^2\right\} \tag{17a}$$

Iterating these equations (using only five steps in the independent variable), the following eigenvalue is obtained:

$$\sigma^2 = 1/117$$

The values of the perturbation functions for this case are:

η	$u(\eta)$	$v(\eta)$	$w(\eta)$	$\left(\frac{\delta P}{\nu\rho}\right) \div \left(\frac{\delta^2 mf}{\nu}\right)$
0	0		0	.333
		-.053		
.2	.35		-.00098	.298
		-.090		
.4	.66		-.00265	.197
		-.032		
.6	.88		-.00324	.043
		+.054		
.8	.98		-.00224	-.142
		+.121		
1.0	1.00		0	-.340

The chief features are that the streamwise velocity perturbation u is much larger than the transverse perturbations v and w, and the pressure perturbation exhibits a node at an intermediate depth.

Viscous Solution for Neutral Stability - Case B

Following the same procedure as that used in Case A the following perturbation equations are obtained:

$$w'''' - 2\sigma^2 w'' + \sigma^4 w = -\sigma\left(\frac{\delta^2 \bar{n}_f}{\nu}\right) v' \qquad (11b)$$

$$v'' - \sigma^2 v = \left(\frac{\delta^2 \bar{v}_0'}{\nu} + \frac{\delta^2 \bar{n}_f}{\nu}\right)\frac{w'}{\sigma} \qquad (12b)$$

In this case, the boundary condition on the free surface is taken from the disappearance of perturbation shear stresses, hence u' and v' must disappear at $\eta = 1$. Since $w' = \alpha u$ from the last of equations (5b), the boundary conditions are

$$\eta = 0: \; u = v = w = 0 \quad \text{and} \quad w' = 0$$

$$\eta = 1: \; u' = v' = w = 0 \quad \text{and} \quad w'' = 0.$$

Performing appropriate integrations of equation (11b) and (12b), the following are obtained:

$$w(\eta) = \sigma\left(\frac{\delta^2 n f}{\nu}\right)\left\{\int_0^{\eta}\int_0^{\eta}\int_{\eta}^{1} v\,d\eta^3 - \left(\frac{\eta^2}{2} - \frac{\eta^3}{6}\right)3\int_0^{1}\int_0^{\eta}\int_{\eta}^{1} v\,d\eta^3\right\}$$

$$+ 2\sigma^2\left\{\int_0^{\eta}\int_0^{\eta} w\,d\eta^2 - \left(\frac{\eta^2}{2} - \frac{\eta^3}{6}\right)3\int_0^{1}\int_0^{\eta} w\,d\eta^2\right\}$$

$$+ \sigma^4\left\{\int_0^{\eta}\int_0^{\eta}\int_{\eta}^{1}\int_0^{\eta} w\,d\eta^4 - \left(\frac{\eta^2}{2} - \frac{\eta^3}{6}\right)3\int_0^{1}\int_0^{\eta}\int_{\eta}^{1}\int_0^{\eta} w\,d\eta^4\right\} \qquad (13b)$$

$$v(\eta) = \left(\frac{\delta^3 v_0'}{\nu} + \frac{\delta^2 n f}{\nu}\right)\int_0^{\eta}\frac{w}{\sigma}\,d\eta - \sigma^2\int_0^{\eta}\int_{\eta}^{1} v\,d\eta^2 \qquad (14b)$$

Iterating these equations for $\frac{\delta^2 n f}{\nu} = 100$ and $\sigma = 1$, again using only five steps of the independent variable, a value of

$$\left(\frac{\delta^2 v_0'}{\nu} + \frac{\delta^2 n f}{\nu}\right) = -3.6$$

is obtained. (In this iteration, the small value of σ made it possible to drop the terms in σ^2 and σ^4 of equation (13b).)

The values of the perturbation functions are:

η	$u(\eta)$	$v(\eta)$	$w(\eta)$	$\left(\frac{\delta p}{\nu\rho}\right) \div \left(\frac{\delta^2 n f}{\nu}\right)$
0		0	0	.551
	-1.0			
.2		-.010	-.20	.566
	-1.7			
.4		+.175	-.53	.562
	- .65			
.6		.519	-.62	.545
	+1.2			
.8		.857	-.45	.527
	+2.2			
1.0		1.000	0	.519

The values of the velocity perturbations are all of the same magnitude, in contrast to the results of Case A. Also, the pressure perturbation is nearly constant with depth.

Effect of Horizontal Curvature of the Stream

The effect of a radius R of cyclonic curvature in Case B is to add a term $2U_0 U_1 / R$ to the left-hand side of the first of equations (5b). Physically, this subtracts from the amount of absolute vorticity opposing the rotation vector, hence is a stabilizing influence. Anticyclonic curvature is a destabilizing factor, the degree of which may be seen by inclusion of this term in the subsequent equations where it is associated with n_f in the 4th-order equation (11b) but does not enter equation (12b). The term $(\delta^2 n_f / \nu)$ in equation (13b) will then be replaced by $(\delta^2 n_f/\nu) - (2\delta^2 U_0/\nu R)$. For a 200 km. radius, the extra term amounts to 10 compared to the previous estimate of 100 for the other term. Recalculating, the necessary eigenvalue is reduced to

$$(\delta^2 U_0'/\nu) + (\delta^2 n_f/\nu) = -3.2$$

which is a slight (but hardly significant) reduction in necessary shear. The modal shape of the velocity perturbations is changed only very slightly.

In Case A. cyclonic curvature introduces a term $-2u_0 u_{tan} \alpha y/R$ to the left-hand side of the second of equations (5a). Thus, its

effect is not in the correct y-phase to permit vortex perturbations and the present analysis must fail.

Nonlinear Velocity Profile - The Cromwell Current

A final example of Case A is the calculation of the eigenvalue and perturbation for a nonlinear profile, that of the upper 200 meters of the Cromwell Current (taken from Ref. 14). The eigenvalue $\sigma^2 = 1/7.46$ gives a cross-stream wavelength of 3.4 km. for the neutral stability perturbation vortex. The perturbation velocity components are:

η	$\delta^2(u_0' + m_f)/\nu$	u	v	w
0	200	0		0
			.233	
.1	320	.076		.0085
			.588	
.2	1200	.159		.0300
			.653	
.3	1200	.266		.0539
			.659	
.4	320	.406		.0780
			.930	
.5	0	.565		.1120
			-.300	
.6	-200	.720		.1010
			-.352	
.7	-600	.855		.0881
			-.509	
.8	-1200	.950		.0695
			-1.085	
.9	-1200	.991		.0298
			-.815	
1.0	-400	1.000		0

$\frac{\delta^2 m_f}{\nu} = 4$

Comparison with Ocean Current Phenomena

The preceding arguments show the possible existence of roll vortices as secondary flows within the structure of ocean currents. It has not been possible to demonstrate the actual existence of such vortex structure from oceanographic data, but there is a certain amount of evidence to suggest its physical reality. (In fact, it is precisely this evidence which led to the present investigation.)

The Cromwell Current, a sub-surface current flowing easterly along the equator in the Pacific, exhibits the necessary geophysical conditions for Case A instability. It is known to possess unusually high mixing in the surface layer, which may be the result of instability of a roll-vortex nature. The velocity at the surface is in the opposite direction to the Cromwell Current, creating a shear which exhibits a difference in velocity of 50 cm/sec for a depth increment of 10 meters, far greater than the effect of the earth's rotation.

The U.S.Navy Oceanographic Office has evolved a procedure for sea surface temperature synoptic analysis (Ref.10) which interprets scattered synoptic temperature data by means of the assumption that the surface current is perpendicular to the gradient of surface temperature. The justification of this assumption is not given; it is presumed that this may be considered an empirical fact, based on extensive practical experience. This procedure has been used (Ref. 11) to interpret the sea surface temperature averaged on a monthly basis in the Gulf Stream. The result is a pattern of alternating warm and cool bands with axes parallel to the Gulf Stream drift, the bands having a

fairly uniform width so that they constitute a transverse periodicity of the Stream with a wavelength of about 60 miles. Since the current data on which the temperature charts are based was averaged on a one-degree latitude-longitude area basis, this 60-mile wavelength may be due to the grid size. However, the result of a vortex structure would be to bring cold, upwelled water to the surface on lines parallel to the current direction, in agreement with the published sea surface temperature charts.

A second observation based on oceanographic data is afforded by Fig. 65 of Stommel's study of the Gulf Stream (Ref. 12). The transverse variation of velocity of the Gulf Stream is calculated from temperature data on the assumption of uniform potential vorticity, and is compared with geostrophic (dynamic) velocity calculations. The differences between results of the two methods of calculation might be claimed as the result of ignoring the vortex structure in performing geostrophic calculations. Comparison of the variations on a numerical basis is now being made. Similar arguments may be based on Fig. 32 of Ref. 12, concerning which Stommel suggests internal inertial gravity or tidal waves acting on the density field as the cause of a false "streakiness" of velocity calculated by geostrophic equation.

Transverse variations in horizontal shear are discussed by von Arx (Ref. 13). These would be expected if a roll-vortex structure exists.

References

1. Taylor, G.I. 1923: Stability of a viscous liquid contained between two rotating cylinders. Phil.Trans. A 223, 289.

2. Goertler, H. 1940: On a three-dimensional instability of laminar boundary layers on concave walls. Nach.Wiss.Ges., Goettingen, Math.Phys.Klasse, New Series, 2, No.1.

3. Kirchgassner, K. 1962: Some examples of the stability theory for flows along concave and other heated walls. Ing.-Arch. 31, 115-124.

4. Hammerlin, G. 1961: Stability of compressible flow along a concave wall with varying temperatures. Dtch.Versuchanstalt Luftfahrt., Ber. 176, 38 pp.

5. Faller, A.J. 1963: An experimental study of the instability of the laminar Ekman boundary layer. J.Fluid Mech. 15, 560-576.

6. Gregory, N., J.T.Stuart and F.S.Walker, 1955: On the stability of three-dimensional boundary layers with application to the flow due to a rotating disc. Phil.Trans. A 248, 155-199.

7. Stern, M.E. 1960: Instability of Ekman flow at large Taylor number. Tellus 12, 399-417.

8. Arons, A.B., A.P.Ingersoll and T.Green, 1961: Experimentally observed instability of a laminar Ekman flow in a rotating basin. Tellus 13, 21-29.

9. von Arx, W. 1962: An introduction to physical oceanography. Addison-Wesley Publishing Company, Inc.

10. Gibson, B.W., April 1962: Sea surface temperature synoptic analysis. Asweps Rep. No. 7, U.S.Navy Hydrographic Office.

11. Perlroth, I. and L. Simpson, 1962: Persistence of composite sea surface temperature patterns for Feb. 1958-61 off Cape Hatteras. U.S.Navy Hydrographic Office IOM 20-62 (30 March,1962) see also Undersea Technology Magazine, July/August, 1962.

12. Stommel, H. 1960: The Gulf Stream. Univ. of California Press.

13. von Arx, W. 1952: Notes on the surface velocity profile and horizontal shear across the width of the Gulf Stream. Tellus 4, 211-214.

14. Knauss, J.A. 1960: Measurements of the Cromwell Current. Deep-Sea Research 6, 265-286.

Stability of a Homogeneous Fluid Cooled Uniformly from Above

by

Theodore D. Foster

Stability of a Homogeneous Fluid Cooled Uniformly from Above

Theodore D. Foster

I. Introduction

Consider an initially homogeneous and isothermal layer of fluid. If the temperature of the top surface is suddenly reduced, a nonlinear temperature gradient develops. This causes a heavier layer of fluid to form on the top of the fluid which will progressively grow thicker. It is the purpose of this paper to examine the stability of such a system.

II. Basic Equations

We will use the set of equations appropriate for an incompressible fluid. In the usual notation we have the Navier-Stokes equation,

$$\rho \frac{\partial \underset{\sim}{u}}{\partial t} + \rho \underset{\sim}{u} \cdot \nabla \underset{\sim}{u} = \rho g \underset{\sim}{k} - \nabla P + \rho \nu \nabla^2 \underset{\sim}{u} \qquad (1)$$

where $\underset{\sim}{k}$ is the unit vector in the z-direction which is vertically downward, the continuity equation,

$$\nabla \cdot \underset{\sim}{u} = 0 \qquad (2)$$

and the heat conduction equation,

$$\frac{\partial T}{\partial t} + \underset{\sim}{u} \cdot \nabla T = \kappa \nabla^2 T \qquad (3)$$

We will assume a linear equation of state,

$$\rho = \rho_I \left[1 - \alpha (T - T_I) \right] \tag{4}$$

Using the Boussinesq approximation equation (1) becomes

$$\frac{\partial \underset{\sim}{u}}{\partial t} + \underset{\sim}{u} \cdot \nabla \underset{\sim}{u} = g \left[1 - \alpha (T - T_I) \right] \underset{\sim}{k} - \frac{1}{\rho_I} \nabla P + \nu \nabla^2 \underset{\sim}{u} \tag{5}$$

Now let us separate the temperature into a horizontal mean, $\overline{T}$, and a fluctuating part, T , so that

$$T = \overline{T}(z,t) + T(x,y,z,t) \tag{6}$$

where, $\langle T \rangle = 0$, the brackets indicating a horizontal average.

Using (2) we can write (3) in the form

$$\frac{\partial T}{\partial t} + \nabla (\underset{\sim}{u} T) = \kappa \nabla^2 T \tag{7}$$

Now taking the horizontal average of (7) and using (6) we find

$$\frac{\partial \overline{T}}{\partial t} + \frac{\partial}{\partial z} \langle w T \rangle = \kappa \frac{\partial^2 \overline{T}}{\partial z^2} \tag{8}$$

Similarly by using (6) in (3) and subtracting off (8) we obtain

$$\frac{\partial T}{\partial t} - \kappa \nabla^2 T = -w \frac{\partial \overline{T}}{\partial z} - H \tag{9}$$

where

$$H \equiv \underset{\sim}{u} \cdot \nabla T - \frac{\partial}{\partial z} \langle w T \rangle \tag{10}$$

Incorporating the mean temperature in the pressure term in (5) and

taking the z-component of the double curl of (5) we obtain

$$\left(\frac{\partial}{\partial t} - \nu\nabla^2\right)\nabla^2 W = -g\alpha\,\nabla_1^2 T + L \tag{11}$$

where

$$\nabla_1^2 = \frac{\partial}{\partial x^2} + \frac{\partial}{\partial y^2} \tag{12}$$

and

$$L \equiv \frac{\partial}{\partial z}\left[\frac{\partial}{\partial x}\left(\underset{\sim}{u}\cdot\nabla\underset{\sim}{u}\right) + \frac{\partial}{\partial y}\left(\underset{\sim}{u}\cdot\nabla v\right)\right] - \nabla_1^2\left(\underset{\sim}{u}\cdot\nabla w\right) \tag{13}$$

Eliminating the pressure from the horizontal terms of (5) we obtain

$$\left(\frac{\partial}{\partial t} - \nu\nabla^2\right)\left(\nabla_1^2 u + \frac{\partial^2 w}{\partial x\,\partial z}\right) = \frac{\partial^2}{\partial x\,\partial y}\left(\underset{\sim}{u}\cdot\nabla v\right) - \frac{\partial^2}{\partial y^2}\left(\underset{\sim}{u}\cdot\nabla u\right) \tag{14}$$

and

$$\left(\frac{\partial}{\partial t} - \nu\nabla^2\right)\left(\nabla_1^2 v + \frac{\partial^2 w}{\partial y\,\partial z}\right) = \frac{\partial^2}{\partial x\,\partial y}\left(\underset{\sim}{u}\cdot\nabla u\right) - \frac{\partial^2}{\partial x^2}\left(\underset{\sim}{u}\cdot\nabla v\right) \tag{15}$$

We will now introduce the dimensionless (primed) parameters:

$$\underset{\sim}{r} = h\,\underset{\sim}{r}' \tag{16}$$

$$\underset{\sim}{u} = \frac{\kappa}{h}\,\underset{\sim}{u}' \tag{17}$$

$$T = \frac{\nu\kappa}{h^3 g\alpha}\,T' \tag{18}$$

$$\bar{T} = \Delta T\,\bar{T}' \tag{19}$$

$$t = \frac{h^2}{\kappa}\,t' \tag{20}$$

$$\sigma = \frac{\nu}{\kappa} \tag{21}$$

where h is the total depth of the fluid layer, and ΔT is the temperature change at the top surface.

We define a Rayleigh number

$$R = \frac{\alpha g}{\kappa \nu} \Delta T h^3 \tag{22}$$

Now our basic equations in dimensionless form become (dropping primes)

$$\frac{\partial \bar{T}}{\partial t} + \frac{1}{R} \frac{\partial}{\partial z} \langle wT \rangle = \frac{\partial^2 \bar{T}}{\partial z^2} \tag{23}$$

$$\frac{\partial T}{\partial t} - \nabla^2 T = -Rw \frac{\partial \bar{T}}{\partial z} - H \tag{24}$$

$$\left(\frac{1}{\sigma} \frac{\partial}{\partial t} - \nabla^2\right) \nabla^2 w = -\nabla_1^2 T + \frac{1}{\sigma} L \tag{25}$$

$$\left(\frac{1}{\sigma} \frac{\partial}{\partial t} - \nabla^2\right)\left(\nabla_1^2 u + \frac{\partial^2 w}{\partial x \partial z}\right) = \frac{1}{\sigma}\left[\frac{\partial^2}{\partial x \partial y}(\underset{\sim}{u} \cdot \nabla v) - \frac{\partial^2}{\partial y^2}(\underset{\sim}{u} \cdot \nabla u)\right] \tag{26}$$

$$\left(\frac{1}{\sigma} \frac{\partial}{\partial t} - \nabla^2\right)\left(\nabla_1^2 v + \frac{\partial^2 w}{\partial y \partial z}\right) = \frac{1}{\sigma}\left[\frac{\partial^2}{\partial x \partial y}(\underset{\sim}{u} \cdot \nabla u) - \frac{\partial^2}{\partial x^2}(\underset{\sim}{u} \cdot \nabla v)\right] \tag{27}$$

III. Boundary Conditions

Mainly in the interest of mathematical simplicity we will assume the so-called "slippery" boundary conditions for the vertical velocity,

$$w = \frac{\partial^2 w}{\partial z^2} = 0 \qquad \text{at} \quad z = 0, 1 \tag{28}$$

We will also make the usual assumption that the temperature fluctuations vanish on the boundaries,

$$T = 0 \qquad \text{at} \quad z = 0, 1 \tag{29}$$

Finally we will assume that the fluid is infinite in horizontal extent.

IV. Perturbation Equations

Let us expand in a power series of the small parameter ϵ:

$$\underset{\sim}{u} = \epsilon \underset{\sim}{u}_1 + \epsilon^2 \underset{\sim}{u}_2 + \cdots \tag{30}$$

$$T = \epsilon T_1 + \epsilon^2 T_2 + \cdots \tag{31}$$

$$\overline{T} = \overline{T}_0 + \epsilon \overline{T}_1 + \epsilon^2 \overline{T}_2 + \cdots \tag{32}$$

$$R = R_0 + \epsilon R_1 + \epsilon^2 R_2 + \cdots \tag{33}$$

A. Zeroth Order Equations

From (23) we obtain our only zeroth order equation

$$\frac{\partial \overline{T}_0}{\partial t} = \frac{\partial^2 \overline{T}_0}{\partial z^2} \tag{34}$$

which we recognize as the heat conduction equation for a fluid at rest.

B. First Order Equations

$$\frac{\partial \overline{T}_1}{\partial t} = \frac{\partial^2 \overline{T}}{\partial z^2} \tag{35}$$

which has the same form as the zeroth order equation (34), and therefore we can set $\overline{T}_1 = 0$.

$$\left(\frac{\partial}{\partial t} - \nabla^2\right) T_1 = - R_0 W_1 \frac{\partial \overline{T}_0}{\partial z} \tag{36}$$

$$\left(\frac{1}{\sigma}\frac{\partial}{\partial t} - \nabla^2\right) \nabla^2 W_1 = - \nabla_1^2 T_1 \tag{37}$$

$$\left(\frac{1}{\sigma}\frac{\partial}{\partial t} - \nabla^2\right)\left(\nabla_1^2 u_1 + \frac{\partial^2 W_1}{\partial x \partial z}\right) = 0 \tag{38}$$

$$\left(\frac{1}{\sigma}\frac{\partial}{\partial t} - \nabla^2\right)\left(\nabla_1^2 v_1 + \frac{\partial^2 W_1}{\partial y \partial z}\right) = 0 \tag{39}$$

C. Second Order Equations

$$\frac{\partial \overline{T}_2}{\partial t} + \frac{1}{R_0}\frac{\partial}{\partial z}\langle W_1 T_1 \rangle = \frac{\partial^2 \overline{T}_2}{\partial z^2} \tag{40}$$

$$\left(\frac{\partial}{\partial t} - \nabla^2\right) T_2 = - R_0 W_2 \frac{\partial \overline{T}_0}{\partial z} - R_1 W_1 \frac{\partial \overline{T}_0}{\partial z} - H_{11} \tag{41}$$

where

$$H_{ij} \equiv \underset{\sim}{u}_i \cdot \nabla T_j - \frac{\partial}{\partial z}\langle W_i T_j \rangle \tag{42}$$

$$\left(\frac{1}{\sigma}\frac{\partial}{\partial t} - \nabla^2\right) \nabla^2 W_2 = - \nabla_1^2 T_2 + \frac{1}{\sigma} L_{11} \tag{43}$$

where

$$L_{ij} \equiv \frac{\partial}{\partial z}\left[\frac{\partial}{\partial x}\left(\underset{\sim}{u}_i \cdot \nabla u_j\right) + \frac{\partial}{\partial y}\left(\underset{\sim}{u}_i \cdot \nabla v_j\right)\right] - \nabla_1^2\left(\underset{\sim}{u}_i \cdot \nabla W_j\right) \tag{44}$$

$$\left(\frac{1}{\sigma}\frac{\partial}{\partial t} - \nabla^2\right)\left(\nabla_1^2 u_2 + \frac{\partial^2 W_2}{\partial x \partial z}\right) = \frac{1}{\sigma}\left[\frac{\partial^2}{\partial x \partial y}\left(\underset{\sim}{u}_1 \cdot \nabla v_1\right) - \frac{\partial^2}{\partial y^2}\left(\underset{\sim}{u}_1 \cdot \nabla u_1\right)\right] \tag{45}$$

$$\left(\frac{1}{\sigma}\frac{\partial}{\partial t} - \nabla^2\right)\left(\nabla_1^2 v_2 + \frac{\partial^2 W_2}{\partial y \partial z}\right) = \frac{1}{\sigma}\left[\frac{\partial^2}{\partial x \partial y}\left(\underset{\sim}{u}_1 \cdot \nabla u_1\right) - \frac{\partial^2}{\partial y^2}\left(\underset{\sim}{u}_1 \cdot \nabla v_1\right)\right] \tag{46}$$

D. Third Order Equations

The only third order equations that we will need are

$$\left(\frac{1}{\sigma}-\nabla^2\right)T_3 = -R_0\left(W_1\frac{\partial \overline{T}_2}{\partial t}-W_3\frac{\partial \overline{T}_0}{\partial z}\right)-R_1\left(W_2\frac{\partial \overline{T}_2}{\partial z}\right)-R_2\left(W_1\frac{\partial \overline{T}_0}{\partial z}\right)-H_{12}-H_{21} \tag{47}$$

$$\left(\frac{1}{\sigma}\frac{\partial}{\partial t}-\nabla^2\right)\nabla^2 W_3 = -\nabla_1^2 T_3+\frac{1}{\Gamma}\left(L_{12}+L_{21}\right) \tag{48}$$

V. The Temperature Gradient

Let us assume the fluid to have the constant mean temperature $\overline{T}_I$ for all $t < 0$. Now let the top surface temperature be suddenly lowered by an amount ΔT at $t = 0$ and remain at that temperature for all $t > 0$. The solution to the zeroth order heat conduction equation (34) in dimensional form is (provided the total fluid depth is much greater than $2\sqrt{\kappa t}$)

$$\overline{T}_0 = \overline{T}_I - \Delta T\left(1-\frac{2}{\sqrt{\pi}}\int_0^{\frac{z}{2\sqrt{\kappa t}}} e^{-\xi^2}\,d\xi\right) \tag{49}$$

We now define an effective penetration depth,

$$d = 2\sqrt{\kappa t} \tag{50}$$

and introduce a new dimensionless parameter

$$\lambda = \frac{d}{h} \tag{51}$$

Now non-dimensionalizing (49) (again dropping primes) we have

$$\bar{T}_0 = \bar{T}_\infty - \left(1 - \frac{2}{\sqrt{\pi}} \int_0^{\frac{z}{\lambda}} e^{-\xi^2} d\xi\right) \tag{52}$$

and the vertical temperature gradient is

$$\frac{\partial \bar{T}_0}{\partial z} = \frac{2}{\lambda \sqrt{\pi}} e^{-\frac{z^2}{\lambda^2}} \tag{53}$$

VI. The Stability Problem

If we operate on the first order equation (36) by $-\nabla_1^2$, and on (37) by $\left(\frac{\partial}{\partial t} - \nabla^2\right)$ and add, we obtain

$$\left(\frac{\partial}{\partial t} - \nabla^2\right)\left(\frac{1}{\sigma}\frac{\partial}{\partial t} - \nabla^2\right)\nabla^2 W_1 = R_0 \frac{\partial \bar{T}_0}{\partial z} \nabla_1^2 W_1 \tag{54}$$

We now make the important assumption that the temperature gradient can be considered quasi-static; that is, the effect of the change in gradient at the instability point is sufficiently small so that the time dependence of the perturbations can be accurately represented by exponential functions

$$W_1(x, y, z, t) = W_1(z) \hat{f}(x, y) e^{\gamma t} \tag{55}$$

Then equation (54) becomes

$$(\gamma - \nabla^2)\left(\frac{1}{\sigma}\gamma - \nabla^2\right)\nabla^2 W_1 = R_0 \frac{\partial \bar{T}_0}{\partial z} \nabla_1^2 W_1 \tag{56}$$

It can be shown that the principle of exchange of stabilities holds for this equation and the marginal state is given by setting $\gamma = 0$. Thus we obtain the equation governing the onset of instability:

$$\nabla^6 W_1 = R_0 \frac{\partial \bar{T}_0}{\partial z} \nabla_1^2 W_1 \tag{57}$$

We will analyse an arbitrary disturbance into normal modes and examine the stability of each mode separately. Consequently we will assume

$$\nabla_1^2 f(x,y) = -a^2 f(x,y) \tag{58}$$

where a is the dimensionless horizontal wave number of the disturbance. Now using (53) the stability equation becomes

$$-(D^2 - a^2)^3 W_1 = a^2 \frac{R_0}{\lambda} \frac{2}{\sqrt{\pi}} e^{-\frac{z^2}{\lambda^2}} W_1 \tag{59}$$

where $D = \frac{d}{dz}$.

Since (59) is a sixth order differential equation with non-constant coefficients, its solution presents a rather difficult mathematical task in general. In the case of small λ the best solution method appears to be a variational method which, since the equation (59) with the "slippery" boundary conditions (28), (29) is self-adjoint, provides upper bounds on the eigenvalues. With the aid of the CDC 1604 computer eigenvalues for three different values of λ were obtained for a wide range of wave numbers:

λ	Minimum R_0	a for Minimum R_0
2.44×10^{-6}	1.2×10^{13}	2.2
2.44×10^{-4}	1.2×10^{9}	2.2
2.44×10^{-3}	1.2×10^{7}	2.2

The most surprising thing about these solutions was that the wave number for minimum Rayleigh number occurred in each case, within the accuracy of the computation, at the same value, $a \simeq 2.2 \simeq \pi/\sqrt{2}$, which is the wave number obtained in the usual convection theory for linear temperature gradients. This means that the most unstable mode occurs at a wavelength of the same order of magnitude as the total depth of fluid, h, and not that of the penetration depth of the temperature gradient, d.

In order to substantiate these variational calculations and to obtain simpler eigenfunctions, equation (59) was also solved by the Fourier expansion technique. Since sine functions satisfy the boundary conditions, we let

$$W_1(z) = \sum_{m=1}^{\infty} A_m \sin m\pi z \qquad (60)$$

substituting into (59) we find

$$\sum_{m=1}^{\infty} \left(m^2\pi^2 + a^2\right)^3 A_m \sin m\pi z = \frac{a^2 R_0}{\lambda} \frac{2}{\sqrt{\pi}} e^{-\frac{z^2}{\lambda^2}} \sum_{m=1}^{\infty} A_m \sin m\pi z \qquad (61)$$

multiplying (61) by $\sin r\pi z$ and integrating from $z = 0$ to $z = 1$ we have

$$(r^2\pi^2+a^2)^3 A_r - \frac{2a^2R_0}{\lambda}\sum_{m=1}^{\infty} A_m I_{mr} = 0 \tag{62}$$

where

$$I_{mr} = \frac{2}{\sqrt{\pi}}\int_0^1 e^{-\frac{z^2}{\lambda^2}} \sin m\pi z \sin r\pi z \, dz \tag{63}$$

(62) is a set of m homogeneous equations for the A_m. Thus in order that this set be consistent, the determinant of the coefficients of the A_m must vanish. Thus

$$\begin{vmatrix} (\pi^2+a^2)^3 - \frac{2a^2R_0}{\lambda} I_{11} & -\frac{2a^2R_0}{\lambda} I_{12} & -\frac{2a^2R_0}{\lambda} I_{13} \cdots \\ -\frac{2a^2R_0}{\lambda} I_{12} & (4\pi^2+a^2)^3 - \frac{2a^2R_0}{\lambda} I_{22} & -\frac{2a^2R_0}{\lambda} I_{23} \cdots \\ -\frac{2a^2R_0}{\lambda} I_{13} & -\frac{2a^2R_0}{\lambda} I_{23} & (9\pi^2+a^2)^3 - \frac{2a^2R_0}{\lambda} I_{33} \cdots \\ \vdots & \vdots & \vdots \end{vmatrix} = 0 \tag{64}$$

The determinant is then truncated to the smallest order compatible with convergent results. In the cases treated 2x2 determinants gave quite good results (Note: Due to lack of time and access to an adequate high-speed computer the integrals (63) were approximated by Simpson's rule using only 10 points and utilizing a somewhat unreliable desk calculator).

λ	R_o (2x2)	R_o (3x3)	A_2/A_1	A_3/A_1
0.3162	1004.7	1005.34	0.0403	0.0023
0.4000	810.1		0.0308	
0.5000	710.2	710.175	0.0224	0.0004
0.5064	706.7		0.0220	

In every calculation the minimum Rayleigh number occurred at $a = \pi/\sqrt{2}$ within the accuracy of the computation, confirming the results of the variational calculations. A log-log plot of minimum R_o versus λ shows a nearly linear relation (see Figure #1). Another somewhat surprising result is that the velocity field penetrates the entire depth of the fluid, and for the cases calculated differed but slightly from the sine curve obtained with a linear temperature gradient. The temperature field was somewhat more distorted (see Figure #2).

The validity of the stability criteria calculated from equation (59) is not clear. An attempt was made to estimate the error in neglecting the time dependence of the coefficients A_m in W_1 (60) on making the quasi-static assumption used in deriving (59). By calculating the rate of change of the ratio A_2/A_1 in going from λ = 0.5000 to λ = 0.5064, it was found that the neglected time dependence terms were 4% and 28% that of the terms retained. It is not clear how to interpret these results. In an attempt to clarify the situation further a finite amplitude analysis following the method developed by Veronis (1963) was made.

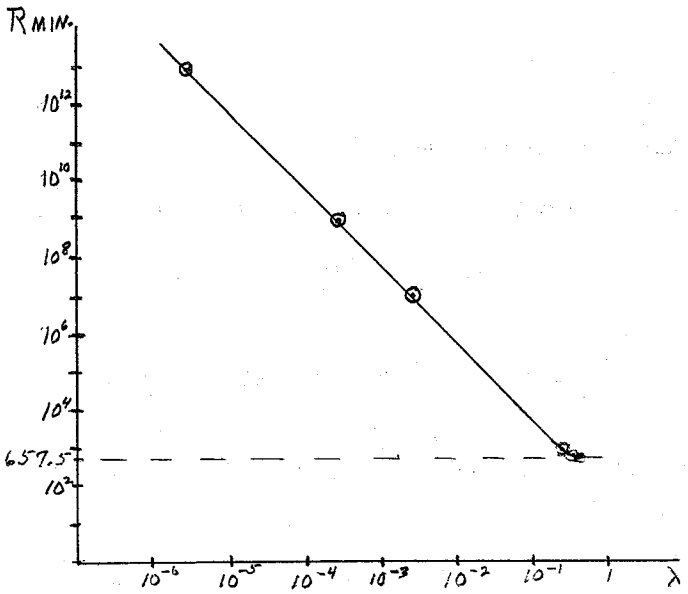

Figure #1

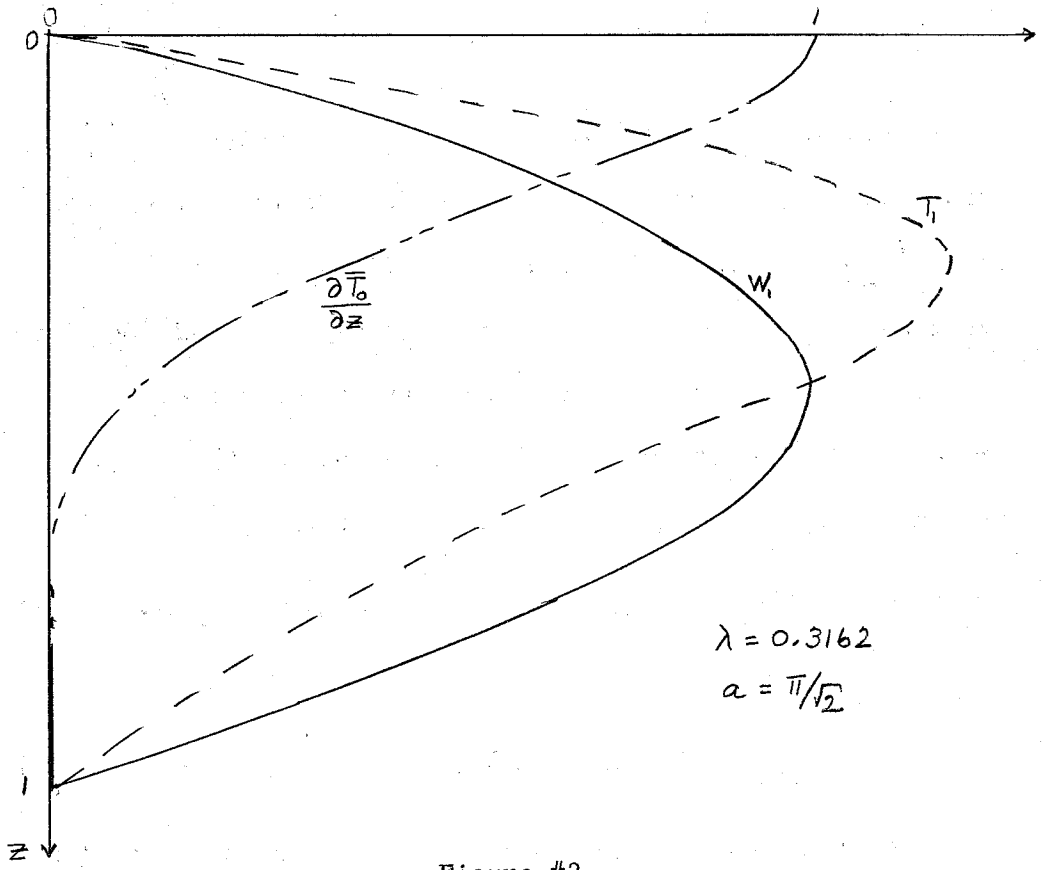

Figure #2

VII Finite Amplitude Analysis

We will only treat the case of two-dimensional convection cells at $\lambda = 0.5$ for $a = \pi/\sqrt{2}$. Now

$$W_1 = (A_1 \sin \pi z + A_2 \sin 2\pi z) \cos ax \tag{65}$$

By solving the time independent version of equation (38) we find

$$u_1 = -\sqrt{2}\,(A_1 \cos \pi z + 2A_2 \cos 2\pi z) \sin ax \tag{66}$$

The time independent form of (37) gives

$$T_1 = -\frac{9}{2}\pi^2 (A_1 \sin \pi z + 9A_2 \sin 2\pi z) \cos ax \tag{67}$$

We now normalize W_1 such that the average of W_1^2 throughout the entire layer of fluid is equal to unity, that is, $(W_1^2)_m = 1$. Now we impose the condition that $(W_1 W)_m = \epsilon$ which has the effect of putting all the amplitude of W_1 into ϵ . The normalization procedure determines the constants $A_1 = 1.9995$ and $A_2 = 0.04482$. Using (65), (66) and (67) we can now determine H_{11} and L_{11} . We find

$$H_{11} = 18\pi^3 A_1 A_2 (\cos \pi z \sin 2\pi z - 2 \sin \pi z \cos 2\pi z) \cos 2ax \tag{68}$$

and

$$L_{11} = 3\pi^3 A_1 A_2 (-\cos \pi z \sin 2\pi z + 2 \sin \pi z \cos 2\pi z) \cos 2ax \tag{69}$$

Combining the time independent forms of equations (40) and (41) we obtain

$$\mathcal{L} W_2 = R_1 \frac{\partial \bar{T}_0}{\partial z} \nabla_1^2 W_1 + \nabla_1^2 H_{11} - \frac{1}{\sigma} \nabla^2 L_{11} \tag{70}$$

where

$$\mathcal{L} \equiv \nabla^6 - R_0 \frac{\partial \bar{T}_0}{\partial z} \nabla_1^2 \tag{71}$$

If we multiply equation (70) by the adjoint of W_1 and average over the entire fluid, both sides of the resulting equation must vanish. For our boundary conditions W_1 is self-adjoint. Now since H_{11} and L_{11} only involve $\cos 2ax$ and W_1 only involves $\cos ax$ the orthogonality of the consines results in

$$R_1 = 0 \tag{72}$$

We can now solve (70) for W_2 by expanding in a Fourier sine series

$$W_2 = \left[\sum_{m=1}^{\infty} B_m \sin m\pi z \right] \cos 2ax \tag{73}$$

In order to simplify succeeding calculations we will assume a Prandtl number, $\sigma = 7.04$, (approximately that of sea water ($20^{\circ}C$, $35^{\circ}/oo$)). Substituting (72) and (73) into (70) multiplying by $\sin r\pi z$ and integrating we obtain a set of n inhomogeneous equations for determining the B_n. Truncating the series to 3 terms and approximating the integrals by Simpson's rule we find, $B_1 = -0.11927$, $B_2 = -0.00463$, $B_3 = 0.00030$. We can now also evaluate u_2, T_2 and hence L_{12}, L_{21}, H_{12}, and H_{21}.

Next, in order to determine ϵ we must go to the third

order equations. The time independent forms of equations (47) and (48) can be combined to give

$$\mathcal{L}W_3 = \left(R_0 \frac{\partial \bar{T}_2}{\partial z} + R_2 \frac{\partial \bar{T}_0}{\partial z}\right)\nabla_1^2 W_1 + \nabla_1^2\left(H_{12} + H_{21}\right) - \frac{1}{\sigma}\left(L_{12} + L_{21}\right) \qquad (74)$$

Now we have to determine $\bar{T}_2$. Using the values of R_0 , W_1 and T_1 already determined we can write equation (40) in the form

$$\frac{\partial^2 \bar{T}_2}{\partial z^2} - \frac{\partial \bar{T}_2}{\partial t} = \sum_{n=1}^{4} G_n \sin n\pi z \qquad (75)$$

where $G_1 = 0.0440$, $G_2 = -0.3927$, $G_3 = -0.1321$, $G_4 = 0.0036$. The boundary conditions are $\bar{T}_2 = 0$ at $z = 0$ and $z = 1$. The solution is straightforward and gives

$$\bar{T}_2 = -\sum_{n=1}^{4} \frac{G_n}{n^2\pi^2}\left(1 - e^{-n^2\pi^2(t-t_0)}\right) \sin n\pi z \qquad (76)$$

where t_0 is the time of onset of instability.

Now multiplying equation (74) by W_1 and averaging, both sides of the resulting equation must vanish thus providing an expression for R_2 in terms of known quantities. After a lengthy and very tedious computation we finally obtain (subject to various human and calculator errors)

$$R_2 = \frac{116.8 - 1.1e^{-\pi^2 t'} - 109.5e^{-4\pi^2 t'} - 1.1e^{-9\pi^2 t'} - 0.00025e^{-16\pi^2 t'}}{4.6549} \qquad (77)$$

where $t' = t - t_0$

To second order we have

$$R = R_0 + \epsilon^2 R_2 \tag{78}$$

or

$$\epsilon^2 = \frac{R - R_0}{R_2} \tag{79}$$

Since at all times $R_2 > 0$ and $\epsilon^2 > 0$, we must have

$$R > R_0 \tag{80}$$

from which we can conclude there is no finite amplitude instability for this case ($\lambda = 0.5$).

We are now in a position to make another estimate of validity of the quasi-static assumption. To second order we now have

$$\overline{T} = \overline{T}_0 + \epsilon^2 \overline{T}_2 \tag{81}$$

Using the values of ϵ^2 (79) and $\overline{T}_2$ (76) calculated above we can determine the time scale for the establishment of a quasi-steady convective flow for $\lambda = 0.5$. Using only the largest term ($n = 2$) in the series expansion for $\overline{T}_2$ and the largest exponential term in ϵ^2 we find that the approximate time for $\epsilon^2 \overline{T}_2$ to reach $\left(1 - \frac{1}{e}\right)$ of its asymptotic ($t' = \infty$) value is

$$t' \simeq 0.00185 \tag{82}$$

which we may take as the time scale for the establishment of

quasi-steady convection. Using equations (50) and (51) we can write

$$\lambda = 2\sqrt{t} \tag{83}$$

and thus the time scale for change in $\bar{T}_o$ is

$$t = 0.0625 \tag{84}$$

which is approximately 34 times (82). During the time it takes for quasi-steady convection to be established λ will change by about 1.5% and R_o by about 0.75%. Thus the assumption that the temperature gradient can be treated quasi-statically would seem to be reasonable for the case of temperature gradients near $\lambda = 0.5$

VIII Preliminary Conclusions

One must first be warned that all the above calculations are of uncertain accuracy and it is precarious to draw any conclusions from these results until they are thoroughly checked.

The most striking result is the occurrence of the minimum Rayleigh number at the same wave number $a = \pi/\sqrt{2}$ for all values of λ . This is in contradiction to the intuitive feeling that the most unstable wave length should be of the same order as the penetration depth and independent of the depth of the fluid. The physical reason for this somewhat odd behavior is that we are dealing with an initially neutrally stable layer of fluid which is free to move through the entire depth of the fluid and not just

in the region of the strong temperature gradient.

The experiments of Spangenberg and Rowland (1961) with convection produced by evaporative cooling at the top of a homogeneous fluid are not entirely in agreement with the above theoretical model. The observed Rayleigh number at onset of instability seems to be one to two orders of magnitude larger than predicted. This may be due to the neglect of surface tension in the theoretical model. While they observed convective instabilities which have a horizontal scale much larger than that of the penetration depth, they did not observe the predicted variation with the total depth of the fluid layer. Possibly this was due to a very slight stabilizing temperature gradient which prevented the predicted large scale velocity field from being established. Some experiments by the author with a homogeneous fluid cooled from above did seem to produce large scale cellular convection but lack of instrumentation prevented obtaining any quantitative data.

The author wishes to acknowledge the many useful discussions with the other members of the Geophysical Fluid Dynamics course and in particular to thank Dr. George Veronis for his extensive guidance through many of the intricacies of the analysis.

References

Spangenberg, W.G. and W.R. Rowland, 1961: "Convective Circulation in Water induced by Evaporative Cooling", Physics of Fluids, 4, 743.

Veronis, G., 1963: "Penetrative Convection", Astrophysical Journal, 137, 641.

Experiments on "Taylor Columns" in a Rotating Barotropic Liquid

by

Alan Ibbetson

Experiments on "Taylor Columns" in a Rotating Barotropic Liquid

A. Ibbetson

Introduction

In 1923, G.I.Taylor carried out the qualitative experiments in which he produced an entirely two-dimensional flow in a rotating liquid by slowly moving a three-dimensional obstacle through it. Since then, there have been many attempts to study this and similar problems (see 1963 G.F.D. lecture notes), but no-one has tried to establish experimentally the conditions for such a flow field to be produced.

A quantitative theoretical criterion for the occurrence of Taylor columns was proposed by Hide (1961), and in a different form by Bolin (1950). It was predicted that if an obstacle of length L and height h moved with speed U through a fluid of depth D rotating with angular velocity Ω, a Taylor column would be formed only if

$$\alpha \frac{U}{L\Omega} < \frac{h}{D}$$

where α is a numerical constant of order unity.

In 1960, the author repeated Taylor's experiments to test these predictions. However the results, using circular cylindrical obstacles such as Taylor used, agreed with the theory only over a limited range of conditions.

In the present experiments therefore, a geometrically simpler obstacle was used in the hope that results would show better agreement with theory. The obstacle was in fact a horizontal cylinder extending along a radius of the tank. It could be moved azimuthally at an angular speed slow compared with the basic rotation rate.

Simplified Theory

Consider an obstacle of height h moving with uniform speed U through an inviscid liquid of uniform depth D which is rotating with angular speed Ω. Provided that the flow is always approximately two-dimensional, it is legitimate to consider vertical filaments of liquid which, during their motion over the obstacle, conserve their circulation.

Thus if the filament shortens in moving over the obstacle, its cross-sectional area increases, so the vertical component of its absolute vorticity decreases by an amount

$$\zeta = 2\Omega h/D. \qquad (1)$$

This change in vorticity of the filament can be balanced by curvature of the trajectory of the filament, the vorticity change generated by this mechanism being $\sim U/r$, where r is the radius of curvature of the trajectory (assumed constant).

Thus

$$U/r \sim -2\Omega h/D. \qquad (2)$$

The formation of a Taylor column requires that $r < L$, where L is the horizontal dimension of the obstacle. Thus

$U/L\Omega < h/D$, which is Hide's criterion.

For an obstacle moving azimuthally as in these experiments, $U = s\omega$, where s = distance radially outward from centre, and ω = relative angular speed of the obstacle, so that

$$r \sim -s\frac{\omega}{2\Omega}\cdot\frac{D}{h} \qquad (3)$$

Apparatus

The rotating tank and the mechanism for producing the slow motion of the obstacle relative to the tank are shown schematically in Fig. 1. The tank was a circular cylinder of 'Plexiglass', 29.2 cm inside diameter fitted with a transparent lid. It was mounted horizontally on a balanced steel turntable. Inside the tank was a close-fitting horizontal false base A below which the mechanism for rotating the obstacle was housed. Throughout these experiments the depth of the tank, from lid to false base, was 10.93 ± 0.05 cm.

The obstacle was a horizontal radial arm B of either square or circular cross section. It was fixed on a vertical shaft C mounted in bearings at the centre of the base. The vertical shaft C was rotated at angular speeds continuously variable from 0.01 to

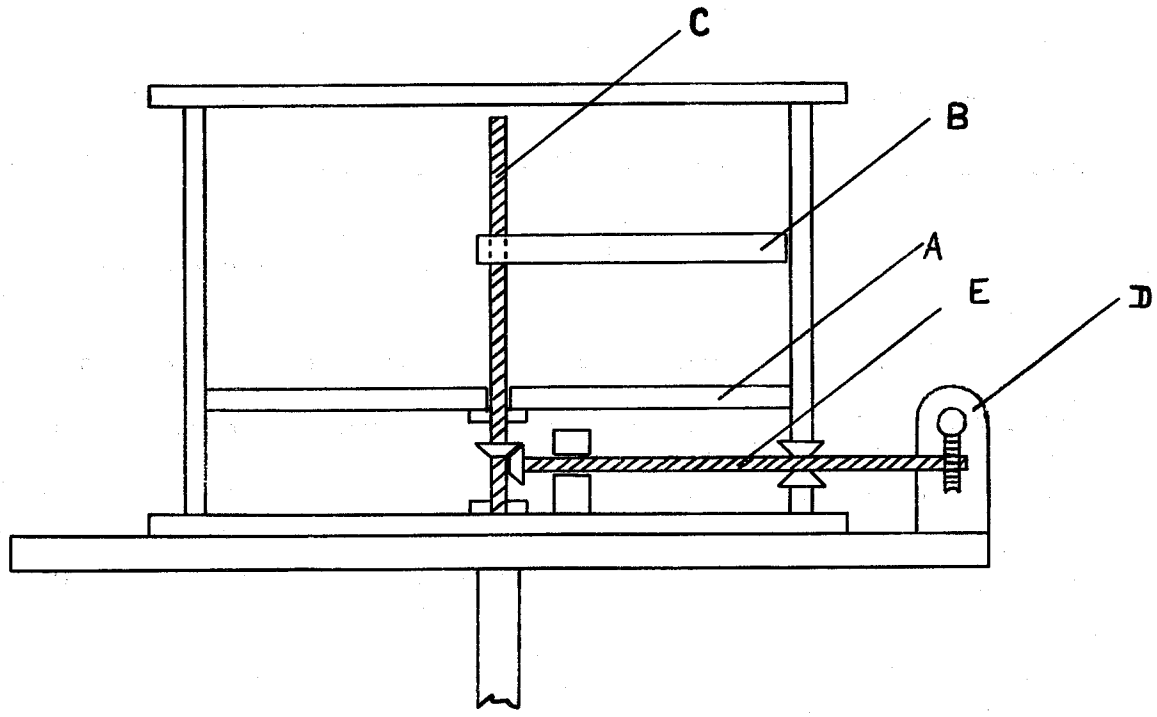

FIGURE 1 : APPARATUS.

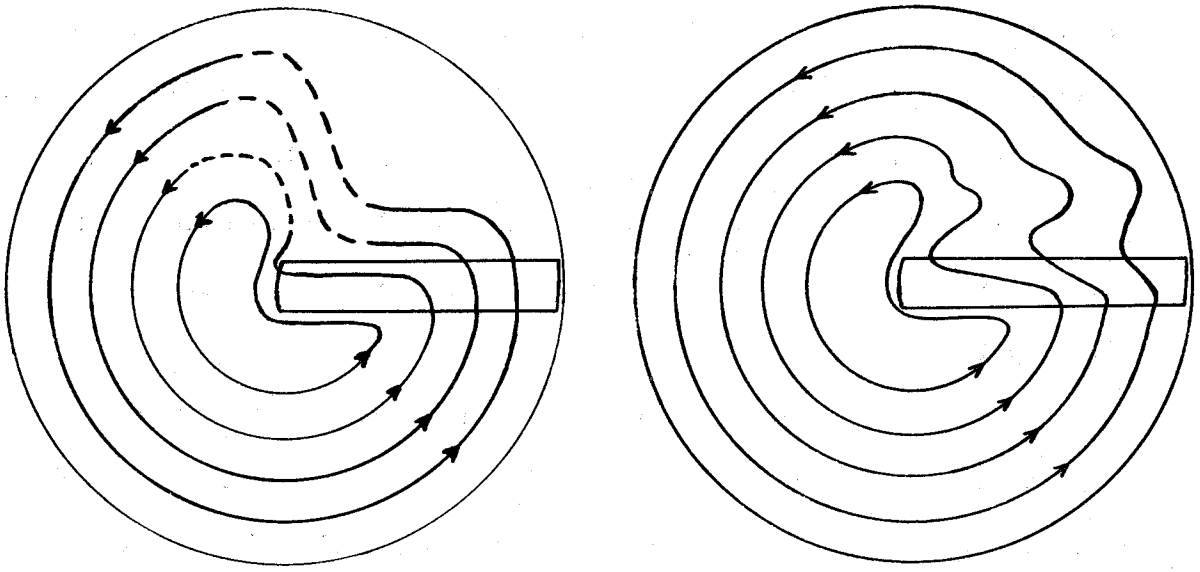

FIGURE 2.

a b

0.10 rad/sec by an electric motor D through a reduction gear, a horizontal rod E, and bevel gears. The vertical position of the obstacle in the tank was adjustable.

A reference grid was marked on the false base to facilitate measurements. The divisions were 1 cm. radially and 15° azimuthally.

The turntable could be rotated at speeds continuously variable from 0 to 10 rad/sec. During the time required for an experiment, fluctuations in angular speed of the turntable were not greater than 0.1%.

Direct observation of the flow field in the rotating tank was made possible by use of a "rotoscope". This consists of a Dove prism which can be rotated about its optic axis at exactly half the angular velocity of the tank. Seen through this rotating prism, the tank appears to be stationary, so that measurements relative to the rotating tank can be made directly.

Visualization of the flow field was achieved by injecting a fine stream of almost neutrally-buoyant dye from a hypodermic needle into the liquid. The needle, which passed through a central hole in the lid of the tank, was attached to the vertical shaft C so as to rotate with it. However, using this method it is possible to trace only one or perhaps two streamlines at one time.

Throughout these experiments, the tank was filled completely with water at a temperature of $23 \pm 2^{\circ}C$. The kinematic viscosity of water in this range is $(0.936 \pm 0.041) \times 10^{-2}$ $cm^2.sec^{-1}$.

Qualitative Observations

Schematic diagrams of the flow fields at some distance above obstacles of square and circular cross sections are shown in Figs. 2a and 2b respectively. In both diagrams the basic rotation, Ω, and the relative rotation of the obstacle, ω, are clockwise. The diagrams show streak-lines relative to the rotating obstacle, so that the liquid appears to be approaching the obstacle with angular speed $\simeq \omega$.

Several features of the flow field should be noted:

a) The velocity field ahead of the obstacle is approximately circular, although measurements show that the azimuthal velocity component V is not equal to ωs, where s is the distance radially outwards.

b) For given values of ω and Ω, there exists a critical radius s_0 at which the flow does not climb over the obstacle, but is deflected inwards, passing round the end of the obstacle.

c) At radii greater than s_0 the flow, on passing over the obstacle, is deflected inwards. Downstream of the obstacle the flow field is different in the two cases: for an obstacle of circular cross section, the streak-lines are oscillatory but are quickly damped by viscous dissipation; for the other obstacle, the streak-lines do not attempt to recover their original radial position, but remain almost parallel to the obstacle. There is a region of unsteady circulation downstream of the obstacle near the rim in this case.

As the kinematic Rossby number ω/Ω decreases, s_o increases so that the flow becomes more and more completely blocked by the obstacle. Theoretically, as $\omega/\Omega \to 0$, no flow over the obstacle is possible, and the Taylor column is complete. Experimentally, when $\omega/\Omega = 2 \times 10^{-3}$, there was still some flow over the obstacle near the wall, but it was small. Toomre has computed the streamlines for a completely blocked flow, and there is at least qualitative agreement between theory and experiment.

Quantitative Experiments

1. In the first experiments carried out, the obstacle was a horizontal cylinder of square cross-section, 2.54 cm x 2.54 cm. It was located about 1 mm above the false base to allow a smooth rotation relative to the tank.

Observations were made of single streak-lines using dye injected from the hypodermic needle at a height of 8.5 cm above the base. With this obstacle, streak-lines passing over it were deflected in an approximately circular path, remaining parallel to the obstacle downstream of it. The distance, δ, of this streak-line parallel to the obstacle from the leading edge of the obstacle was measured as a function of ω for fixed values of Ω and s, using the grid on the base and a square grid marked on the obstacle as reference scales. Provided that $\delta > 0$, the radius of curvature of the streak-line, R, is approximately equal to δ. These

measurements were repeated for different values of s and Ω over the observable range.

A typical set of results of these measurements is given in Fig. 3. δ is the radius of curvature of the streak-line, L the breadth of the obstacle, and ω the relative angular velocity of the obstacle. It is obvious that these results do not agree with the simple theory which predicts that $\delta/L \propto \omega$.

However, it is found that graphs of $\ln \omega$ vs. δ/L are, within the experimental errors, straight lines (see Fig. 4). The relationship is therefore expressible as

$$\omega = \omega_0 (\Omega, s)\, e^{K(s)\,\delta/L},$$

where $K(s)$ is the slope of the straight lines, and ω_0 is the value of ω at which $\delta = 0$.

Values of K as a function of s are given below:

K	S, cms
0.667	4.2
0.690	7.2
0.91	10.6
1.35	11.7
2.08	12.7

Radius of tank = 14.6 cms

h = 2.54 cm

D = 10.93 cm

It is seen that for $s \ll R$, K is approximately constant, suggesting that the large variation of K with s near the wall is a viscous boundary layer effect.

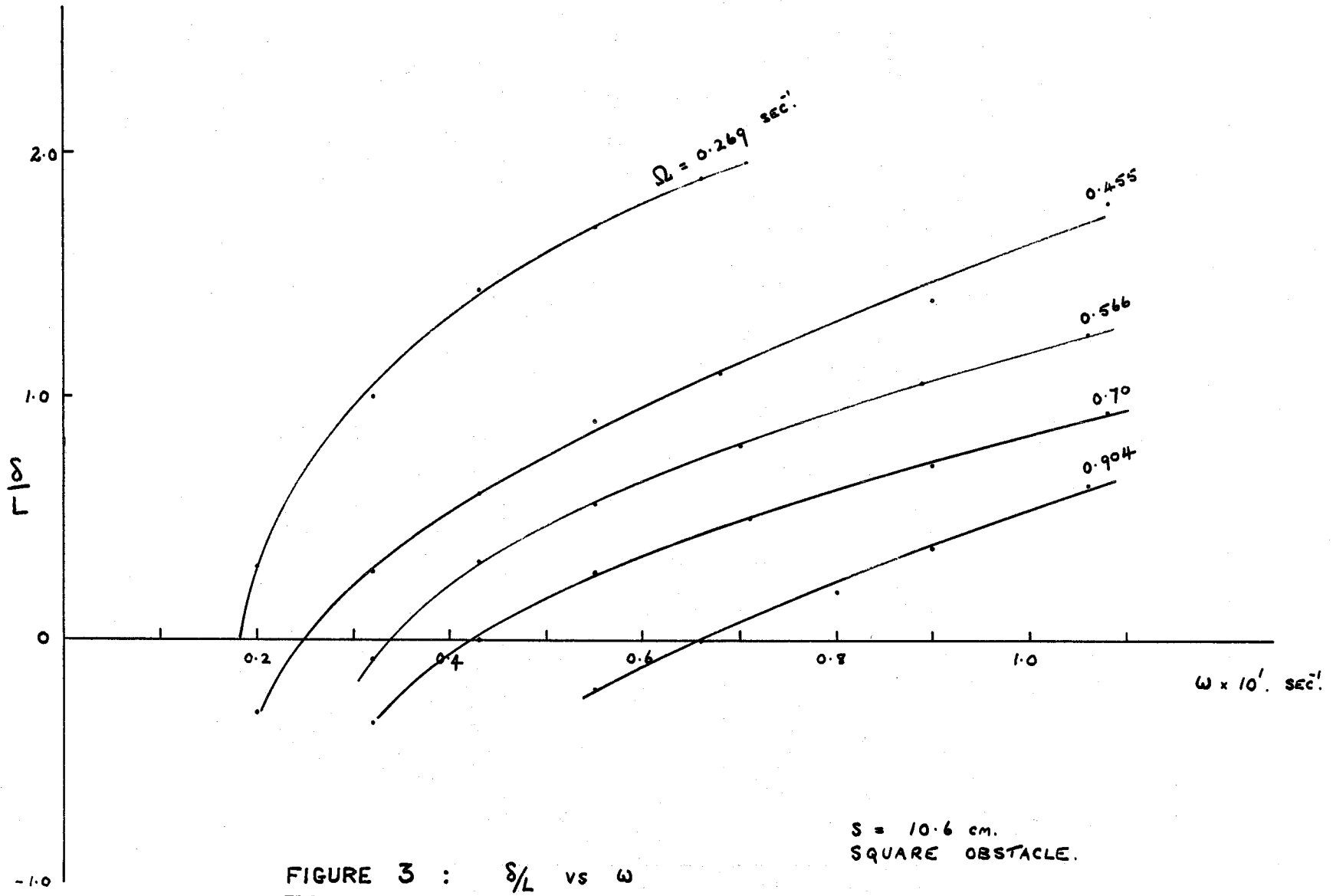

S = 10·6 cm.
SQUARE OBSTACLE.

FIGURE 3 : δ/L vs ω

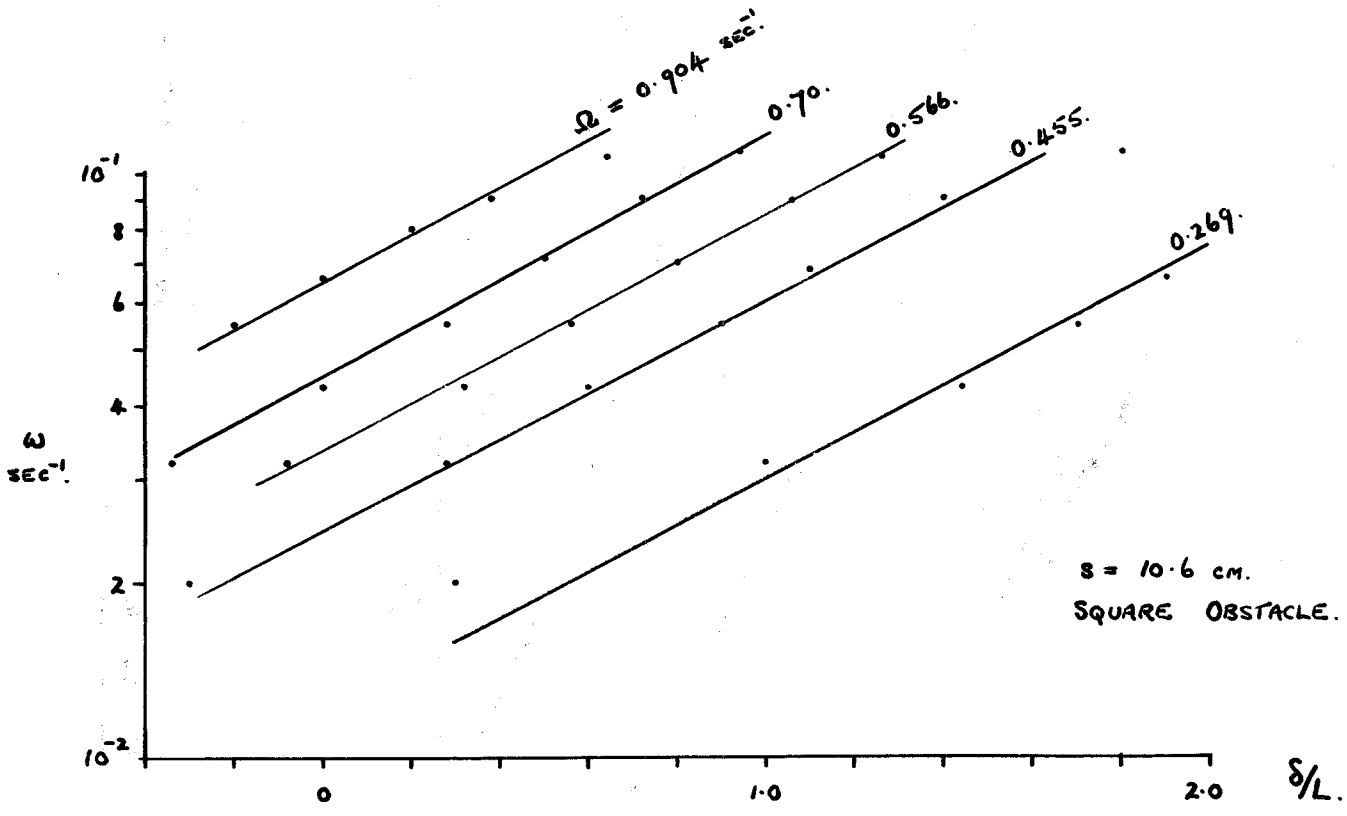

Log$_e$ ω vs δ/L.

FIGURE 4.

2. The distinct lack of agreement between observation and theory in the first experiments suggested the use of a less blunt obstacle. In the next experiments, therefore, the obstacle was a horizontal circular cylinder, diameter 2.54 cm. To minimize any possible boundary layer effects it was mounted equidistant from the lid and the base of the tank.

The radii of curvature of streak-lines passing over the obstacle in this case was not even approximately constant, so that no quantity corresponding to δ could be defined. It was therefore decided to measure only the critical value of the relative speed of the obstacle, ω_0, at which the flow at radius s was just blocked, i.e. at which $\delta = 0$. The experiments were repeated varying Ω and s as widely as possible.

The results are plotted in Fig. 5, which shows the dynamical Rossby number, $s\omega_0/L\Omega$, at which blocking just occurs, as a function of Ω^2. In Fig. 6 a corresponding graph for the obstacle of square cross section is given.

During these experiments, some measurements of the azimuthal velocity of the liquid ahead of the obstacle relative to the tank were made by timing the motion of a dye streak between two of the grid markings on the base. (Ideally in this experiment, this relative velocity upstream of the obstacle would be zero, but the situation is altered by the finite size of the tank and the blocking action itself.) Approximate radial profiles of the induced fluid velocity

FIGURE 5 : Rossby No. $\frac{S\omega_0}{L\Omega}$ vs Ω^2. (CIRCULAR OBSTACLE).

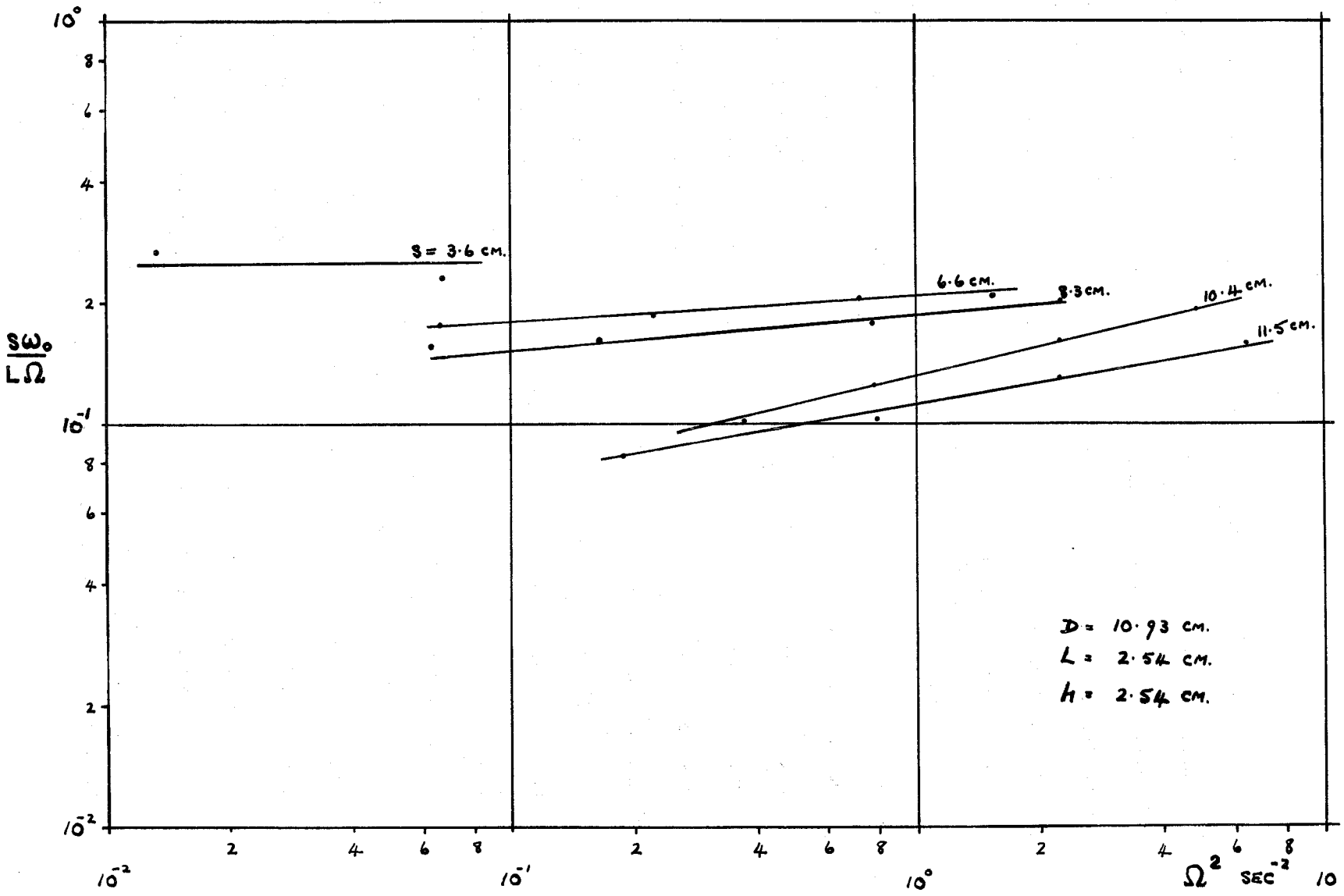

FIGURE 6 : ROSSBY No. $\frac{S\omega_0}{L\Omega}$ VS. Ω^2. (SQUARE OBSTACLE).

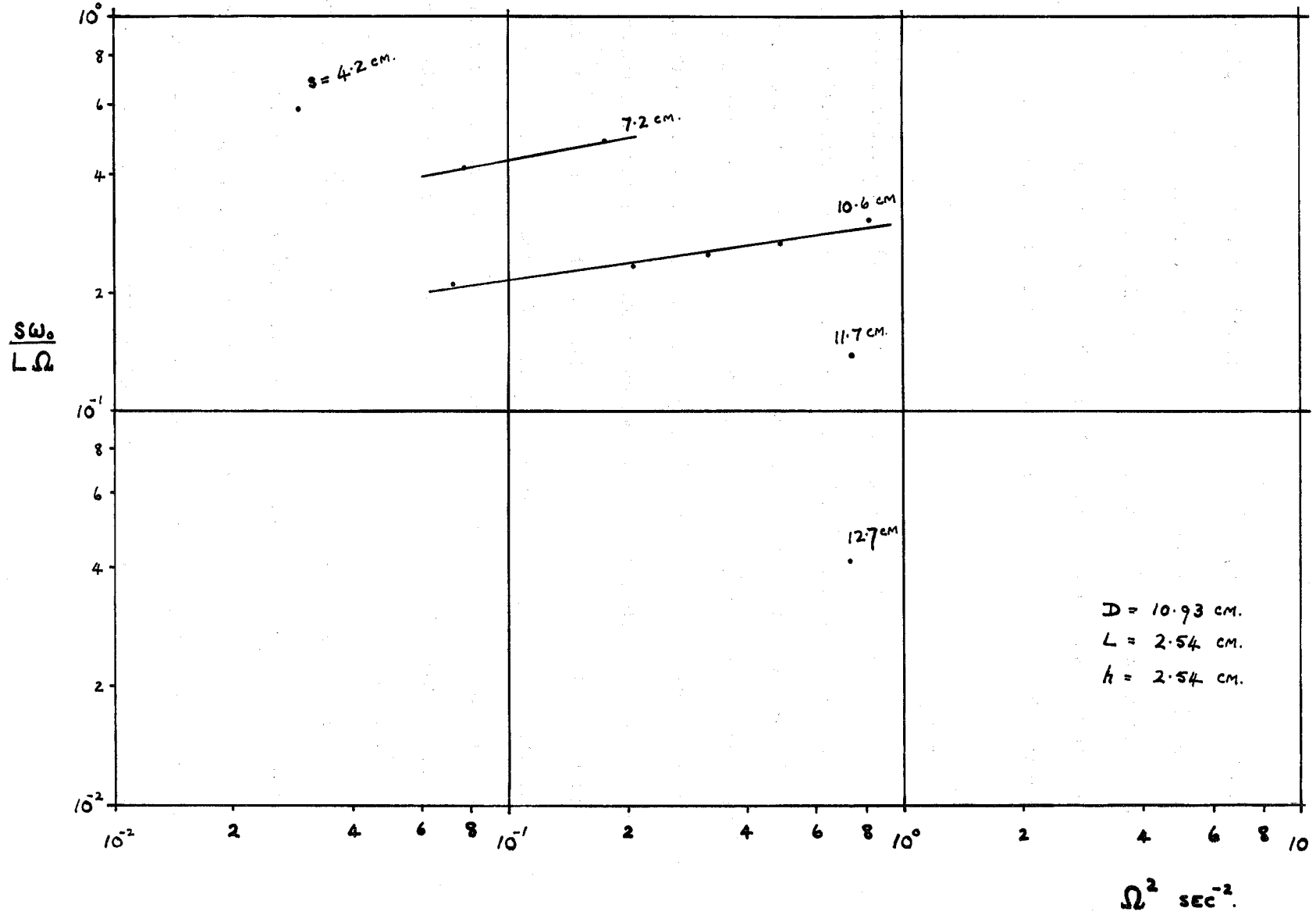

relative to the tank, ω_f , upstream of the obstacle are plotted in Fig. 7 as ω_f/ω vs s/R , R being the radius of the tank. It is seen that ω_f/ω is constant up to the radius s_o at which the flow ceases to be completely blocked, and that it then decreases abruptly, although it appears never to become zero.

Discussion

1. The results (Figs. 5 and 6) show that a well-defined Taylor column (where the flow over an obstacle is completely blocked) can be produced at Rossby numbers below about 2×10^{-1}, when the vertical aspect ratio h/D is 0.232. It is seen that the critical Rossby number - Taylor number relationship is not simple, but it would be hoped that at larger values of Taylor number, a simpler asymptotic behaviour would occur. The fit of data having different values of s on these graphs is better for the circular cross section obstacle than for the other. Variation of the other parameters in the problem (h , D , L , ν) is necessary before definite conclusions can be drawn.

2. Explanation of the relationship $\delta/L \propto \ln \omega$ is at present impossible. Moore has suggested that the model of vertical filaments of fluid shortening as the pass over the obstacle is probably inadequate, especially if the obstacle has a blunt leading edge. But no other model yet proposed has yielded better agreement with observations.

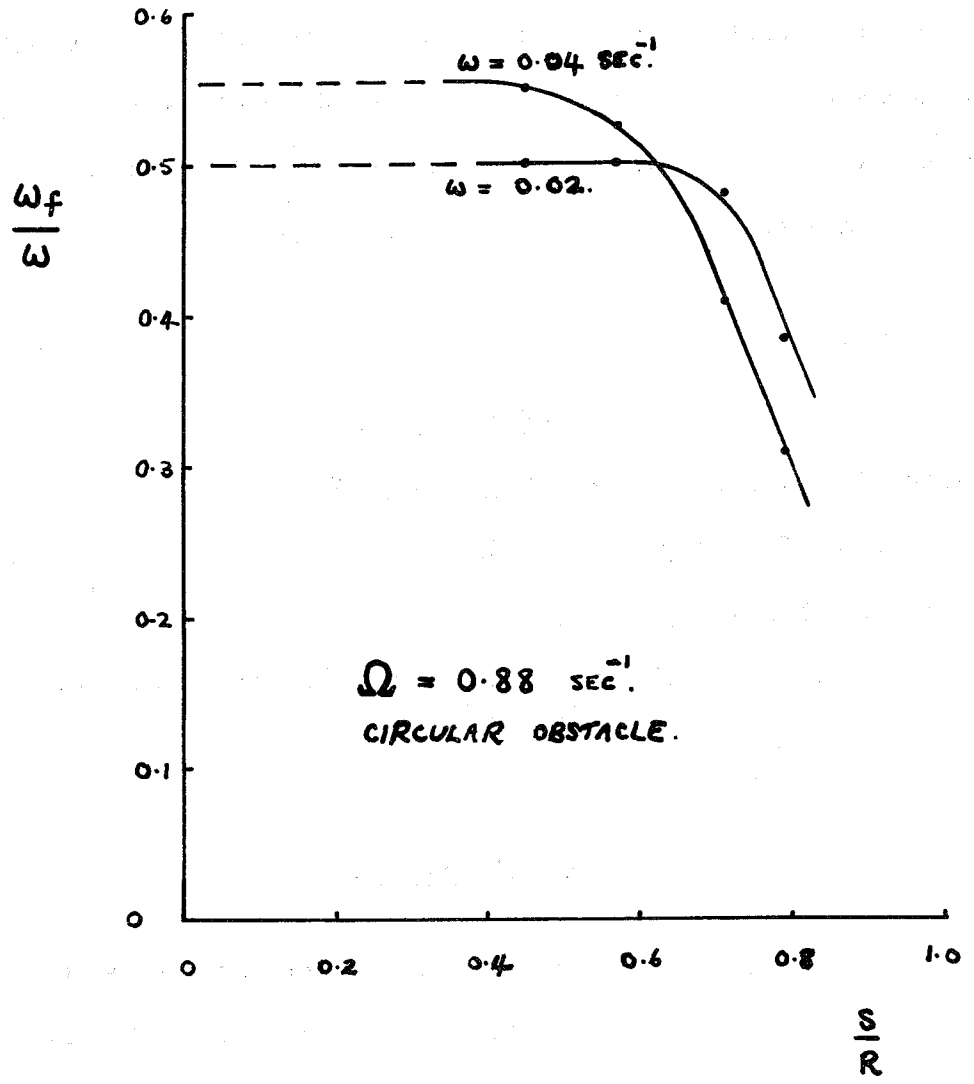

FIGURE 7 : $\frac{\omega f}{\omega}$ vs. $\frac{S}{R}$.

3. No measurements of the variation of flow field with height have been made here, but qualitative observations show that a) in the region of complete blocking, the flow is two-dimensional (away from boundary layer), b) the flow over the obstacle is not accurately two-dimensional, but the variation with height is small enough to be neglected in a preliminary investigation.

References

1. Taylor, G.I. (1923) Proc.Roy.Soc.A. 104, 213.

2. Hide, R. (1961) Nature 190, 895.

3. Bolin, B. (1950) Tellus 2, 184.

4. Hide, R., et al (1961) Technical Summary Report, Contract No. AF. 61(052) - 216.

Acknowledgements

The author wishes to thank Dr. Alan Faller for the use of laboratory facilities, and Prof. Hide, Dr. Moore, and Dr. Toomre for invaluable discussions.

A Weak Source Disk in a Rotating Fluid in a Circular Cylinder of Finite Length

by

J. D. Lin

A Weak Source Disk in a Rotating Fluid in a Circular Cylinder of Finite Length

J. D. Lin

1. Introduction

Theoretical investigations of a small initial disturbance on a slowly moving body started from rest along the axis of a rotating fluid, e.g. Morgan (1951) Stewartson (1952, 1953), show that the disturbance will set up a Taylor column and ultimately a steady two-dimensional flow field consistent with the experimental result of Taylor (1922). All investigations are so far based on the condition of an infinite extent of fluid in the direction of rotating axis. For most physical problems, this boundary condition is generally replaced either by a free surface or by a solid wall. It is of interest to ask whether a Taylor column could be set up or what kind of flow field would be led to by the disturbance in the presence of a solid wall normal to the axis of a rotating fluid. The present study is an initial attempt to investigate this problem based on a simple model, a weak source disk located at one end of a circular cylinder of finite length containing a rotating fluid initially under solid body rotation.

2. Analysis

Consider a circular cylinder containing homogeneous, incompressible and inviscid fluid rotating initially as a solid body about its own axis with an angular velocity Ω. Relative to the cylindrical coordinates (r, θ, z) fixed on the cylinder the linearized equations of axisymmetric motion induced by a weak source flow initially started from rest on the disk $r \leq 1$ at $z = 0$ are

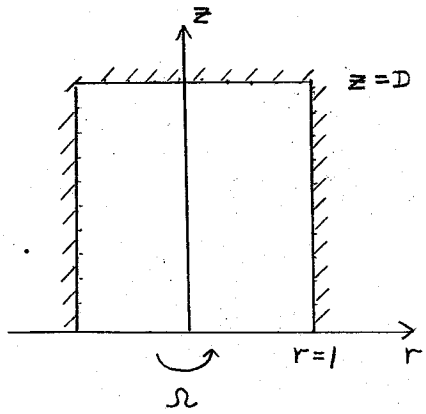

$$\frac{\partial u_r}{\partial t} - 2\Omega u_\theta = -\frac{\partial p}{\partial r}$$

$$\frac{\partial u_\theta}{\partial t} + 2\Omega u_r = 0 \qquad (1)$$

$$\frac{\partial u_z}{\partial t} = -\frac{\partial p}{\partial z}$$

and

$$\frac{1}{r}\frac{\partial r u_r}{\partial r} + \frac{\partial u_z}{\partial z} = 0$$

where $p = \frac{p}{\rho} - \frac{1}{2} r^2 \Omega^2$. Defining a stream function, $\psi(r, z, t)$, as

$$u_r = \frac{1}{r}\frac{\partial \psi}{\partial z}, \quad u_z = -\frac{1}{r}\frac{\partial \psi}{\partial r} \qquad (2)$$

then (1) may be reduced to

$$\frac{\partial^2}{\partial t^2} D^2 \psi + 4\Omega^2 \frac{\partial^2 \psi}{\partial z^2} = 0 \quad , \quad D^2 = r\frac{\partial}{\partial r}\frac{1}{r}\frac{\partial}{\partial r} + \frac{\partial^2}{\partial z^2} \tag{3}$$

After the solution of ψ is obtained, the velocity component, u_θ , may be computed from the second equation of (1).

The initial conditions are $u_r = u_\theta = u_z = 0$ when $t = 0$ or in terms of the stream function

$$\psi(r, z, 0) = \frac{\partial}{\partial t}\psi(r, z, 0) = 0 \tag{4}$$

everywhere in the fluid. The boundary conditions for $t > 0$ are prescribed by

$$u_z(r, D, t) = 0, \quad \text{for} \quad 0 \le r \le 1 ,$$

$$u_r(1, z, t) = 0, \quad \text{for} \quad 0 \le z \le D , \tag{5}$$

and

$$u_z(r, 0, t) = V(1 - e^{-2\Omega\beta t}) J_0(\alpha_i r), \text{ for } \quad 0 \le r \le 1 ,$$

where α_i is the root of $J_1(\alpha_i) = 0$.

The first two boundary conditions represent the condition of zero normal velocity at the end of the cylinder, $z = D$, and on the inner surface, $r = 1$, while the last is the distribution of the source flow on the disk, $r \le 1$, at $z = 0$. V and β are constants. An impulsive start of the disturbance may be represented by letting β tend to infinity.

The choice of $J_0(\alpha_i r)$ is to insure that the total mass flux across the disk is zero.

Taking the Laplace transform, defined by

$\tilde{f}(p) = \int_0^\infty e^{-pt} f(t)\,dt$, of (3) and using (4), one has

$$\frac{\partial^2 \tilde{\psi}}{\partial r^2} - \frac{1}{r}\frac{\partial \tilde{\psi}}{\partial r} + \left(1 + \frac{4\Omega^2}{p^2}\right)\frac{\partial^2 \tilde{\psi}}{\partial z^2} = 0 \qquad (6)$$

while the boundary conditions of (5) become for $R(p) > 0$

$$\tilde{u}_z(r, D, p) = 0 \quad \text{for} \quad 0 \le r \le 1$$

$$\tilde{u}_r(1, z, p) = 0 \quad \text{for} \quad 0 \le z \le D \qquad (7)$$

and

$$\tilde{u}_z(r, 0, p) = \frac{2\Omega\beta}{p(p+2\Omega\beta)} V J_0(\alpha_i r), \text{ for } \quad 0 < r \le 1.$$

The appropriate solution satisfying (6) and (7) may be found as

$$\tilde{\psi}(r, z, p) = \frac{V r J_1(\alpha_i r)}{\alpha_i} \frac{2\Omega\beta}{p(p+2\Omega\beta)} \frac{\sinh \frac{\alpha_i p(z-D)}{\sqrt{p^2+4\Omega^2}}}{\sinh \frac{\alpha_i p D}{\sqrt{p^2+4\Omega^2}}} \qquad (8)$$

then, by the inversion formula, one has

$$\psi(r, z, t) = \frac{V r J_1(\alpha_i r)}{\alpha_i} \frac{1}{2\pi i} \int_{c-i\alpha}^{c+i\alpha} \frac{2\Omega\beta e^{pt}}{p(p+2\Omega\beta)} \frac{\sinh \frac{\alpha_i p(z-D)}{\sqrt{p^2+4\Omega^2}}}{\sinh \frac{\alpha_i p D}{\sqrt{p^2+4\Omega^2}}} \qquad (9)$$

for $t > 0$.

An examination of the Bromwich integral will indicate that there are simple poles at $p=0$, $-2\beta\Omega$ and $\pm 2\Omega\lambda_n$ for $n = 1, 2, 3, \ldots$, where $\lambda_n = \left(1 + \frac{\alpha_i^2 D^2}{n^2\pi^2}\right)^{-\frac{1}{2}}$. Since $0 < \lambda_n \leq 2\Omega$, the infinite number of simple poles are located between $p = \pm i2\Omega$ on the imaginary axis. Then, the contributions to the integral are all from the sum of the residues from these poles. Hence, one has

$$\psi(r,z,t) = -\frac{Vr J_1(\alpha_i r)}{\alpha_i}\left[1-\frac{z}{D} - \frac{\sinh\frac{\beta\alpha_i(D-z)}{\sqrt{p^2+4\Omega^2}}}{\sinh\frac{\beta\alpha_i D}{\sqrt{p^2+4\Omega^2}}}e^{-2\Omega\beta t}\right.$$

$$\left. - \frac{2}{\pi}\sum_{n=1}^{\infty}\frac{\cos(2\Omega\lambda_n t + \tan^{-1}\frac{\lambda_n}{\beta})\sin\frac{n\pi z}{D}}{n\left(1+\frac{n^2\pi^2}{\alpha_i^2 D^2}\right)\left(1+\frac{\lambda_n^2}{\beta^2}\right)^{1/2}}\right] \qquad (10)$$

3. Discussion of the Results

The solution of (10) may be reduced to a simpler form for the case of an impulsive start of the source flow by $\beta \to \infty$. The velocity components are then given by

$$u_z(r,z,t) = V J_0(\alpha_i r)\left[1-\frac{z}{D} - \frac{2}{\pi}\sum_{n=1}^{\infty}\frac{\cos 2\Omega\lambda_n t \sin\frac{n\pi z}{D}}{n\left(1+\frac{n^2\pi^2}{\alpha_i^2 D^2}\right)}\right.$$

$$u_r(r,z,t) = \frac{V J_1(\alpha_i r)}{\alpha_i D}\left[1+2\sum_{n=1}^{\infty}\frac{\cos 2\Omega\lambda_n t\cos\frac{n\pi z}{D}}{1+\frac{n^2\pi^2}{\alpha_i^2 D^2}}\right] \qquad (11)$$

and

$$u_\theta(r,z,t) = -\frac{2V J_1(\alpha_i r)}{\alpha_i D}\left[\Omega t + \sum_{n=1}^{\infty} \frac{\sin 2\Omega\lambda_n t \cos\frac{n\pi z}{D}}{n\left(1+\frac{n^2\pi^2}{\alpha_i^2 D^2}\right)}\right]$$

From these velocity components, it is seen that a steady two-dimensional flow field cannot ultimately be set up in this model and the standing waves are also excited in the cylinder. The circumferential velocity component, u_θ, decreases linearly with time and tends to reduce the momentum of the fluid in the cylinder. This phenomenon is due to tha fact that, for this particular model, the fluid with a smaller angular momentum is induced into the central region while the same fluid of higher momentum is drawn from the outer region. However, $u_\theta = O(u_r \Omega t)$ and the linear analysis requires that $u_\theta << r\Omega$, the distance of this radial convection, $u_r t$, is then very small compared with the radial dimension of the cylinder. The solution is valid for all $t > 0$ within the validity of the linearized equations of motion used in this treatment.

References

Taylor, G.I. (1922) Proc.Roy.Soc. A 100, 144.

Morgan, G.W. (1951) Proc.Roy.Soc. A 206, 109.

Stewartson, K. (1952) Proc.Camb.Phil.Soc. A 48, 168.

Stewartson, K. (1953) Q.J.M.A.M. 6, 45.

Baroclinic Instability

by

Lorenz Magaard

Baroclinic Instability

Lorenz Magaard

I) The Perturbation Equation

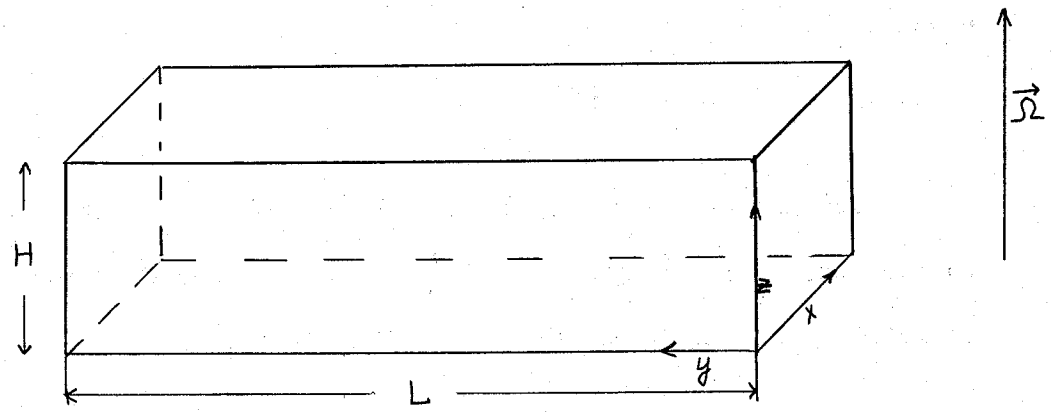

We consider a parallel current $\bar{u}(y,z)$ in x-direction in a stratified[1] fluid (density $\bar{\rho}(y,z)$) which rotates with the constant angular velocity parallel to the z-axis. We assume fixed walls at $y = 0$ and $y = L$ and a finite depth H . We assume further $\frac{\partial}{\partial x} = 0$ for the mean field. Using the Boussinesq approximation we have for the hydrostatic balance

$$\frac{\partial \bar{p}}{\partial z} = -g\bar{\rho} \tag{1}$$

where $\bar{p}$ is the mean pressure and g the acceleration of gravity and for the geostrophic balance

[1] incompressible

$$f\bar{u} = -\frac{1}{\rho_0}\frac{\partial \bar{p}}{\partial y} \tag{2}$$

where $f = 2|\vec{\Omega}|$ and $\rho_0 = \frac{1}{LH}\int_0^H\int_0^L \bar{\rho}(y,z)\,dy\,dz$.

Eliminating $\bar{p}$ from (1) and (2) we get the thermal wind equation

$$f\frac{\partial \bar{u}}{\partial z} = \frac{g}{\rho_0}\frac{\partial \bar{\rho}}{\partial y}. \tag{3}$$

For the perturbation terms u', v', w' (velocity components), p' (pressure) and ρ' (density) the equations of motion, continuity and incompressibility are

$$\frac{\partial u'}{\partial t} + \bar{u}\frac{\partial u'}{\partial x} + v'\frac{\partial \bar{u}}{\partial y} + w'\frac{\partial \bar{u}}{\partial z} - fv' = -\frac{1}{\rho_0}\frac{\partial p'}{\partial x} \tag{4}$$

$$\frac{\partial v'}{\partial t} + \bar{u}\frac{\partial v'}{\partial x} + fu' = -\frac{1}{\rho_0}\frac{\partial p'}{\partial y} \tag{5}$$

$$0 = -\frac{1}{\rho_0}\frac{\partial p'}{\partial z} - g\frac{\rho'}{\rho_0} \tag{6}$$

$$\frac{\partial u'}{\partial x} + \frac{\partial v'}{\partial y} + \frac{\partial w'}{\partial z} = 0 \tag{7}$$

$$\frac{\partial \rho'}{\partial t} + v'\frac{\partial \bar{\rho}}{\partial y} + w'\frac{\partial \bar{\rho}}{\partial z} + \bar{u}\frac{\partial \rho'}{\partial x} = 0 \tag{8}$$

We have used the Boussinesq approximation in (4) and (5) and the quasi-hydrostatic approximation in (6).

We eliminate ρ' from (6) and $\frac{\partial \bar{\rho}}{\partial y}$ from (3) and scale

$$x = L x_1 \; ; \quad y = L y_1 \; ; \quad z = H z_1 \; ; \quad t = \frac{L}{u^*} t_1$$

$$\bar{u} = u^* \bar{u}_1 \; ; \quad u' = u^* u_1' \; ; \quad v' = u^* v_1' \; ; \quad w' = R_0 u^* \frac{H}{L} w_1'$$

$$p' = \rho_0 L u^* f p_1'$$

to get

$$\left(-v_1' + \frac{\partial p_1'}{\partial x_1}\right) R_0^0 + \left(\frac{\partial u_1'}{\partial t_1} + v_1 \frac{\partial \bar{u}_1}{\partial y_1} + \bar{u}_1 \frac{\partial u_1}{\partial x_1}\right) R_0' + w_1' \frac{\partial u_1'}{\partial z_1} R_0^2 = 0 \qquad (9)$$

$$\left(u_1' + \frac{\partial p_1'}{\partial y_1}\right) R_0^0 + \left(\frac{\partial v_1'}{\partial t_1} + \bar{u}_1 \frac{\partial v_1}{\partial x_1}\right) R_0' \quad = 0 \qquad (10)$$

$$\left(\frac{\partial u_1'}{\partial x_1} + \frac{\partial v_1}{\partial y_1}\right) R_0^0 + \frac{\partial w_1'}{\partial z_1} R_0' \quad = 0 \qquad (11)$$

$$\left(v_1' \frac{\partial \bar{u}_1}{\partial z_1} - \frac{\partial^2 p_1'}{\partial z_1 \partial t_1} - \bar{u}_1 \frac{\partial^2 p_1'}{\partial z_1 \partial x_1} - \frac{1}{F} w_1'\right) R_0^0 \; = 0 \qquad (12)$$

From these equations we have the Rossby number $R_0 = \frac{u^*}{fL}$ and the Froude number $F = \frac{f^2 L^2}{g s H^2}$ where $S = -\frac{1}{\rho_0} \frac{\partial \bar{\rho}}{\partial z}$ is the static stability which we assume to be positive.

We assume

$$u_1'(x_1, y_1, z_1, t_1) = u_1(y_1, z_1)\, e^{i\alpha(x_1 - \beta t_1)}$$

$$v_1'(x_1, y_1, z_1, t_1) = v_1(y_1, z_1)\, e^{i\alpha(x_1 - \beta t_1)}$$

$$w_1'(x_1, y_1, z_1, t_1) = w_1(y_1, z_1)\, e^{i\alpha(x_1 - \beta t_1)}$$

$$p_1'(x_1, y_1, z_1, t_1) = p_1(y_1, z_1)\, e^{i\alpha(x_1 - \beta t_1)}$$

and eliminate u_1, v_1 and w_1 from (9), (10) and (12) to get from (11)

$$\left\{(\bar{u}_1 - \beta)\left[\frac{\partial^2 p_1}{\partial y_1^2} + \frac{\partial}{\partial z_1}\left(F\frac{\partial}{\partial z_1}p_1\right) - \alpha^2 p_1\right] - p_1\left[\frac{\partial^2 \bar{u}_1}{\partial y_1^2} + \frac{\partial}{\partial z_1}\left(F\frac{\partial \bar{u}_1}{\partial z_1}\right)\right]\right\} \cdot R_0' + \quad (13)$$

$$+ \left\{\dots\right\} R_0^2 + \dots = 0$$

We divide by R_0, neglect terms of order R_0^n with $n \geq 1$ (quasi-geostrophic approximation) to get the coefficient of R_0' in (13). Rescaling this we get

$$(\bar{u} - c)\left[\frac{\partial^2 p}{\partial y^2} + \frac{\partial}{\partial z}\left(\Gamma\frac{\partial p}{\partial z}\right) - k^2 p\right] - p\, D = 0 \quad (14)$$

where $D(y,z) = \frac{\partial^2 \bar{u}}{\partial y^2} + \frac{\partial}{\partial z}\left(\Gamma\frac{\partial \bar{u}}{\partial z}\right)$; $\Gamma = \frac{f^2}{gs}$; $c = u^*\beta$; $k = \frac{\alpha}{L}$

so that $p'(x, y, z, t) = p(y, z)\, e^{ik(x - ct)}$.

The boundary conditions are

$$v = 0 \quad \text{at} \quad y = 0 \quad \text{and} \quad y = L \quad (15)$$

and

$$w = 0 \qquad z = 0 \qquad z = H. \tag{16}$$

Using the quasi-geostrophic approximation we get

$$p = 0 \qquad y = 0 \qquad y = L \tag{17}$$

and

$$(\bar{u} - c)\frac{\partial p}{\partial z} - \frac{\partial \bar{u}}{\partial z} p = 0 \qquad z = 0 \qquad z = H. \tag{18}$$

Calling $p(y,z) = \psi(y,z)$ we have the perturbation equation

$$(\bar{u} - c)\left[\frac{\partial^2 \psi}{\partial y^2} + \frac{\partial}{\partial z}\left(r\frac{\partial \psi}{\partial z}\right) - k^2\psi\right] - \psi D = 0 \tag{19}$$

and the boundary conditions

$$\psi = 0 \qquad y = 0 \qquad y = L \tag{20}$$

and

$$(\bar{u} - c)\frac{\partial \psi}{\partial z} - \frac{\partial \bar{u}}{\partial z}\psi = 0 \qquad z = 0 \qquad z = H \tag{21}$$

If we introduce

$$\phi = \frac{\psi}{\bar{u} - c} \tag{22}$$

as a new unknown function we get an equivalent formulation of the problem (19) - (21):

$$\frac{\partial}{\partial y}\left[(\bar{u}-c)^2\frac{\partial \phi}{\partial y}\right]+\frac{\partial}{\partial z}\left[(\bar{u}-c)^2\Gamma\frac{\partial \phi}{\partial z}\right]-k^2(\bar{u}-c)^2\phi=0 \qquad (23)$$

$$\phi=0 \quad \text{at} \quad y=0 \quad \text{and} \quad y=L \qquad (24)$$

$$\frac{\partial \phi}{\partial z} \quad \text{at} \quad z=0 \quad \text{and} \quad z=H. \qquad (25)$$

Equations (19) - (25) have also been derived by Stern $(1963)_2$ from the law of conservation of potential vorticity.

II) Discussion of the Problem and some Stability Theorems

Equation (19) is a self-adjoint elliptic equation because of $\Gamma > 0$. It is in general a singular differential equation. We have not yet been able to prove the existence of solutions ψ and eigenvalues c of the boundary problem (19) - (21) in the general case. But on the one hand we are able to do that for special cases and on the other hand we can derive useful theorems without having proved the existence.

At first, some definitions: We call $\bar{u}(y,z)$ unstable with respect to the wavenumber k if the corresponding equations (19) - (21) have solutions $\psi^{(n)}(y,z,k)$ with eigenvalues $c^{(n)}(k)=c_r^{(n)}(k)+i\,c_i^{(n)}(k)$ with $c_i^{(n)}(k)>0$ for at least one n. If $\bar{u}(y,z)$ is unstable with respect to any k, we call $\bar{u}(y,z)$ unstable.

Theorem 1 (semicircle theorem): If $\bar{u}(y,z)$ is unstable, then the inequality

$$\left[c_r - \tfrac{1}{2}(a+b)\right]^2 + c_i^2 \leq \left[\tfrac{1}{2}(b-a)\right]^2$$

holds, where $a = \min \bar{u}$ and $b = \max \bar{u}$. Thus the complex wave velocity $c^{(n)}$ for any unstable mode must lie inside the semicircle in the upper half-plane which has the range of $\bar{u}$ for diameter. Especially the inequality

$$a \leq c_r \leq b$$

holds for c_r.

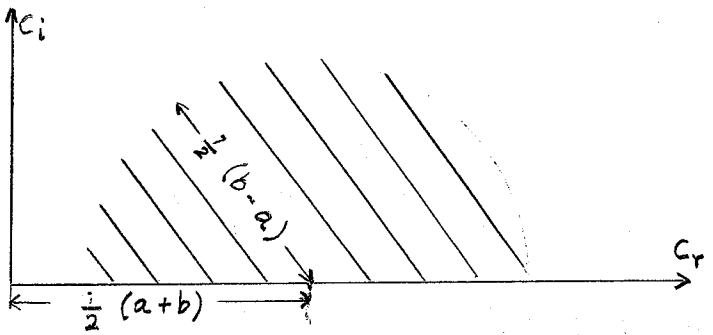

Proof: We assume that $\bar{u}$ is unstable, i.e. there exist solutions $\phi^{(n)}$ of (23) - (25) with $c_i^{(n)} > 0$ for at least one n (the index n is left out for the rest of the proof). We multiply (23) by the complex conjugate ϕ^* and integrate to get

$$\int_0^H \int_0^L \left\{ \phi^* \frac{\partial}{\partial y}\left[(\bar{u}-c)^2 \frac{\partial \phi}{\partial y}\right] + \phi^* \frac{\partial}{\partial z}\left[(\bar{u}-c)^2 \frac{\partial \phi}{\partial z}\right] - k^2 (\bar{u}-c)^2 \phi^* \phi \right\} dy\, dz = 0 \qquad (26)$$

Using (24) and (25) we get

$$\int_0^H \int_0^L (\bar{u}-c)^2 \chi \, dy\, dz \tag{27}$$

where χ is the positive definite form

$$\chi = \frac{\partial \phi^*}{\partial y}\frac{\partial \phi}{\partial y} + \Gamma \frac{\partial \phi^*}{\partial z}\frac{\partial \phi}{\partial z} + k^2 \phi^* \phi. \tag{28}$$

We split up (27) in into its real and imaginary part

$$\int_0^H \int_0^L \left[(\bar{u}-c_r)^2 - c_i^2\right] \chi \, dy\, dz = 0 \tag{29}$$

and

$$c_i \int_0^H \int_0^L (\bar{u}-c_r)\chi \, dy\, dz = 0. \tag{30}$$

Because of $c_i \neq 0$ we have

$$c_r \int_0^H \int_0^L \chi \, dy\, dz = \int_0^H \int_0^L \bar{u}\chi \, dy\, dz \tag{31}$$

and from (29) and (31) we get

$$(c_r^2 + c_i^2) \int_0^H \int_0^L \chi \, dy\, dz = \int_0^H \int_0^L \bar{u}^2 \chi \, dy\, dz. \tag{32}$$

Now

$$0 \geq \int_0^H \int_0^L (\bar{u}-a)(\bar{u}-b)\chi \, dy\,dz = \int_0^H \int_0^L \bar{u}^2 \chi \, dy\,dz - \tag{33}$$

$$-(a+b)\int_0^H \int_0^L \bar{u}\chi \, dy\,dz + ab \int_0^H \int_0^L \chi \, dy\,dz =$$

$$= \left\{(c_r^2+c_i^2) - (a+b)c_r + ab\right\} \int_0^H \int_0^L \chi \, dy\,dz .$$

Thus we have

$$c_r^2 + c_i^2 - (a+b)\, c_r + ab \leq 0 \tag{34}$$

which is equivalent to

$$\left[c_r - \tfrac{1}{2}(a+b)\right]^2 + c_i^2 \leq \left[\tfrac{1}{2}(b-a)\right]^2 \tag{35}$$

which had to be proved.

This semicircle theorem was first given by Howard (1961) for the case $\bar{u} = \bar{u}(z)$. Eckart (1963) has shown that it is also valid for compressible media.

Theorem 2: If $\frac{\partial \bar{u}}{\partial z} = 0$ at $z = 0$ and $z = H$ and if $D \not\equiv 0$ a necessary condition for $\bar{u}(y,z)$ to be unstable is that $D(y,z)$ changes its sign in the interior of the fluid.

Proof: We multiply (19) by the complex conjugate ψ^* and integrate using (20) and (21) to get

$$\int_0^H\int_0^L \left(\frac{\partial\psi}{\partial y}\frac{\partial\psi^*}{\partial y}+\Gamma\frac{\partial\psi}{\partial z}\frac{\partial\psi^*}{\partial z}+k^2\psi\psi^*\right)dy\,dz + \tag{36}$$

$$+\int_0^H\int_0^L \frac{\psi\psi^* D}{\bar{u}-c_r-ic_i}\,dy\,dz = 0$$

The imaginary part of (36) is

$$c_i\int_0^H\int_0^L \frac{\psi\psi^* D}{(\bar{u}-c_r)^2+c_i^2}\,dy\,dz = 0. \tag{37}$$

Because of $c_i > 0$ it follows

$$\int_0^H\int_0^L \frac{\psi\psi^* D}{(\bar{u}-c_r)^2+c_i^2}\,dy\,dz = 0 \tag{38}$$

which can only be satisfied if D changes its sign in the interior of the fluid.

Theorem 2 was given by Stern $(1963)_2$ and is an extension of Rayleigh's theorem (see Lin (1955)).

Theorem 3: If $\frac{\partial\bar{u}}{\partial z}=0$ at $z=H$ and $\frac{\partial\bar{u}}{\partial z}$ has no zeroes at $z=0$ a sufficient condition for $\bar{u}$ to be stable is $D=0$.

Proof: We multiply (19) again by ψ^* and integrate using (20), (21) and $D\equiv 0$ to get

$$c^* \int_0^L \left\{ \Gamma(0) \frac{\partial \psi^*}{\partial z} \frac{\partial \psi}{\partial z} \frac{1}{\frac{\partial \bar{u}}{\partial z}} \right\}\Bigg|_{z=0} dy = \int_0^L \left\{ \Gamma(0) \frac{\partial \psi^*}{\partial z} \frac{\partial \psi}{\partial z} \frac{\bar{u}}{\frac{\partial \bar{u}}{\partial z}} \right\}\Bigg|_{z=0} dy + \tag{39}$$

$$+ \int_0^H \int_0^L \left[\frac{\partial \psi}{\partial y} \frac{\partial \psi^*}{\partial y} + \Gamma \frac{\partial \psi}{\partial z} \frac{\partial \psi^*}{\partial z} + k^2 \psi \psi^* \right] dy\, dz .$$

From (39) we see that c^* is real, i.e. c is real so that $\bar{u}$ is stable.

Theorem 3 was given by Stern $(1963)_1$.

In case of $D \equiv 0$ the problem (19) - (21) becomes separable if $\frac{\partial \Gamma}{\partial y} = 0$, $\bar{u}\Big|_{z=0} = \bar{u}_0 = \text{const.}$ and $\frac{\partial \bar{u}}{\partial z}\Big|_{z=0} = \left(\frac{\partial \bar{u}}{\partial z}\right)_0 = \text{const.}$ If also $\Gamma = \Gamma_0 = $ const. we can find the explicit solution and eigenvalues of the problem to be

$$\psi^{(n)}(y, z, k) = A^{(n)} \cosh \alpha_n (z - H) \sin \frac{n\pi}{L} y \tag{40}$$

where $A^{(n)}$ is an arbitrary constant and $\alpha_n^2 = \frac{1}{\Gamma_0}\left(k^2 + \frac{n^2\pi^2}{L^2}\right)$ and

$$c^{(n)}(k) = c_r^{(n)}(k) = \bar{u}_0 + \left(\frac{\partial \bar{u}}{\partial z}\right)_0 \frac{\coth \alpha_n H}{\alpha_n} \tag{41}$$

III) Marginal Instability

If one knows that a field $\bar{u}(y, z)$ is stable one would like to know some more on the "degree of it's stability". Therefore one tries to find out if there is a small variation of

$\bar{u}(y,z)$ so that the varied field is unstable. If there is such a variation of $\bar{u}(y,z)$ we call $\bar{u}(y,z)$ marginally unstable.

We define that as follows: A stable field $\hat{\bar{u}}(y,z)$ is said to be marginally unstable[1] if there is a function $\bar{u}(y,z,\mu)$ and a real number μ_1 with the following properties:

1) $\bar{u}(y,z,\mu)$ is at least twice differentiable with respect to μ at $\mu = 0$

2) $\lim_{\mu\to 0} \bar{u}(y,z,\mu) = \hat{\bar{u}}(y,z)$

3) For $\bar{u}(y,z,\mu)$ there are solutions of (19) - (21) $\psi^{(n)}(y,z,k^2,\mu)$ and eigenvalues $c^{(n)}(k,\mu)$

4) $\lim_{\mu\to 0}(\psi^{(n)}\psi^{(n)*}) = \hat{\psi}^{(n)}\hat{\psi}^{(n)*} = \hat{\psi}^{(n)2}$

and

$$\lim_{\mu\to 0} c^{(n)}(k,\mu) = \hat{c}_r^{(n)}(k)$$

where $\hat{\psi}^{(n)}$ and $\hat{c}^{(n)}$ are the solutions and eigenvalues of (19) - (21) for the stable field $\hat{\bar{u}}(y,z)$.

5) $c_i^{(n)}(k,\mu) > 0$ for $0 < \mu \leq \mu_1$ for at least one n .

A field, which is marginally unstable with respect to any k, will be called marginally unstable.

A stable field $\bar{u}(y,z)$ which is not marginally unstable will be called very stable.

---

[1] with respect to the wave number k .

IV) The Stability of Fields $\bar{u}(y,z)$ for which $D \equiv 0$

We assume $\frac{\partial \hat{\bar{u}}}{\partial z} = 0$ at $z = H$ and $\frac{\partial \hat{\bar{u}}}{\partial z} > 0$ at $z = 0$. According to theorem 3 we know that these $\hat{\bar{u}}(y,z)$ are stable because of $D \equiv 0$. We shall now try to find out whether these fields are marginally unstable or not. For that purpose we assume to have a $\bar{u}(y,z,\mu)$ satisfying the condition III) 1) - 4). (In following the index n will be left out.) We multiply (19) by ψ^* and integrate using (20) and (21) and take the imaginary part of the result to get

$$c_i \int_0^L \frac{\Gamma(0)\psi\psi^* \frac{\partial \bar{u}}{\partial z}\Big|_{z=0}}{(\bar{u}-c_r)^2 + c_i^2} dy = -\int_0^H \int_0^L \frac{\psi\psi^* D c_i \, dy\, dz}{(\bar{u}-c_r)^2 + c_i^2} . \tag{42}$$

We split up the integral on the right-hand side of (42) into two parts:

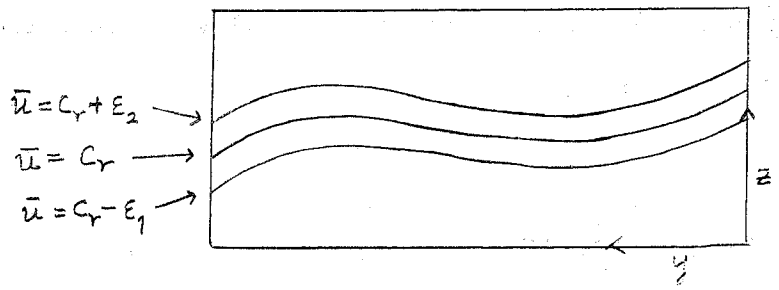

The first part is taken over the region between the curves $\bar{u} = c_r + \varepsilon_2$ and $\bar{u} = c_r - \varepsilon_1$, which we shall call C. The other part is taken over the rest R. The value of ε is chosen so that in the region C the coordinate transformation

$$\begin{aligned} r &= \bar{u}(y, z, \mu) - c_r \\ s &= \int \sqrt{1 + \left(\frac{dz}{dy}\right)^2}\, dy \end{aligned} \tag{43}$$

is unique where $z = z(y)$ is the curve $\bar{u} = c_r$. Thus we get for the right-hand side of (42)

$$-\int_{\bar{u}=c_r} \int_{c_r-\varepsilon_1}^{c_r+\varepsilon_2} \frac{\psi\psi^* D}{|\nabla \bar{u}|} \frac{c_i}{(\bar{u}-c_r)^2 + c_i^2}\, d\bar{u}\, ds - \tag{44}$$

$$-\iint_R \frac{\psi\psi^* D c_i\, dy\, dz}{(\bar{u}-c_r)^2 + c_i^2} .$$

We expand (44) with respect to μ and write down the terms up to the first order in μ:

$$\left\{ -\pi \int_{\hat{u}=\hat{c}} \frac{\hat{\psi}^2}{|\nabla \hat{u}|} \frac{\partial}{\partial \mu} D \Big|_{\mu=0} ds \right\} \mu + \ldots \quad . \tag{45}$$

Thus (44) is positive for $0 < \mu < \mu_1$, if (45) is positive, where μ_1 is a convenient $\mu \neq 0$. Thus we get from (42) the following

Theorem 4: A necessary and sufficient condition for a field $\hat{\bar{u}}(y,z)$, for which $D \equiv 0$ and $\frac{\partial \hat{\bar{u}}}{\partial z} = 0$ at $z = H$ and $\frac{\partial \hat{\bar{u}}}{\partial z} > 0$ at $z = 0$, to be marginally unstable[1] is that there exists a function $\bar{u}(y,z,\mu)$, which satisfies the conditions III) 1) - 4) and also the inequality

$$\int_{\hat{\bar{u}} = \hat{c}^{(n)}(k)} \frac{\hat{\psi}^2}{|\nabla \hat{\bar{u}}|} \left. \frac{\partial D}{\partial \mu} \right|_{\mu=0} ds < 0 \tag{46}$$

for at least one n.

Theorem 4 was given by Stern $(1963)_1$.

If the curve $\hat{\bar{u}} = \hat{c}^{(n)}(k)$ does not intersect the ground $z = 0$, we get from (42) and (45) using (21)

$$\left. \frac{\partial c_i^{(n)}(k)}{\partial \mu} \right|_{\mu=0} = \frac{-\pi \int_{\hat{\bar{u}} = \hat{c}^{(n)}k} \hat{\psi}^2 |\nabla \hat{\bar{u}}|^{-1} \left. \frac{\partial D}{\partial \mu} \right|_{\mu=0} d\ell}{\Gamma(0) \int_0^{\infty} \left. \frac{\hat{\psi}_z^2}{\frac{\partial \hat{\bar{u}}}{\partial z}} \right|_{z=0} dy} \tag{47}$$

---

[1] with respect to

We shall now try to get further conclusions from theorem 4:

We take

$$\bar{u}(y,z,\mu) = \hat{\bar{u}}(y,z) + \mu\,\bar{u}_1(y,z). \tag{48}$$

So we have satisfied III) 1) and 2). We choose $\bar{u}_1(y,z)$ so that the corresponding D_1 is negative definite. We have then fulfilled (46) because of $\left.\frac{\partial D}{\partial \mu}\right|_{\mu=0} = D_1$.

So we get the

Theorem 5: A field $\hat{\bar{u}}(y,z)$ for which $D \equiv 0$ and $\frac{\partial \hat{\bar{u}}}{\partial z} = 0$ at $z = H$ and $\frac{\partial \hat{\bar{u}}}{\partial z} > 0$ at $z = 0$ is marginally unstable if there exists a function $\bar{u}_1(y,z)$ which has a negative definite corresponding D_1 and which satisfies the conditions III) 3) and 4).

V) Concluding Remarks

We cannot be satisfied at this state of development of the theory. The thing most lacking is an existing proof for the solution of (19) - (21). We should be able to make it in the case $D \equiv 0$. The case $D \not\equiv 0$ which leads in general to a singular equation (19) will require a more intensive and careful treatment. Having proved the existence one will probably never be able to find the explicit solutions and eigenvalues but perhaps one can succeed in finding more general criteria for stable or unstable modes.

The theorems 1) - 3) do not need the existence proof, but the theorems 4) and 5) do. The theorems 1) - 3) particularly 2) and 3) are rather special ones so the further treatment mentioned above is very necessary.

Acknowledgements

I am very grateful that the Fellowship Committee gave me the possibility to participate in this course at the Woods Hole Oceanographic Institution.

I wish to thank all other participants for helping me in many cases.

Especially I wish to thank Dr. Melvin Stern. He introduced me to the problem of baroclinic instability, made his unpublished papers available to me and helped me by a lot of very useful discussions.

References

Eckart, C. (1963): An unpublished manuscript.

Howard, L.N. (1961): Note on a paper of John W. Miles. J.Fluid Mech., 10(4), p.509.

Lin, C.C. (1955): The Theory of Hydrodynamic Stability. Cambridge University Press.

Stern, M.E. $(1963)_1$: Marginally Unstable Baroclinic Atmospheres. Unpublished manuscript.

Stern, M.E. $(1963)_2$: Two Theorems related to the Stability of Baroclinic Jets. Unpublished manuscript.

Internal Waves with Stratification and an Inclined Rotation Vector

by

P. B. Rhines

Internal Waves with Stratification and an Inclined Rotation Vector

P. B. Rhines

Abstract

The effect of an inclined rotation vector on internal waves has been considered by Phillips (1963) and others. This paper investigates the response of a similar system, with both horizontal and vertical mean density gradients, to wave-like perturbations. Gravity waves are found, for realistic values of the parameters, to dominate the system, with some few exceptions. (Shear interactions with the waves are neglected.) Stability characteristics of the system are also considered.

Phillips (1963) and others have considered the propagation of inertial waves in a homogeneous incompressible fluid when the rotation vector $\underline{\Omega}$ is not vertical. The frequency of such waves is determined by the component of $\underline{\Omega}$ along the propagation direction, hence the waves are anisotropic. When reflection from a plane surface occurs, the linearity of the equations requires that the frequency remain the same. This reflection must therefore take place about the direction of $\underline{\Omega}$ or its perpendicular, rather than about the surface normal.

Since the projection of the wavenumber on the boundary must be conserved through the reflection, the incident and reflected waves will

generally have different wavenumbers. As a result energy is transferred between wavenumbers at the same frequency.

In Fig. 1 the reflected wavenumber $\underline{k}'$ is plotted with respect to the direction of the reflected wave. Near 90^{o}, the projection of $\underline{k}'$ becomes small and, ~~for~~ an inviscid system, its magnitude goes to ∞ .

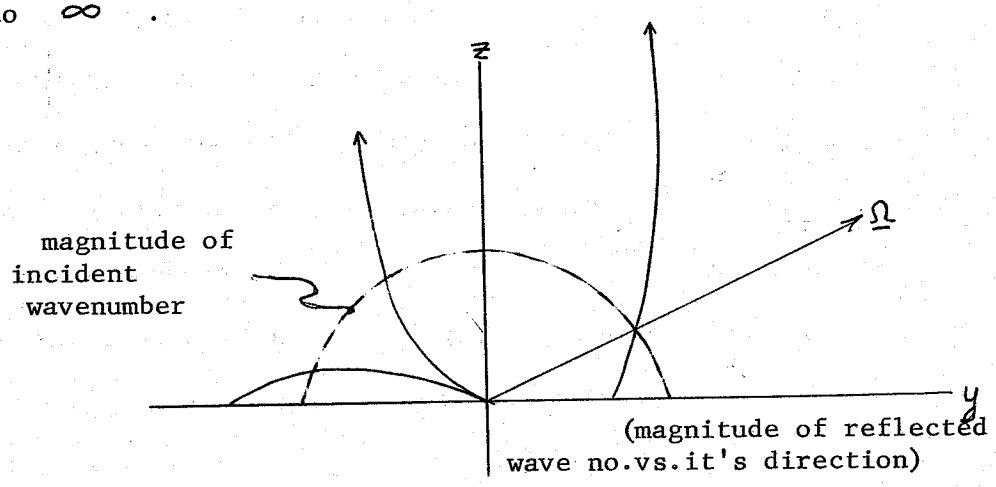

Figure 1.

The behavior of internal waves in a more general system will be considered here. With account taken of density stratification, a result more representative of the oceans would be expected. And since the density gradient changes greatly with depth, the propagation and reflection of waves near the bottom might differ from that near the surface. The presence of different reflection laws at surface and bottom could in turn produce energy trapping in regions of the ocean.

The inviscid equations considered take account of small mean horizontal and vertical density gradients and an inclined rotation

vector. The Boussinesq approximation is made, so that density variations in the momentum equations will be considered only in the buoyancy terms. If the z-axis is taken vertically, with $\underline{\Omega}$ in the yz-plane, the equations of motion are then

$$\frac{\partial u}{\partial x} + \frac{\partial v}{\partial y} + \frac{\partial w}{\partial z} = 0 \tag{1}$$

$$\frac{\partial u}{\partial t} + u\frac{\partial u}{\partial x} - \lambda v + \mu w = -\frac{1}{\bar{\rho}}\frac{\partial p}{\partial x} \tag{2}$$

$$\frac{\partial v}{\partial t} + u\frac{\partial v}{\partial x} + \lambda u = -\frac{1}{\bar{\rho}}\frac{\partial p}{\partial y} \tag{3}$$

$$\frac{\partial w}{\partial t} + u\frac{\partial w}{\partial x} - \mu u = -\frac{1}{\bar{\rho}}\frac{\partial p}{\partial z} - g\hat{\rho} \tag{4}$$

Where the hydrostatic pressure has been removed, the non-linear terms not involving u have been dropped, since the perturbation velocities are to be small, and

$$\lambda = 2\Omega \sin\theta, \qquad \mu = 2\Omega\cos\theta, \quad \text{and} \quad \rho = \bar{\rho}(1+\hat{\rho})$$

(θ is the angle from $\underline{\Omega}$ to the horizontal.)

The motions of the fluid will be considered adiabatic, and the fluid incompressible so that

$$\bar{\rho}\left(\frac{\partial \hat{\rho}}{\partial t} + u\frac{\partial \hat{\rho}}{\partial x}\right) + v\frac{\partial \bar{\rho}}{\partial y} + w\frac{\partial \bar{\rho}}{\partial z} = 0 \tag{5}$$

The existence of a mean horizontal variation of density requires a mean shear of the u velocity. The y- and z-momentum equations give

$$\lambda\frac{\partial u}{\partial z} = \frac{g}{\bar{\rho}}\frac{\partial \bar{\rho}}{\partial y} \tag{6}$$

$$-\mu\frac{\partial u}{\partial y} = \frac{g}{\bar{\rho}}\frac{\partial \bar{\rho}}{\partial z} \tag{7}$$

for the mean flow, since

$$\frac{\partial}{\partial y}\left(\frac{\partial P}{\partial z}\right) = \frac{\partial}{\partial z}\left(\frac{\partial P}{\partial y}\right) = -g\frac{\partial \bar{\rho}}{\partial y}$$

where P is the hydrostatic pressure.

Equations (6) and (7) give the shear of u required to make the system statically stable; thus the retention of the $u\frac{\partial}{\partial x}$ terms in the basic equations is necessary. The interaction of the shear with the system will, however, be neglected by assuming a large mean flow U so that

$$u = U + u' + \epsilon_1 z + \epsilon_2 y$$

and the non-linear terms

$$u\frac{\partial u}{\partial x},\quad u\frac{\partial v}{\partial x},\quad u\frac{\partial w}{\partial x},\quad \bar{\rho}u\frac{\partial \hat{\rho}}{\partial x}$$

will be approximated by

$$U\frac{\partial u}{\partial x},\quad U\frac{\partial v}{\partial x}\quad \cdots\cdots$$

and then eliminated by adopting the substantial time derivative:

$$\frac{D}{Dt} = \frac{\partial}{\partial t} + U\frac{\partial}{\partial x}\ .$$

This corresponds to redefining time with respect to a translating origin. If exponential density profiles are chosen so that $\frac{1}{\bar{\rho}}\frac{\partial \bar{\rho}}{\partial z}$, $\frac{1}{\bar{\rho}}\frac{\partial \bar{\rho}}{\partial y}$ are constant, the equations will all have constant coefficients.

A wave-like perturbation in three dimensions,

$$\exp i\,(\sigma t + k x + l y + m z)$$

will be assumed. If the equations are then solved for σ, we find

$$\sigma^3 + \sigma\left[\frac{-(k^2+l^2)N_z^2 + km\,N_y^2 - (l\mu + m\lambda)^2}{k^2+l^2+m^2}\right] + \tag{8}$$

$$+ i\,\frac{k\,N_y^2\,(l\mu + m\lambda)}{k^2+m^2+l^2} = 0$$

where

$$-\frac{g}{\bar{\rho}}\frac{\partial \bar{\rho}}{\partial z} = N_z^2 \quad \text{and} \quad \frac{-g}{\bar{\rho}}\frac{\partial \bar{\rho}}{\partial y}$$

(N_z is the Väisälä frequency, if the compressibility of the fluid is neglected.)

The frequency of the motions with respect to a fixed observer is then

$$\sigma^* = \sigma - k U$$

Some special cases of this result will now be considered. If only vertical density stratification is considered, $N_u = 0$ and U may be set equal to zero, giving $\sigma^* = \sigma$. If also the waves do not depend on x, $k = 0$, and we have

$$\sigma^{-2} = \sigma^{*-2} = \frac{l^2 N_z^2 + (l\mu + m\lambda)^2}{l^2 + m^2}$$

This is conveniently reduced to

$$\sigma^2 = N_z^2 \cos^2\varphi + 4\frac{\underline{\Omega}\cdot\underline{k}}{|\underline{k}|^2} \qquad (9)$$

$$= N_z^2 \cos^2\varphi + 4\Omega^2 \cos^2\delta \qquad \text{(See Fig.2)}$$

$$\left(\underline{k} = k\underline{j}_1 + l\underline{j}_2 + m\underline{j}_3,\ \underline{\Omega} = \frac{\mu}{2}\underline{j}_2 + \frac{\lambda}{2}\underline{j}_3\right)$$

The first or Väisälä term is strongest in the horizontal direction; the inertial term is determined by the component of $\underline{\Omega}$ along the propagation direction. The orders of magnitude of the terms may be compared; in the second term $4\Omega^2 \cong 4\cdot 10^{-8}$. The density is largely temperature determined, with an equation of state $\rho = \rho_0(1 - \alpha T)$.

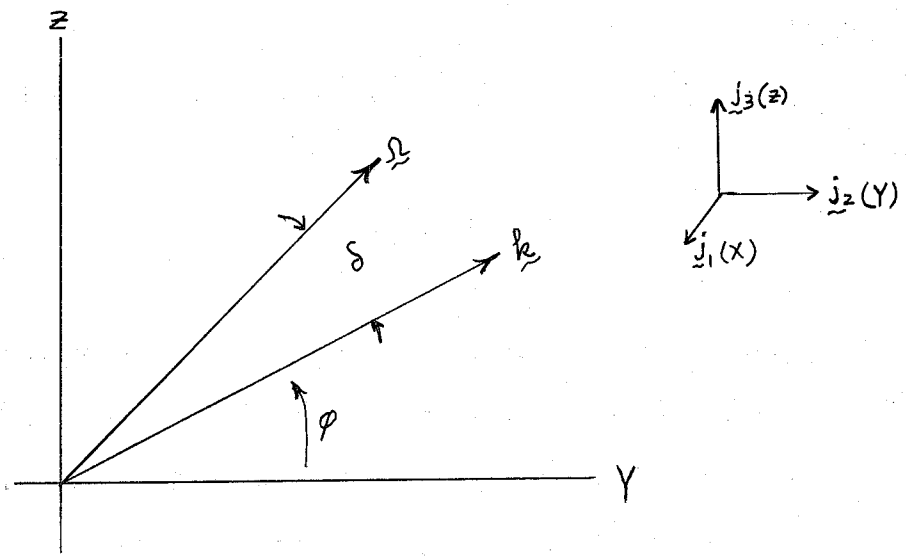

Figure 2.

Then

$$\frac{g}{\bar{\rho}} \frac{\delta \bar{\rho}}{\delta z} \cong \frac{g}{\rho_0} \rho_0 \alpha \frac{\partial T}{\partial t} \quad \text{or with} \quad \alpha = 9 \times 10^{-6}$$

(Eckart, 1960)

$N_z^2 \cong 10^{-9}$ for a temperature gradient of 1°/km. N_z^2 is rarely this low; Eckart (1960) gives typical values of from 10^{-3} to 10^{-4} for the upper 2000 meters of the sea. Knowledge of the values of α and $\frac{\delta T}{\delta z}$ at extreme depths is not reliable, but there would seem to be no widespread occurrence of values of N_z^2 less than 10^{-7}.

The stability frequency would thus be dominant except for small values of $\left(\frac{\cos^2 \varphi}{\cos^2 \delta} \right)$. It is found that for $N_z^2 \cong 10^{-5}$ and $\underline{\Omega}$ near the vertical, the waves must be travelling within about 3° of the vertical, for inertial motions to prevail. At this attitude, however, the reflection conditions mentioned earlier require the reflected wavenumber to be very near zero, and the amplitude of the waves similarly near zero. Practically speaking, therefore, waves are reflected about the surface normal except possibly in restricted bottom areas where the density gradient is extremely small.

The particle velocities are found by taking axes based on the propagation direction, and solving the original equations for $u = u(v)$ (v is now normal to $\underline{k}$ in the zy-plane, and u normal

to both $\underline{k}$ and v). We get

$$u = \pm iv\left[1 - \frac{N_z^2 \cos^2\phi}{\sigma^2}\right]^{1/2}$$

$$= \pm iv\left[\frac{1}{1 + \frac{N_z^2 \cos^2\phi}{4\Omega^2 \cos^2\delta}}\right]$$

Hence pure vertical waves ($N_z = 0$) are circularly polarized, and have circular particle paths. In general the paths are ellipses; clearly, for typical values of N_z and Ω , $u << v$ and the ellipses degenerate almost to straight lines. Since the fluid is incompressible, the continuity equation

$$ku + lv + mw \equiv (\underline{k}, \underline{q}) = 0$$

requires that the waves be transverse. The particles move in plane sheets oriented normal to $\underline{k}$.

The motivation for including a horizontal density gradient is to try to balance the dominant effects of the vertical gradient. Letting $N_y^2 \neq 0$ and $v \neq 0$, but with $k = 0$ still, we have

$$\sigma^2 = N_z^2 \cos^2\phi + 4\Omega^2 \cos^2\delta - \frac{lmN_y^2}{l^2 + m^2}$$

$$= N_z^2 \cos^2\phi + 4\Omega^2 \cos^2\delta - \frac{N_y^2}{2} \sin 2\phi .$$

It is possible for N_y to balance N_z if

$$\frac{N_y^2}{N_z^2} \approx \cot\phi$$

However this merely moves the narrow "window" for inertial waves away from the vertical; it remains narrow. If, for example, $N_y^2 = \frac{1}{10} N_z^2$, the inertial effects dominate in a 4^o sector at about 85^o from the horizontal. Reflection of these waves by a horizontal plane is now possible, since the reflected wavenumber does not go to zero as in the previous case.

Some interesting considerations arise from the above cases. If N_z^2 in eq. (9) is slightly negative (unstable stratification) rotation may keep the system stable for some wavenumbers. If we then let $\delta = \varphi$ (horizontal rotation vector) and if

$$\frac{4\Omega^2}{|N_z^2|} > 1$$

the system is stable to disturbances in any direction. Physically, one would reason that a displaced particle of fluid initiating instability would be deflected around by the Coriolis force, and stability would result.

We may also consider the system

$$\sigma^2 = -\frac{N_y^2}{2} \sin 2\varphi$$

obtained by setting $N_z = 0$ and letting Ω approach zero while the product $\cdot \lambda \frac{\partial u}{\partial z}$ is kept large enough to maintain zero-order stability. We see that the system is stable for waves propagating in quadrants I and III of the yz-plane, and unstable for quadrants II and IV assuming the density increases as y increases. (See Fig.3)

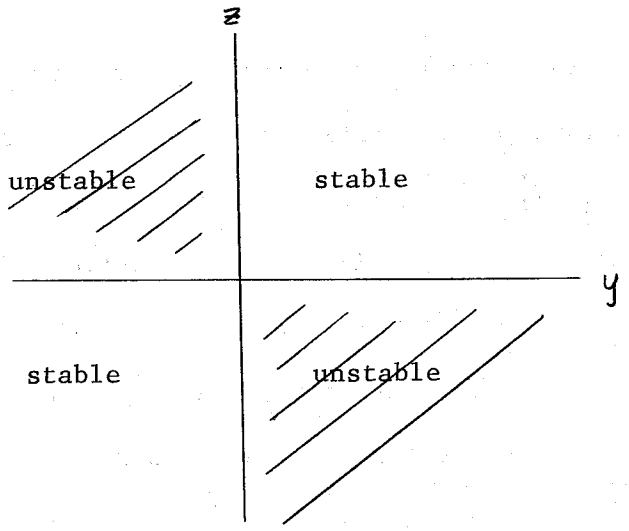

Figure 3.

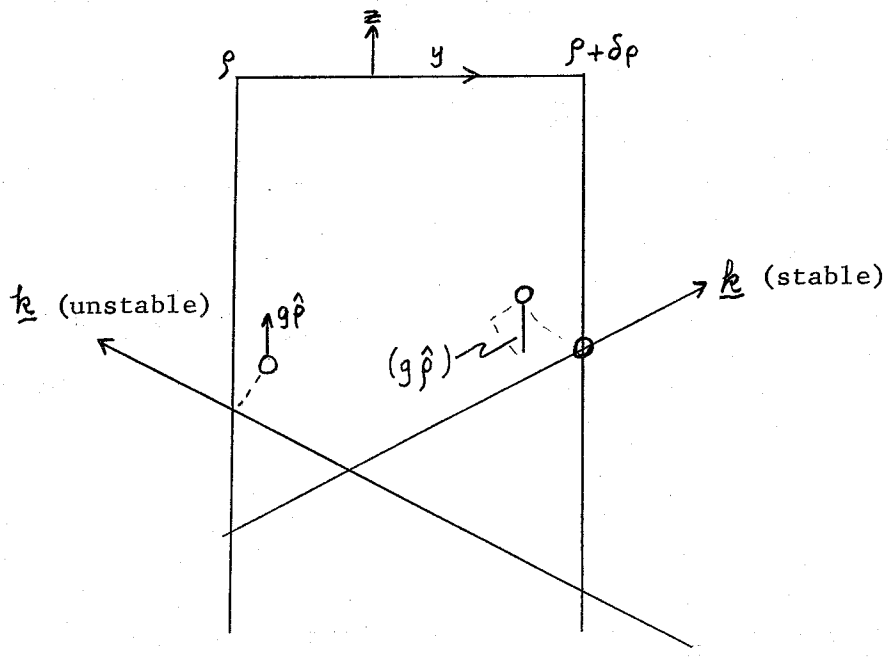

Figure 4.

In Fig. 4, a particle displaced upwards from the propagation axis in the first quadrant comes into a region of lower density and

experiences a force downwards of magnitude $g\hat{\rho}$. The pressure gradient along $\underset{\sim}{k}$, due to the motion is given, from eqs. (3) and (4), by

$$\frac{\partial p'}{\partial y}\sin\varphi + \frac{\partial p'}{\partial z}\cos\varphi =$$

$$\frac{l\frac{\partial p'}{\partial y} + m\frac{\partial p'}{\partial z}}{|k|} = -\bar{\rho}\left[\frac{l(v_r + Vv_x) + m(w_r + Vw_x) + gw\hat{\rho}}{\underset{\sim}{k}}\right]$$

Since $lv + mw = 0$,

the force along $\underset{\sim}{k}$ due to this gradient becomes just

$$g\hat{\rho}\sin\varphi$$

and the net restoring force is transverse; the particle is drawn back to its original position. Similarly, in the case of inertial waves, the component of the Coriolis force along the propagation direction is just balanced by the induced pressure gradient.

If, on the other hand, $\underset{\sim}{k}$ is in quadrants II or IV, a particle displaced upwards is lighter than its surroundings, and continues to rise.

If eq. (8) is written as

$$\sigma^3 + a\sigma + ib = 0$$

where $a < 0$ generally, the roots are given by

$$\sigma_1 = W^{1/3}e^{i\pi/6} + \frac{-a}{3}W^{-1/3}e^{-i\pi/6}$$

$$\sigma_2 = W^{1/3}e^{5\pi/6} + \frac{-a}{3}W^{-1/3}e^{-5\pi/6}$$

$$\sigma_3 = -i\left[W^{1/3} - \frac{-a}{3}W^{-1/3}\right]$$

where $W = \left[-\frac{b}{2} + \sqrt{\frac{b^2}{4} - \frac{a^3}{27}} \right]$

Here $\sigma_1 = -\overline{\sigma_2}$ and σ_3 is pure imaginary.

Generally

$$|b| << |a|$$

so that, after some manipulation, the roots become approximately:

(See Fig. 5)

$$\sigma_1 = \sqrt{-a} - \frac{i}{2}\frac{b}{-a}$$

$$\sigma_2 = -\sqrt{-a} - \frac{i}{2}\frac{b}{-a}$$

$$\sigma_3 = \frac{ib}{-a} \qquad (a<0)$$

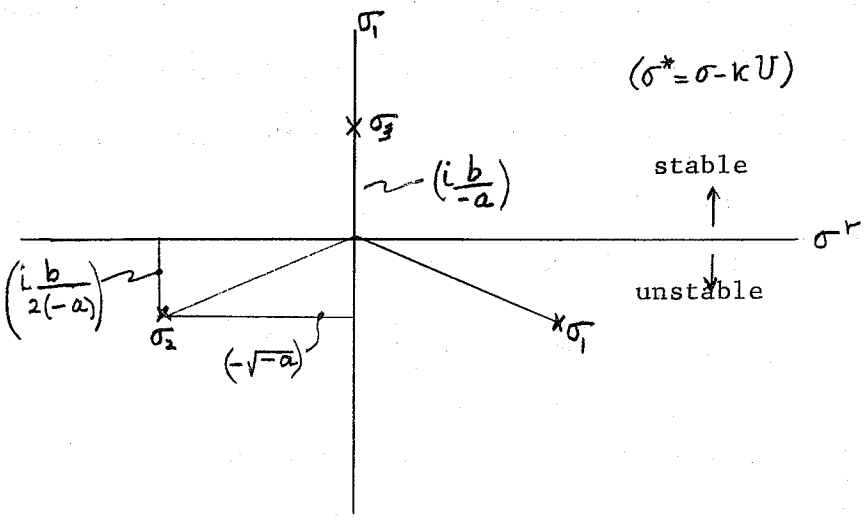

Figure 5

Thus the real parts of σ_1 and σ_2 (the frequency) are the same as we obtained before (with the addition of dependence on k) and

the imaginary parts are:

$$\sigma_2^i = \sigma_1^i = -\frac{1}{2} \frac{k N_y^2 (l\mu + m\lambda)}{(k^2+l^2)N_z^2 - lm N_y^2 + (l\mu+m\lambda)^2}$$

and $$\sigma_3^i = -2\sigma_2^i$$

Even though N_y^2 is generally considered much smaller than N_z^2, the magnitude of the imaginary parts can still exceed that of the real parts.

The system is, therefore, unstable due to the simultaneous presence of rotation, horizontal density stratification, and propagation of waves in the x-direction ($K \neq 0$). The imaginary parts change sign if either $\underline{\Omega} \cdot k$ or N_y^2 change sign. Then σ_1 and σ_2 (overstable roots) become stable and σ_3 represents non-oscillatory growth. Note that changing back to fixed coordinates merely changes the frequency by kU ; the growth parameters are unaffected.

When the dominant density variation is vertical and the rotation small, we have

$$\sigma_1^i \cong -\frac{1}{2} \frac{k N_y^2 (l\mu + m\lambda)}{(k^2+l^2) N_z^2} \tag{10}$$

If the rotation rate is large, however,

$$\sigma_1^i \cong -\frac{1}{2} \frac{k N_y^2}{(l\mu+m\lambda)} \tag{11}$$

and where slight rotation is necessary to destabilize the system in (10) an increased rotation rate tends to stabilize the system in (11).

The physical situation for the instability is not clear; presumably it might arise as in the second special case where the sign of the Coriolis force would determine whether overstability or pure instability occurred.

Conclusion

The motivation for this work was to find whether or not the influence of the dominant stability of the ocean on internal wave propagation is balanced by other effects. It has been suggested that the inclusion of the shear interaction with the waves might have produced more conclusive results than this analysis reveals. It is hoped that some physical reasoning may justify the instability considered in the last section.

References

Bjerknes, Physikalishe Hydrodynamik (1933)

Eckart Hydro.of Oceans and Atmospheres (1960)

Fjeldstad Internal Waves. Geofys.Pub. Oslo (1933)

Phillips Physics of Fluids 4, 513. (1963)

Radiative Structure of Sound and Shock Waves

by

Robert Stein

Contents

Radiative Structure of Sound and Shock Waves

Robert Stein

I. Introduction

Radiation effects on the propagation of sound and shock waves are significant at high temperatures such as occur in stars and behind shock fronts in interstellar matter.

The upper chromosphere and corona of the sun are hotter than the underlying layers and are heated by acoustic waves. A broad frequency spectrum of waves is generated by turbulent gas motions but only certain frequencies are propagated through the atmosphere. Observed oscillations in the solar atmosphere have periods of about 300 sec. The limits of the pass band depend upon the interaction of radiation with the medium.

Shock waves occur in pulsating (variable) stars. They are observable only to the extent that they modify the radiation from the star, so that the relation between shock structure and radiation is essential for understanding what is happening in the star.

Shock waves occur also in collisions of interstellar gas clouds and in supernova explosions. In these cases radiation acts primarily to cool the region behind the shock front.

In the following pages I will first review the general nature of the interaction of the radiation field with matter and then consider its effects on sound and shock waves.

II. The Radiation Field

The radiation field interacts with matter through emission and absorption photons and generation of a radiation pressure. For the fluid media, the absorption of photons acts as an energy source and their emission as an energy sink. Let us call the net rate of energy transfer from the radiation field to the fluid per unit volume

$$Q_r = \text{absorption} - \text{emission} \quad \frac{\text{ergs}}{\text{cm}^3\text{sec}}$$

Then the energy conservation equations for the fluid and the radiation field are:

$$\frac{\partial e}{\partial t} + \nabla \cdot \underset{\sim}{\mathcal{F}} = Q_r \qquad \text{Fluid}$$

$$\frac{\partial e_r}{\partial t} + \nabla \cdot \underset{\sim}{F}_r = -Q_r \qquad \text{Radiation} \tag{2.1}$$

where e and $\mathcal{F}$ are the energy density and flux of the fluid and e_r and F_r are the energy density and flux of radiation. In a steady state the energy equation for the radiation field reduces to

$$\nabla \cdot \underset{\sim}{F}_r = -Q_r \tag{2.2}$$

and for steady-state problems it is often convenient to express the radiation-matter interaction in terms of the radiative energy flux.

Consider now the radiation field in some detail in order to derive explicit expressions for the rates of emission and absorption and the radiative energy flux.

The radiation field can be described most simply by the distribution function of photons in phase space.

$$f_\nu(\underset{\sim}{x}, \hat{\mu}, t)\, d^3\underset{\sim}{x}\, d\nu\, d\Omega$$

= number of photons in the frequency interval $(\nu, \nu + d\nu)$, in $d^3\underset{\sim}{x}$ at $\underset{\sim}{x}$, moving in the direction $\hat{\mu}$, in a beam of solid angle $d\Omega$, at time t.

The absorption of photons is determined by the opacity per unit length

$$\kappa = 1/\text{photon mean free path}$$

so that the fractional change in the number of photons on traversing an element of distance ds in a given direction is

$$\frac{df}{f} = -\kappa\, ds \tag{2.3}$$

The distance, in units of the photon mean free path, is called the optical depth τ:

$$d\tau = \kappa\, ds$$

$$\tau_{12} = \int_1^2 \kappa\, ds \tag{2.4}$$

Thus,

$$f = f_0 e^{-\tau}$$

We can now derive an explicit expression for the distribution function by the following physical argument. The number of photons at a given point moving in a given direction, $f(\underset{\sim}{x}, \hat{\mu})$, is the sum of contributions due to the emission $S(\tau')$ from all elements behind

the point considered (in the direction $-\hat{\mu}$), with each separate contribution diminished by absorption according to $f = f_0 e^{-\tau}$. Thus, the distribution function (either monochromatic or integrated over frequency) is

$$\boxed{f(\underset{\sim}{x}, \hat{\mu}) = \int_0^\infty S(\tau') e^{-\tau'} d\tau'} \qquad (2.5)$$

where the integral is from $\underset{\sim}{x}$ along the direction $-\hat{\mu}$ to ∞ and where S is the rate of emission of photons. A photon of frequency ν has energy $h\nu$, so the flux of radiative energy is

$$F_{ir} = \int h\nu c f_\nu(\underset{\sim}{x}, \hat{\mu}) \mu_i \, d\Omega \, d\nu \qquad (2.6)$$

Hereafter, I will be considering the special case of plane parallel flow

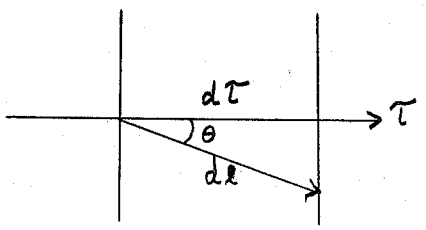

$\mu = \cos\theta$

$d\tau = \mu \, d\ell$

The distribution function is then

$$f(\tau,\mu) = \int_{-\infty}^{\tau} S(\tau') e^{-\left(\frac{\tau-\tau'}{\mu}\right)} \frac{d\tau'}{\mu}, \quad \mu > 0$$

$$f(\tau,\mu) = -\int_{\tau}^{\infty} S(\tau') e^{-\left(\frac{\tau-\tau'}{\mu}\right)} \frac{d\tau'}{\mu}, \quad \mu < 0$$

---

and the radiative flux is

$$\boxed{\begin{aligned} F(\tau) &= \int h\nu c f_\nu(\tau,\mu) \mu \, d\mu \, d\phi \, d\nu \\ &= 2\pi \int_{-\infty}^{\tau} 2(\tau') E_2(\tau-\tau') d\tau' \\ &\quad - 2\pi \int_{\tau}^{\infty} 2(\tau') E_2(\tau'-\tau) d\tau' \end{aligned}} \qquad (2.7)$$

where we have used the exponential integral functions

$$E_n(x) = \int_0^1 e^{-x/\mu} \mu^{n-2} d\mu$$

and where $\mathcal{Q} = \int h\nu c S d\nu$ is the energy source function, (the rate of emission of energy per unit volume).

Now consider the rates of absorption and emission of energy. Since the energy of a photon of frequency ν is $h\nu$ and $ds/dt = c$ the rate of absorption of energy is

$$A = \int d\Omega \int d\nu \left(\kappa h\nu c f_\nu\right). \quad \left(\frac{ergs}{cm^3 sec}\right)$$

We have integrated over all photon directions and frequencies to get the total rate. Substitute the explicit expression for

$$\begin{aligned} A &= \iint \kappa \left(\int h\nu c S d\nu\right) e^{-\tau} d\tau d\Omega \\ &= \kappa \iint \mathcal{Q} e^{-\tau} d\tau d\Omega = \kappa \iint \mathcal{Q} e^{-\tau} \kappa dr d\Omega \\ &= 4\pi \kappa \int \kappa \mathcal{Q} \frac{e^{-\tau}}{4\pi r^2} d^3r = 4\pi \kappa J \end{aligned} \tag{2.8}$$

or in one-dimensional form

$$\begin{aligned} A &= \kappa \int_{-\infty}^{\tau} \int_0^1 \mathcal{Q} e^{-\left(\frac{\tau-\tau'}{\mu}\right)} \frac{1}{\mu} d\mu d\tau' \\ &\quad - \kappa \int_{\tau}^{\infty} \int_{-1}^{0} \mathcal{Q} e^{-\left(\frac{\tau-\tau'}{\mu}\right)} \frac{1}{\mu} d\mu d\tau' \\ &= \kappa \int_{-\infty}^{\infty} \mathcal{Q} E_1(|\tau'-\tau|) d\tau' = 2\kappa J \end{aligned} \tag{2.9}$$

where $J = \frac{1}{4\pi}\int h\nu c f \, d\Omega$. J is called the mean intensity and is the average total rate of energy transport through a point by photons. The physical interpretation of J is as follows: The mean total rate of energy transport through a point is proportional to the rate of emission of energy by each volume element which is $\kappa 2 \, d^3 r$. This radiation falls off as $1/r^2$ and is attenuated as $e^{-\tau}$ where τ is the optical distance from the given point to the volume element emitting the radiation. The product is integrated over the whole volume and the average value is obtained by dividing by 4π.

From this physical picture, one can see that the rate of emission of energy in a given direction per unit volume is

$$\kappa 2$$

Thus the total rate of emission of energy is

$$E = 4\pi \kappa 2$$

In local thermodynamic equilibrium, which I shall assume throughout this paper

$$2 = \frac{\sigma}{\pi} T^4 \qquad (2.10)$$

so

$$E = 4\kappa\sigma T^4 \quad \left(\frac{ergs}{cm^3 \, sec}\right) \qquad (2.11)$$

Thus the rate of energy transfer from the radiation field to the fluid is

$$\boxed{Q_r = A - E = 4\sigma K\left[\int K T^4 \frac{e^{-\tau}}{4\pi r^2}\, d^3r - T^4\right]} \qquad (2.12)$$

(For further discussion of radiation field see Chandrasekhar, Stellar Structure, Chap. V, Dover.)

Finally, we derive the perturbation of Q_r due to a temperature perturbation in the medium. (ref. Spiegel, Ap. J., 126, 202, (57)). Consider a disturbance to the steady state temperature distribution, and let

$$T(\underset{\sim}{x}, t) = T_0(\underset{\sim}{x}) + \theta(\underset{\sim}{x}, t),$$

where $\theta(\underset{\sim}{x}, t)$ is the fluctuation in the temperature, and assume $|\theta| << T_0$. We can then linearize the expression for Q_r in the disturbance θ. For any quantity f, set

$$f(\underset{\sim}{x}, t) = f_0(\underset{\sim}{x}) + \frac{\partial f_0}{\partial T_0}\,\theta(\underset{\sim}{x}, t).$$

The steady-state condition is one of radiative equilibrium, that is, no net heat transfer; therefore

$$T_0^4 = \int K_0 T_0^4 \frac{e^{-\tau_0}}{4\pi r^2}\, d^3r$$

Then the perturbation of Q_r is

$$Q_r' = 16\sigma K\left[\int K_0 T_0^3 \theta \frac{e^{-\tau_0}}{4\pi r^2}\, d^3r - T_0^3\theta + \frac{1}{4}\int\left(\frac{\partial K_0}{\partial T_0}\theta - K_0\int\frac{\partial K_0}{\partial T_0}\theta\, ds\right) T_0^4 \frac{e^{-\tau_0}}{4\pi r^2}\, d^3r\right] \qquad (2.13)$$

The first term above is the perturbation of the mean intensity received at a point, the second term is the local emission loss,

while the last term is the effect of the perturbation of the opacity κ.

For the special case of an infinite homogeneous steady state, i.e.

$$T_0 = \rho_0 = \kappa_0 = \text{constant}$$

$$\tau_0 = \kappa_0 r$$

and

$$\alpha = \frac{\partial \kappa_0}{\partial T_0} = \text{constant},$$

we have

$$Q_r' = q_r^* \left[\int \kappa \theta \frac{e^{-kr}}{4\pi r^2} d^3r - \theta + \frac{\alpha T_0}{4} \int (\theta - \kappa \int \theta \, dr') \frac{e^{-kr}}{4\pi r^2} d^3r \right]$$

where $q_r^* = 16 \kappa_0 \sigma T_0^3$. Take the Fourier transform of the temperature fluctuation

$$\theta(\underline{x}, t) = \int \phi(\underline{k}, t) e^{i \underline{k} \cdot \underline{x}} d^3\underline{k}$$

i.e. analyze it into space harmonics. Then, the Fourier transform of the perturbed energy source Q_r' is

$$F.T. \left[Q_r'(\underline{x}, t) \right] = -\sigma(\kappa) \phi(\underline{k}, t)$$

$$\sigma(\kappa) = q_r^* \left(1 - \frac{\kappa}{\kappa} \tan^{-1} \frac{\kappa}{\kappa} \right) \qquad (2.14)$$

---

where to first order the absorption coefficient perturbation has no effect, (the perturbation in the absorption coefficient κ is just balanced by altered emission). Thus

$$Q_r'(\underline{x},t) = q^* \int \underline{K}(|\underline{x}-\underline{x}'|)\,\theta(\underline{x}',t)\,d^3\underline{x}'$$

$$\underline{K}(\underline{r}) = K_0 \frac{e^{-K_0 r}}{4\pi r^2} - \delta^3(\underline{r}) \qquad (2.15)$$

$$q^* = 16\,\sigma K_0 T_0^3$$

There are two limiting cases:

a) Long mfp, $K \to 0$

This is the case of an optically-thin fluctuation; that is, the characteristic dimensions of the fluctuation are much smaller than the photon mean free path.

$$q^* \underline{K} \to -q^* \delta^3(\underline{x}), \quad Q_r \to -q^* \theta$$

$$\sigma(K) \to +q^*$$

And we have Newton's law of radiation. In this case, equilibrium (damping of the fluctuations) is reached almost entirely by emission losses.

b) Short mfp, $K \to \infty$

This is the case of an optically-thick fluctuation. Then expanding $\sigma(K)$ or $\underline{K}(r)$

$$\sigma(K) \to \left(\frac{q^*}{3K^2}\right) K^2$$

$$Q_r' \to -\left(\frac{q^*}{3K^2}\right) \nabla^2 \theta$$

This is a diffusion equation, i.e. the photons escape by random walk, damping is by diffusion and self-absorption if significant.

III. Radiative Damping of Sound Waves

Radiation transfers energy from the hotter condensations of the sound waves to the cooler rarefactions and thus tends to have a damping effect. There are two limiting cases when the radiation does not damp the sound waves. If the oscillations are too rapid to permit the temperature fluctuations to be smoothed out, (i.e. the heat developed in a compression does not have time to escape), then the cycle is adiabatic and the work done in producing a given compression is recovered in the expansion. If the period of the motion is long, the heat escapes as it is produced and no temperature fluctuations can develop. The cycle is now isothermal and again no energy is dissipated. The difference is that in the isothermal case the pressure fluctuations are less for a given volume change.

In the intermediate case, when the period of the oscillations is neither so long that the temperature remains constant nor so short that heat cannot escape, the work expended in producing a given compression goes partially into heat which escapes via radiation to the colder regions thus dissipating energy. Then the work done in a compression is not completely recovered in a rarefaction and the waves are damped.

A. Basic Equations

Let us consider small disturbances in a homogeneous inviscid fluid in uniform motion with velocity $\vec{u}$.

$$\underline{u} = \bar{\underline{u}} + \underline{u}'$$

$$\rho = \rho_0 + \rho'$$

$$p = p_0 + p'$$

$$T = T_0 + T'$$

Since the variations are much less than the mean values, the equations of motion can be linearized. Consider the equations in a coordinate system moving with the fluid so $\bar{\underline{u}} = 0$. Then

$$\frac{\partial \rho'}{\partial t} + \rho_0 \frac{\partial u_j'}{\partial x_j} = 0$$

$$\frac{\partial u_i'}{\partial t} = -\frac{1}{\rho_0} \frac{\partial p'}{\partial x_i}$$

$$\rho_0 C_v \frac{\partial T'}{\partial t} + p_0 \frac{\partial u_j'}{\partial x_j} = \frac{\partial}{\partial x_j}\left(k_0 \frac{\partial T'}{\partial x_j}\right) + Q' \qquad (3.1)$$

$$p' = \frac{p_0}{\rho_0} \rho' + R \rho_0 T'$$

where Q' = radiative heat exchange rate per unit volume. We have seen that

$$Q'(\underline{x},t) = \rho_0 C_v q_r \int K(\underline{x}-\underline{x}',t)\, T'(\underline{x}',t)\, d^3\underline{x}'$$

$$K(\underline{x}) = K \frac{e^{-k|\underline{x}|}}{4\pi r^2 |\underline{x}|^2} - \delta^3(\underline{x}) \qquad (3.2)$$

$$q_r = \frac{16 K \sigma T^3}{\rho C_v}$$

where $[q_r] = t^{-1}$ is the inverse of the radiative cooling time, and $[K] = L^{-1}$ is the inverse of the photon mean free path. Eliminating the velocity gives the equations for the propagation of a small

disturbance in an inviscid fluid,

$$\boxed{\begin{aligned} &\frac{\partial^2 \rho'}{\partial t^2} - \frac{p_0}{\rho_0}\frac{\partial^2 \rho'}{\partial x_j^2} - R\rho_0 \frac{\partial^2 T'}{\partial x_j^2} = 0 \\ &\frac{\partial T'}{\partial t} = \frac{p_0}{C_v \rho_0^2}\frac{\partial \rho'}{\partial t} + \frac{Q'}{\rho_0 C_v} + K_c \frac{\partial^2 T'}{\partial x_j^2} \end{aligned}} \qquad (3.3)$$

where $K_c = \frac{k}{\rho C_v}$ is the thermomeactric conductivity.

Henceforth, we will neglect heat conductivity, which is similar to radiative heat transfer in the limit of long wavelength.

Take the Fourier transform of the equations,

$$f'(\underline{x},t) = \int \hat{f}(\underline{k},t)\, e^{i\underline{k}\cdot\underline{x}}\, d^3k,$$

and

$$F.T.\left[Q'/\rho C_v\right] = -\sigma(k)\hat{T}(\underline{k},t)$$

where

$$\sigma(k) = q_0\left(1 - \frac{K}{k}\tan^{-1}\frac{k}{K}\right).$$

The result is:

$$\frac{\partial^2 \hat{\rho}}{\partial t^2} + k^2 \frac{p_0}{\rho_0}\hat{\rho} + k^2 R\rho_0 \hat{T} = 0$$

$$\frac{\partial \hat{T}}{\partial t} = \frac{p_0}{\rho_0^2 C_v}\frac{\partial \hat{\rho}}{\partial t} - \sigma(k)\hat{T}$$

Differentiating the 1st equation with respect to t and substituting for $\frac{\partial \hat{\rho}}{\partial t}$, eliminates $\hat{\rho}$ and gives

$$\boxed{\frac{\rho_0}{p_0}\left(\frac{\partial}{\partial t} + \sigma\right)\frac{\partial^2 \hat{T}}{\partial t^2} + \left(\gamma\frac{\partial}{\partial t} + \sigma\right)k^2\hat{T} = 0} \qquad (3.4)$$

This has periodic solutions of the form

$$\hat{T}(\underline{k},t) = \hat{T}(\underline{k},0)e^{i\omega t}$$

and we get the Dispersion Relation

$$\boxed{-i\omega^3 - \sigma\omega^2 + i\omega\left(\frac{\gamma p_0}{\rho_0}\right)k^2 + \sigma\frac{p_0}{\rho_0}k^2 = 0} \tag{3.5}$$

B. Space Damping

First we will investigate the space behavior of the sound waves for given real frequency ω. In general k will be complex, $k = k + ik_I$. The real part gives the wavelength and the imaginary part, the damping distance. Consider the conditions necessary for undamped propagation, $k_I \longrightarrow 0$. Then the real and imaginary parts of the dispersion relation must vanish.

$$\sigma\left(-\omega^2 + \frac{p_0}{\rho_0}k^2\right) = 0$$

$$i\omega\left(-\omega^2 + \frac{\gamma p_0}{\rho_0}k^2\right) = 0$$

These equations have two solutions:

a) $k^2 = \left(\frac{\rho_0}{\gamma p_0}\right)\omega^2, \quad \sigma = 0$

so either $q_r = 0$ or $k = 0$.

This is the case of small radiation losses, $q_r << \omega$ and the motion is adiabatic.

b) $k^2 = \left(\frac{\rho_0}{p_0}\right)\omega^2, \quad \omega = 0$

This is the case of large radiation losses, $q_r >> \omega$ and the motion is isothermal.

An alternative way of looking at these limiting cases is to

consider the limits

a) $q_f \to 0$, $\sigma << \omega$, small radiation losses

so $-i\omega^3 + i\omega\left(\frac{\gamma p_0}{\rho_0}\right)k^2 = 0$

and $k^2 = \left(\frac{\rho_0}{\gamma p_0}\right)\omega^2$ unless $\omega = 0$

b) $q_f \to \infty$, $\sigma >> \omega$, large radiative damping

so $-\omega^2 + \frac{p_0}{\rho_0}k^2 = 0$

and $k^2 = \left(\frac{\rho_0}{p_0}\right)\omega^2$

In both cases there is no energy loss. The radiation either has no effect or keeps the medium isothermal. The work done in producing a given compression is recovered in the expansion since pressure is a function of density. In general the radiation will damp the oscillations since it will transfer heat irreversibly from a hotter to a cooler region increasing the entropy. The amount of damping depends on the ratio ω/q_f, which is the radiative cooling time/period.

We can gain further insight by considering two other limiting cases: (ref. Rayleigh, Theory of Sound)

a) $k >> K$

This is the limit of optically-thin fluctuations. Here, $\sigma \to q_f$ (Newton's law of cooling), and

$$k^2 = \frac{\omega^2}{p_0/\rho_0}\,\frac{q_f + i\omega}{q_f + i\gamma\omega}$$

So

$$|K| = \frac{\omega}{\sqrt{P_0/\rho_0}} \left[1 - \omega^2 \frac{(\gamma^2-1)}{q_f^2+\gamma^2\omega^2} \right]^{1/4}$$

$$\phi = \frac{1}{2} \tan^{-1} \left(- \frac{\omega q_f (\gamma-1)}{q_f^2+\gamma\omega^2} \right) \qquad (3.6)$$

In general ϕ is small, so

$$\cos\phi \approx 1 \quad \text{and} \quad \sin\phi \approx \tan\phi = -\frac{1}{2} \frac{\omega q_f (\gamma-1)}{q_f^2+\gamma\omega^2}$$

Then the ratio of the damping constant to the wave number is

$$\left| \frac{K_I}{K_R} \right| = \frac{\gamma-1}{2} \frac{\omega q_f}{q_f^2+\gamma\omega^2} \qquad (3.7)$$

This has a peak at $\omega/q_f = \gamma^{-1/2}$ where it has the value $\frac{\gamma-1}{4\sqrt{\gamma}}$ and it falls to zero as $\omega \to 0$ or ∞ . The inverse ratio $\left|\frac{K_R}{K_I}\right|$ is the damping distance in wavelength units. It is infinite at $\omega \to 0$ or ∞ and has a minimum at $\omega/q_f = \gamma^{-1/2}$. If we put this ratio in dimensionless units, scaling ω by q_f we get

$$\left| \frac{K_R}{K_I} \right| = \frac{2}{\gamma-1} \frac{1+\gamma\omega'^2}{\omega'}$$

where $\omega' = \omega/q_f$. The damping thus depends only on ω/q_f in the optically-thin case. (See accompanying graph, p.110). The limit of small q_f is

$$|K| = \frac{\omega}{\sqrt{\gamma P_0/\rho_0}} \left(1 + \frac{1}{4} \left(\frac{q_f}{\omega} \right)^2 \frac{\gamma^2-1}{\gamma} \right)$$

$$\phi = \pi - \frac{q_f}{2\omega} \left(\frac{\gamma-1}{\gamma} \right)$$

so the wave propagates in the $-\underset{\sim}{K}$ direction and

$$K_R = -\frac{\omega}{c}\left(1+\frac{1}{4}\frac{q_\sigma^2}{\omega^2}\frac{\gamma^2-1}{\gamma^2}\right)$$

$$K_I = \frac{q_\sigma}{2c}.$$

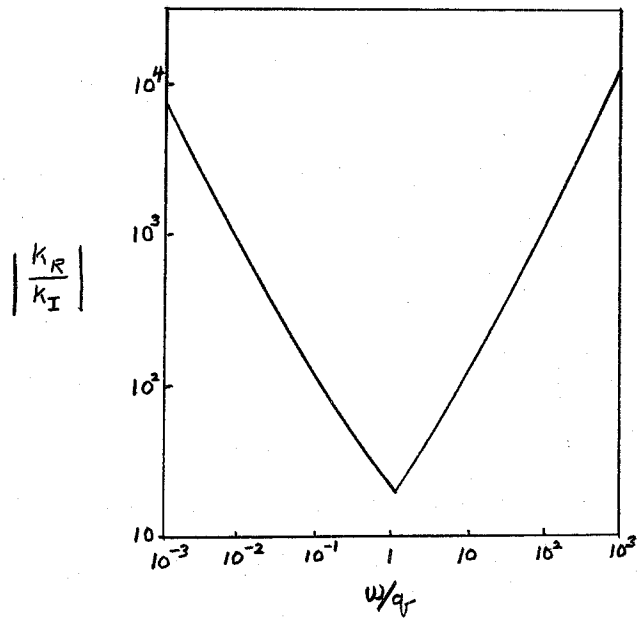

Damping Distance

b) $K << \kappa$

This is the limit of optically-thick fluctuations. Here

$$\sigma(K) = \frac{q_\sigma}{3\kappa_R^2} K^2$$

This corresponds to diffusion of radiation (Eddington approximation) and has the same form as heat conduction. The dispersion relation

gives $$K^4 + K^2\left(-\frac{\rho_0}{p_0}\omega^2 + i\gamma\omega q_f'\right) - i\omega^3\frac{\rho_0}{p_0}q_f' = 0$$

where $$q_f' = \frac{3K_R^2}{q_f}$$

For small q_f, the 0th order solution is

$$K^2 = \frac{\omega^2}{(\gamma p_0/\rho_0)}$$

Substituting this in the small term K^4, gives

$$iK^2\left(\gamma\omega\frac{3K^2}{q_f} - i\frac{\rho_0}{p_0}\omega^2\right) - i\omega^3\frac{\rho_0}{p_0}\frac{3K^2}{q_f} + \frac{\omega^4}{(\gamma p_0/\rho_0)^2} = 0$$

so $$K^2 = \frac{\omega^2}{(\gamma p_0/\rho_0)}\left[1 - i\frac{\gamma-1}{\gamma}\frac{q_f\omega}{3K^2}\frac{1}{(\gamma p_0/\rho_0)}\right]$$

so $$K = -\frac{\omega}{c}\left[1 - i\frac{\gamma-1}{\gamma}\frac{q_f\omega}{6K^2c^2}\right] \qquad (3.8)$$

To solve the general case numerically for the wavelength and damping distance, cast the dispersion relation into non-dimensional form by scaling the variables

$$\omega' = \left(\frac{\omega}{q_f}\right), \quad K' = \left(\frac{K}{K_c}\right)$$

Then we get the dispersion relation

$$\boxed{-i\omega'^3 - \sigma'\omega'^2 + i\omega'\gamma\lambda^2K'^2 + \sigma'\lambda^2K'^2 = 0} \qquad (3.9)$$

where

$$\boxed{\begin{aligned} &\omega' = \omega/q_f, \quad K' = \frac{K}{K_c} \\ &\sigma' = 1 - \frac{1}{K'}\tan^{-1}K' \\ &\lambda^2 = \frac{p_0}{\rho_0}\frac{K_c^2}{q_f^2} \\ &\gamma = C_p/C_v \end{aligned}} \qquad (3.10)$$

note: λ = cooling distance/photon mean free path.

Hereafter, we will drop the primes on the dimensionless variables and work only with dimensionless quantities.

We want to solve for $k(\omega) = k_{12} + i\, k_I$.

From k_R, we can compute the effective γ for radiation

$$\gamma = 1 + \frac{2}{f}$$

where f = number of degrees of freedom

= 3 translational + others.

Then $$c^2 = \frac{\gamma_{eff}\, p_0}{\rho_0} = \left(\frac{g_r \omega}{k\, k_R}\right)^2$$

so

$$\boxed{\gamma_{eff} = \left(\frac{\omega}{\lambda\, k_R}\right)^2} \qquad (3.11)$$

and the damping distance is

$$\boxed{\frac{d}{k} = \frac{1}{k_I}} \qquad (3.12)$$

For a compressible gas in a gravitational field, acoustic waves will not propagate vertically if

$$\omega^2 < \omega_1^2 = \frac{\gamma^2 g^2}{4c^2}$$

and gravity waves will not propagate if

$$\omega^2 > \omega_2^2 = \frac{(\gamma-1)\, g^2}{c^2}\left(1 - \frac{\beta}{\beta_a}\right)$$

where $\beta(z) = \frac{dT}{dz}$ and $\beta_a = \left(\frac{dT}{dz}\right)_{\text{adiabatic}}$.

(ref. D.Moore and E.Spiegel, to be published Ap.J. Nov.1963).

Thus there exists a stop band of frequencies that will not be propagated in an atmosphere and the lower pass band is strongly dependent on the effect of radiation since γ_{eff} is near 1.

c) Time Damping

Now we will investigate the time behavior of the sound waves for given real wave number K. The dispersion relation we found was

$$\omega^3 - i\sigma\omega^2 - \omega\left(\frac{\gamma p_0}{\rho_0}\right)K^2 + i\sigma\left(\frac{p_0}{\rho_0}\right)K^2 = 0$$

In general ω will be complex, $\omega = \omega_R + i\omega_I$, where the real part is the frequency and the imaginary part the inverse of the damping time.

The condition for undamped propagation, $\omega_I \to 0$, is the same as found before, i.e. either

$$\omega^2 = \left(\frac{\gamma p_0}{\rho_0}\right)K^2 \quad \text{when} \quad q_r \to 0$$

or

$$\omega^2 = \left(\frac{p_0}{\rho_0}\right)K^2 \quad \text{when} \quad \omega << q_r$$

Consider the two limiting cases of weak and strong radiation, i.e. $q_r \to 0, \infty$.

a) $\omega >> q_r$, the cooling time is much greater than the period. The 0th order solution,

$$\omega = \gamma^{1/2} c K,$$

is real so there is no damping. Substitute this 0th order solution into the small terms in the dispersion relation. Then

$$\omega^3 - \omega\gamma c^2 k^2 - i\sigma c^2 k^2 (\gamma - 1) = 0$$

where c is the isothermal sound speed, $c^2 = p_0/\rho_0$. The solution of $x^3 + ax + b = 0$ is

$$X = \begin{cases} A + B \\ -\frac{A+B}{2} \pm i\sqrt{3}\,\frac{A-B}{2} \end{cases}$$

where

$$\begin{Bmatrix} A \\ B \end{Bmatrix} = \left[-\frac{b}{2} \pm \sqrt{\frac{b^2}{4} + \frac{a^3}{27}} \right]^{1/3}$$

Here

$$a = -\gamma c^2 k^2$$
$$b = -i\sigma(\gamma - 1)c^2 k^2 << a$$

so

$$A + B = b\left(\frac{3}{a^3}\right)^{1/2} = (\gamma - 1)\left(\frac{3}{\gamma^3}\right)^{1/2} \frac{\sigma}{ck}$$

$$A - B = 2\left(\frac{a}{3}\right)^{1/2}\left(1 + \frac{9}{8}\,\frac{b^2}{a^3}\right)$$

$$= 2i\left(\frac{\gamma}{3}\right)^{1/2} ck \left(1 + \frac{9}{8}\,\frac{(\gamma-1)^2}{\gamma^3}\,\frac{\sigma^2}{c^2k^2}\right)$$

then

$$\omega = \begin{cases} (\gamma - 1)\left(\frac{3}{\gamma^3}\right)^{1/2} \frac{\sigma}{ck} \\ \pm \gamma^{1/2} ck \left[1 + \frac{\gamma - 1}{\gamma}\,\frac{\sigma}{c^2k^2}\left(\frac{9}{8}\,\frac{\gamma - 1}{\gamma^2}\,\sigma \mp 3^{1/2}\right)\right] \end{cases} \tag{3.13}$$

Thus ω is real to first order.

b) $\omega << q_T$, the cooling time is much less than the period.

The 0th order solution,

$$\omega = cK,$$

is real. Substitute this solution into the small terms in the dispersion relation. Then

$$\omega^2 = c^2K^2\left[1 + i(\gamma-1)\frac{cK}{\sigma}\right]$$

so
$$|\omega| = cK\left[1 + (\gamma-1)^2\left(\frac{cK}{\sigma}\right)^2\right]^{1/4}$$

$$\varphi = \tfrac{1}{2}\tan^{-1}\left[(\gamma-1)\frac{cK}{\sigma}\right]$$

In this case, φ is small so

$$\cos\varphi = 1, \quad \sin\varphi = \varphi = \frac{\gamma-1}{2}\frac{cK}{\sigma}$$

Then the real and imaginary parts of ω are

$$\omega_R = cK\left(1 + \left(\frac{\gamma-1}{2}\frac{cK}{\sigma}\right)^2\right)$$

$$\omega_I = \frac{\gamma-1}{2}\frac{c^2K^2}{\sigma} \tag{3.14}$$

Thus the damping time in units of the period is

$$\frac{\omega_R}{\omega_I} = \frac{2}{\gamma-1}\frac{\sigma}{cK}\left(1 + \left(\frac{\gamma-1}{2}\frac{cK}{\sigma}\right)^2\right) \tag{3.15}$$

This goes to infinity as $K \to 0$ or ∞ and has a minimum value of

$$\left(\frac{\omega_R}{\omega_I}\right)_{min.} = 2$$

at
$$K = \left(\frac{\gamma-1}{2}\frac{c}{\sigma}\right)^{-1}.$$

The full dispersion relation is a cubic equation for ω. In non-dimensional form

$$\omega'^3 - i\sigma'\omega'^2 - \omega'\gamma\lambda^2K'^2 + i\sigma'\lambda^2K'^2 = 0$$

where $\omega' = \omega/q_f$, $K' = K/\kappa$ and $\lambda = \frac{c\kappa}{q_f}$

and $c = p_0/\rho_0$ is the isothermal sound speed. The solution is

$$\omega = \begin{cases} A + B - p/3 \\ -\frac{A+B}{2} - \frac{p}{3} \pm i\sqrt{3}\,\frac{A-B}{2} \end{cases}$$

where

$$A = \left[-\frac{b}{2} + \sqrt{\frac{b^2}{4} + \frac{a^3}{27}} \right]^{1/3}$$

$$B = \left[-\frac{b}{2} - \sqrt{\frac{b^2}{4} + \frac{a^3}{27}} \right]^{1/3}$$

and

$$p = -i\sigma'$$

$$a = \frac{\sigma'^2}{3} - \gamma\lambda^2 K'^2$$

$$b = \frac{i\sigma'}{3}\left[\lambda^2 K'^2 (3-\gamma) + \frac{2}{9}\sigma'^2\right]$$

IV. Radiative Structure of Shock Waves

A shock front is the piling up of fluid that occurs because a disturbance in supersonic flow cannot propagate signals upstream. Shock fronts are narrow layers in a fluid where the gradients of velocity and temperature are large and where irreversible processes therefore occur. These transition zones are of the order of one particle mean free path thick so that the model of the fluid as a continuum is not valid in the transition layer. However, it is possible to study the flow through such a discontinuity by treating the equations of motion as conservation laws and deriving jump conditions at the discontinuity. To treat the structure of the

shock transition, it is necessary to consider the molecular and atomic processes that occur.

In the shock transition, the kinetic energy of the mass flow ahead of the shock is converted into thermal energy. This occurs by elastic collisions of the atomic particles in a distance of the order of one mean free path. The thermal energy is then redistributed among the various degrees of freedom of the system, (excitation, ionization or dissociation of atoms and molecules and radiation, over distances depending on the rates of the various processes.

I will consider only the effects of radiation on the shock structure. Viscosity and conduction act over much shorter distances than radiation and their effects can therefore be included in the discontinuity at the shock interface. I will consider only steady plane-parallel (one-dimensional) flow, in the coordinate system moving with the shock front, so that the shock is stationary.

A. Conservation Laws

The equations of motion for inviscid steady flow in one-dimension are

$$\frac{d}{dx}(\rho u) = 0$$

$$\rho u \frac{du}{dx} = -\frac{dp}{dx}$$

$$\rho c_v u \frac{dT}{dx} + p \frac{du}{dx} = -\frac{dF_r}{dx} + Q$$

where F_r is the radiative energy flux (ergs/cm^{2}sec) and Q is the rate of energy input from other sources. The pressure is

$$p = \frac{R}{\mu} \rho T$$

for an ideal gas, or including radiation pressure

$$P = \frac{R}{\mu}\rho T + \frac{1}{3}aT^3$$

where μ is the mean molecular weight. If the radiation pressure is neglected, the equations of motion can be put in the form of conservation laws

$$\boxed{\begin{aligned} &\frac{d}{dx}(\rho u) = 0 \\ &\frac{d}{dx}(\rho u^2 + P) = 0 \\ &\frac{d}{dx}\left[\rho u\left(c_p T + \tfrac{1}{2}u^2\right) + F_r\right] = Q \end{aligned}} \qquad (4.1)$$

In integrated form these are the Rankine-Hugoniot Shock Relations

$$\boxed{\begin{aligned} &\rho u = \rho_1 u_1 \\ &\rho u^2 + P = \rho_1 u_1^2 + P_1 \\ &\rho u\left(c_p T + \tfrac{1}{2}u^2\right) + F_r - \int Q\,dx = \rho_1 u_1\left(c_p T_1 + \tfrac{1}{2}u_1^2\right) \end{aligned}} \qquad (4.2)$$

where the subscript 1 denotes the state at some given point X_1, here taken far ahead of the shock, $X_1 \longrightarrow \infty$, so $F_{r1} = 0$. These relations must hold everywhere, even across a shock transition.

If all the irreversible processes, (radiation, conduction, viscosity, ionization, etc.), are confined to an infinitesimal layer, the shock structure shrinks to a sharp discontinuity where the state of the fluid is constant ahead (1) and behind (2) the shock.

$$\boxed{\begin{aligned} &\frac{u_2}{u_1} = \frac{1}{\gamma+1}\left(\gamma - 1 + \frac{2}{M_1^2}\right) \\ &\frac{T_2}{T_1} = 1 + \frac{2(\gamma-1)}{(\gamma+1)^2}\left(M_1^2 - 1\right)\left(\gamma + \frac{1}{M_1^2}\right) \\ &\frac{P_2}{P_1} = \frac{1}{\gamma+1}\left(1 - \gamma + 2\gamma M_1^2\right) \end{aligned}} \qquad (4.3)$$

(ref.Patterson, Molecular Flow of Gases, Wiley, 1956.)

B. Radiative Shock Structure

Consider now the effect of radiation on the shock structure. All other dissipative processes are lumped into the discontinuity at the shock face. Thus we assume the photon mean free path is much greater than the particle mean free path, so that all collisional relaxation processes are completed in essentially zero optical depth behind the shock. In this section we will consider a closed, (i.e. infinite), system, with plane parallel flow through a normal shock front.

Gas is heated on passing through a shock front and will emit radiation. Some of the emitted radiation from behind the shock will pass forward through the shock face, (since the photon mean free path is greater than the particle mean free path the shock transition is optically thin), and will be absorbed by the gas ahead of the shock heating it. Thus, the gas will come into the shock with a higher temperature and so a lower velocity than without radiation. The conservation laws may now be applied at the shock face giving the new temperature immediately behind the shock.

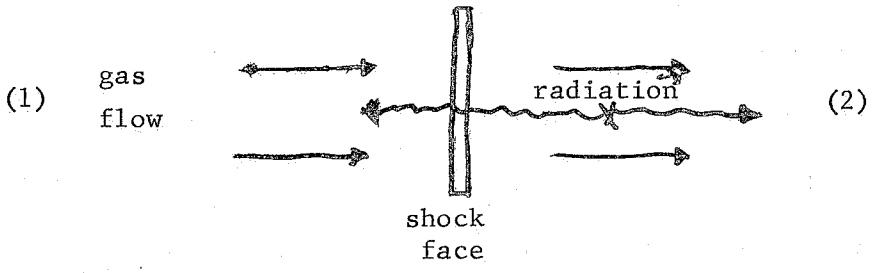

If the flow velocity ahead of the shock is large the temperature behind the shock will be greater than without radiation, since the temperature jump starts from a higher value. If the flow velocity ahead

of the shock is small, and it decreases as the gas is preheated, then just ahead of the shock face the flow will become either slightly supersonic or possibly subsonic, and the temperature behind the shock will be less than without radiation. Thus for low Mach numbers radiation reduces the discontinuity in the state of the gas.

For very strong shocks with very high temperatures behind them, the radiation through the shock is strong and the gas in front is heated up sufficiently to radiate. Thus photons coming through the shock will be absorbed and reemitted, and so diffuse forward, heating up the gas above its asymptotic value T_1 to large optical distance. Behind the shock, the temperature falls to its asymptotic value T_2 within one photon mean free path since the gas can radiate energy to the colder region in front of the shock.

Far away from the shock front the asymptotic state of the gas is the same as without radiation, since the radiation is confined to the region around the shock. That is, the radiative flux goes to zero as $x \longrightarrow \pm \infty$.

The total rate of radiation of energy from behind a strong shock is nearly equal to the rate at which non-thermal kinetic energy is carried through the shock front. We can write the energy conservation equation as

$$\int Q_r\,dx + \int Q_i\,dx = \tfrac{1}{2}\rho_s u_s^3 + \frac{\gamma}{\gamma-1} P_s u_s - \tfrac{1}{2}\rho_2 u_2^3 - \frac{\gamma}{\gamma-1} P_2 u_2$$

where the subscript s refers to values just ahead of the shock and 2 refers to asymptotic values far behind the shock. Q_r is the rate

of energy radiation by the fluid and Q_i the rate of energy absorption by ionization. For a strong shock

$$p_2 \approx \rho_s u_s^2$$

$$u_2 << u_s$$

$$p_s u_s << \tfrac{1}{2} \rho_s u_s^3$$

and the energy absorbed by ionization is later released by recombination so $\int Q_i \, dx \approx 0$. Thus

$$\int Q_r \, dx \leq \tfrac{1}{2} \rho_s u_s^3 \qquad (4.4)$$

If we represent the radiation leaving the high-temperature region behind the shock by two anti-parallel beams of flux $F_{\pm}$ then the flux forward through the shock is

$$F_- = \tfrac{1}{2} \int Q_r \, dx \leq \tfrac{1}{4} \rho_s u_s^3$$

(ref. Skalafuris, thesis, Brandeis Univ. 1963).

For shocks where the effect of radiation is small, we can derive an analytic expression for the radiative structure by a perturbation expansion about the "no-radiation" structure. (ref. Heaslet and Baldwin, Physics of Fluids, 6, 781, 1963). The conservation laws can be written as

$$\rho u = m$$

$$m u + p = m C_1$$

$$m \left(C_p T + \tfrac{1}{2} u^2 \right) + F_r = m C_2$$

and $p = R \rho T$. Here, m, C_1 and C_2 are constants. Then the momentum conservation law implies

$$T = \frac{1}{R} \left(C_1 - u \right) u \qquad (4.5)$$

and substituting this in the energy conservation law gives

$$u^2 - \frac{2\gamma}{\gamma+1} c_1 u + \frac{2(\gamma-1)}{\gamma+1} c_2 = \frac{2(\gamma-1)}{m(\gamma+1)} F_r$$

Now at $x = \pm \infty$ the radiative flux $F_r = 0$ and the velocity has its "no-radiation" values $u = u_1$, u_2, so the above equation has the form

$$\boxed{(u-u_1)(u-u_2) = K F_r} \tag{4.6}$$

where $K = \frac{2(\gamma-1)}{m(\gamma+1)}$

Expand u about the "no-radiation" values

$$\left.\begin{aligned} u &= u_0 + \delta u \\ T &= \frac{1}{R}(c_1 - u_0 - \delta u)(u_0 + \delta u) \\ &= \frac{1}{R}(c_1 - u_0)u_0 + \frac{1}{R}(c_1 - 2u_0)\delta u \\ &= T_0 + \delta T \end{aligned}\right\} \tag{4.7}$$

so

and $(u-u_1)(u-u_2) = (u_0 - u_1 + \delta u)(u_0 - u_2 + \delta u)$

$= (u_0 - u_1$

so the first order equation is

$$(2u_0 - u_1 - u_2)\,\delta u = K F_r(T_0) \tag{4.8}$$

The radiative flux plane parallel flow, assuming local thermodynamic equilibrium, is given by the expression

$$F_r(\tau) = 2\sigma\left[\int_{-\infty}^{\tau} T^4 E_2(\tau - \tau')\,d\tau' - \int_{\tau}^{\infty} T^4 E_2(\tau' - \tau)\,d\tau'\right]$$

then

$$F_r(\tau < 0) = 2\sigma\left[T_1^4 \int_{-\infty}^{\tau} E_2(\tau - \tau')\,d\tau' - T_1^4 \int_{\tau}^{0} E_2(\tau - \tau')\,d\tau' - T_2^4 \int_{0}^{\infty} E_2(\tau' - \tau)\,d\tau'\right]$$

and $\int_a^b E_n(x)\,dx = -E_{n+1}(x)\Big|_a^b$

so $F_r(\tau<0) = -2\sigma(T_2^4 - T_1^4)E_3(|\tau|)$

and $F_r(\tau>0) = 2\sigma\left[T_1^4\int_{-\infty}^{0} E_2(\tau-\tau')\,d\tau' + T_2^4\int_0^{\tau} E_2(\tau-\tau')\,d\tau' - T_2^4\int_{\tau}^{\infty} E_2(\tau'-\tau)\,d\tau'\right]$

$= -2\sigma(T_2^4 - T_1^4)E_3(|\tau|).$

Thus

$$F_{r0}(\tau) = -2\sigma(T_2^4 - T_1^4)E_3(|\tau|) \tag{4.9}$$

---

note: the flux is always in the direction of $-\tau$

so

$$\delta u(\tau) = -\frac{2\sigma K}{2u_0 - u_1 - u_2}(T_2^4 - T_1^4)E_3(|\tau|).$$

Thus the first order corrections to the velocity are

$$\boxed{\begin{aligned}\delta u(\tau<0) &= -\frac{2\sigma K}{u_1 - u_2}(T_2^4 - T_1^4)E_3(|\tau|)\\ \delta u(\tau>0) &= +\frac{2\sigma K}{u_1 - u_2}(T_2^4 - T_1^4)E_3(|\tau|)\end{aligned}} \tag{4.10}$$

The temperature correction is given by

$$\delta T = (C_1 - 2u_0)\,\delta u$$

where $C_1 = u_1 + \frac{P_1}{m}$

Ahead of the shock

$u_1^2 > \gamma P_1/\rho_1$ so $\rho_1 u_1^2 > \gamma P_1$ and $\gamma > 1$

Thus ahead of the shock $C_1 - 2u_0 = C_1 - 2u_1 < 0$ so $\delta T > 0$.

Behind the shock $C_1 - 2u_0 = C_1 - 2u_2$

and $u_2 = \frac{u_1}{\gamma+1}\left(\gamma-1+\frac{2}{M_1^2}\right)$

so $c_1 - 2u_2 = u_1 + \frac{P_1}{\rho_1 u_1} - 2u_1\frac{\gamma-1}{\gamma+1} - \frac{4u_1}{(\gamma+1)M_1^2}$

$$= u_1\left(\frac{P_1}{\rho_1 u_1^2} + 1 - 2\frac{\gamma-1}{\gamma+1} - \frac{4}{(\gamma+1)M_1^2}\right)$$

$$= u_1\left(\frac{1}{\gamma M_1^2} + 1 - 2\frac{\gamma-1}{\gamma+1} - \frac{4}{(\gamma+1)M_1^2}\right)$$

$$= u_1\left(1 - 2\frac{\gamma-1}{\gamma+1} - \frac{3\gamma-1}{\gamma(\gamma+1)}\frac{1}{M_1^2}\right)$$

Thus

$$\delta T(\tau>0) < 0 \quad \text{for } M_1^2 < \frac{3\gamma-1}{\gamma(3-\gamma)}$$

$$\delta T(\tau<0) > 0 \quad \text{for } M_1^2 > \frac{3\gamma-1}{\gamma(3-\gamma)}$$

The temperature is rounded off for a weak shock and peaked for a strong shock.

$$\boxed{\begin{aligned}\delta T(\tau<0) &= 2\sigma K u_1\left(1-\frac{1}{\gamma M_1^2}\right)\frac{T_2^4 - T_1^4}{u_1-u_2}E_3(|\tau|)\\ \delta T(\tau>0) &= 2\sigma K u_1\left(\frac{3-\gamma}{\gamma+1} - \frac{3\gamma-1}{(\gamma+1)\gamma M_1^2}\right)\frac{T_2^4 - T_1^4}{u_1-u_2}E_3(|\tau|)\end{aligned}} \qquad (4.11)$$

For an infinitely strong shock the rise in temperature behind the shock is $\frac{3-\gamma}{\gamma+1} \leq 1$ times the rise in front.

Note: $E_n(x) \sim \frac{e^{-x}}{x}$ for $x \to \infty$

These distributions look like this:

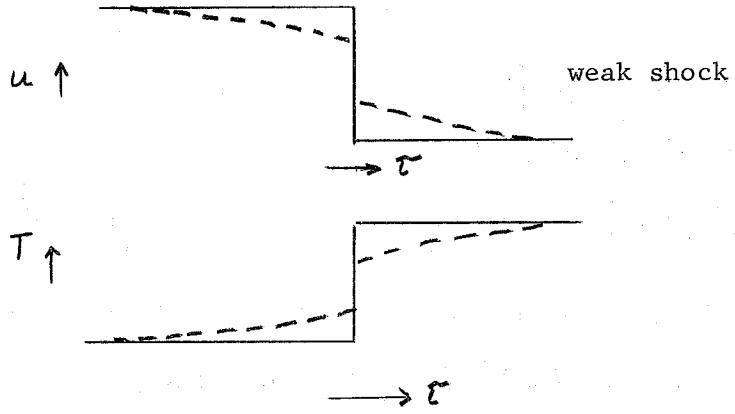

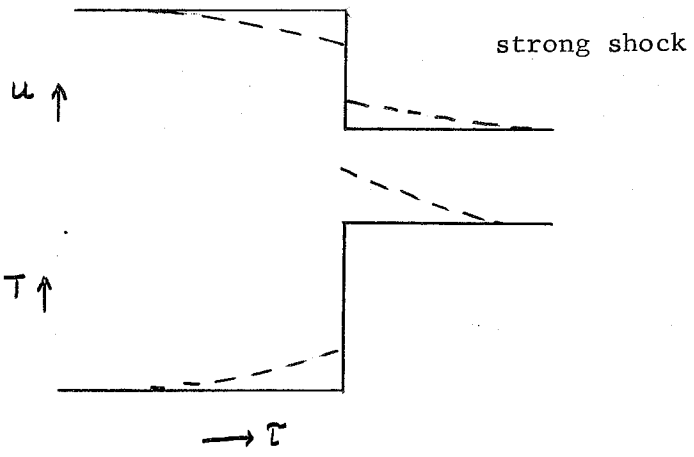

where the decay distance is of order $\tau = 1$, i.e. one photon mean free path.

The condition that there be no discontinuity is

$$-\delta u(0_-) + \delta u(0_+) \geq u_1 - u_2$$

or

$$2\sigma\left(K\,\frac{T_2^4 - T_1^4}{u_1 - u_2}\right. \geq u_1 - u_2$$

or

$$2\sigma K \geq \frac{(u_1 - u_2)^2}{T_2^4 - T_1^4}.$$

Use $T = \frac{1}{R}(c_1 - u)u$

and scale the velocities by $c_1 = u_1\left(1 + \frac{1}{\gamma M_1^2}\right)$. Then the condition for no discontinuity becomes

$$K^* = \frac{2\sigma K c_1^6}{R^4} \geq \frac{(u_1 - u_2)^2}{\left[u_2^4(1-u_2)^4 - u_1^4(1-u_1)^4\right]} \tag{4.12}$$

This is the condition that the flow ahead of the shock becomes subsonic on preheating.

We can obtain an approximate solution for the structure of shocks with large radiative effects and gain a physical picture of

the radiative processes occurring in a shock transition by constructing a crude model. Assume that away from the shock all quantities change slowly, while just behind the shock face is an optically-thin region of rapid change in which absorption can be neglected. The basic conservation law is

$$(u-u_1)(u-u_2) = K F_r$$

where the radiative flux is

$$F_r = 2\sigma \left\{ \int_{-\infty}^{\tau} T^4 E_2(\tau-\tau')\, d\tau' - \int_{\tau}^{\infty} T^4 E_2(\tau'-\tau)\, d\tau' \right\}$$

and

$$\frac{dF_r}{d\tau} = 4\pi \left(\frac{\sigma}{\pi} T^4 - J \right)$$

$$J = \frac{1}{2} \int_{-\infty}^{\infty} T^4 E_1(|\tau-\tau'|)\, d\tau'$$

Away from the shock, we expand T^4 in a Taylor series about the point τ, carry out the integration explicitly, and keep only the lowest order term

$$F_r = -\frac{16\sigma T^3}{3} \frac{dT}{d\tau}$$

since all higher derivatives are small. This is the Eddington approximation and is equivalent to expanding the distribution function in Legendre polynomials and neglecting the second anisotropic term proportional to $P_2(\cos\theta)$. This approximation will hold where the distribution of photons is nearly isotropic, i.e. away from any disturbance. It thus applies ahead of and far behind the shock. In the shock transition layer, the region of rapid change, we neglect absorption in the equation for the flux, so

$$\frac{dF_r}{d\tau} = 4\sigma T^4 = \frac{4\sigma}{R^4} u^4 (c_1 - u)^4$$

and we use this relation in the conservation law differentiated with respect to τ. We get the following set of equations:

$$\frac{du}{d\tau} = -\frac{3R^4}{16\sigma K}\left[\frac{(u-u_1)(u-u_2)}{u^3(c_1-u)^3(c_1-2u)}\right] \qquad \text{away from shock}$$

$$\frac{du}{d\tau} = \frac{4\sigma K}{R^4}\left[\frac{u^4(c_1-u)^4}{2u-u_1-u_2}\right] \qquad \text{shock transition layer}$$

In non-dimensional form scaling the velocities by c_1, the equations become

$$\boxed{\frac{du}{d\tau''} = -\frac{(u-u_1)(u-u_2)}{u^3(1-u)^3(1-2u)} \qquad \text{Eddington}}$$

$$\boxed{\frac{du}{d\tau'} = \frac{u^4(1-u)^4}{2u-u_1-u_2} \qquad \text{shock layer}} \qquad (4.13)$$

where the reduced optical depths are

$$\tau'' = \frac{3R^4}{16\sigma K c_1^6}\tau \qquad \text{Eddington}$$

$$\tau' = \frac{4\sigma K c_1^6}{R^4}\tau \qquad \text{shock layer}$$

First, note that since these are both first order equations with different expressions for the derivative, the slopes of the solutions will not in general match. We do not have the usual kind of boundary layer problem, for our solution will be continuous but only piecewise smooth. Because the shock layer solution is valid

only at small optical depths, (it does not tend to the asymptotic value u_2), yet does not fit smoothly onto an Eddington solution, (that does go to u_2 as $\tau \to +\infty$), the solution of the model is not unique. The switchover from the optically-thin to the Eddington approximation may be done at any point, giving a whole family of solutions corresponding to different radiation strengths. Another physical condition is necessary to choose a unique solution and $\pm$ will use the condition that the thickness of the optically-thin region be one in the reduced optical depth, τ'.

Second, the parameter determining the importance of the radiative effects is

$$K^* = \frac{2\sigma(\gamma-1)c_1^6}{\rho_1 u_1 (\gamma+1) R^4} = 2.7 \times 10^{-37} \left(\frac{\gamma-1}{\gamma+1}\right)\left(1+\frac{1}{\gamma M_1^2}\right)^6 \frac{u_1^5}{\rho_1}$$

since $c_1 = u_1 + \frac{p_1}{\rho_1 u_1} = u_1\left(1+\frac{1}{\gamma M_1^2}\right)$. The independent variables τ', τ'' are reciprical in their dependence on the shock velocity u_1. For a strong shock, the region of rapid change, (shock transition layer), will be of thickness 1 in τ' which is of order u_1^{-6} in τ, while the extent of the diffusion region ahead of the shock will be of order 1 in τ'' which is of order u_1^6 in τ. Thus the radiation can diffuse many photon mean free paths away from a medium strong shock.

Third, for $K^* \to 0$, $\left(\frac{du}{d\tau}\right)_{\text{shock layer}} \longrightarrow 0$ so $u =$ constant in the transition region, while in the Eddington region of the shock $\left(\frac{du}{d\tau}\right)_{\text{Eddington}} \longrightarrow \infty$ unless $u = u_1$ or u_2. Thus we recover the "no-radiation" solution. On the other hand, for $K^* \to \infty$, $\left(\frac{du}{d\tau}\right)_{\text{Eddington}} \longrightarrow 0$ and $\left(\frac{du}{d\tau}\right)_{\text{shock layer}} \longrightarrow \infty$, so there is

an extremely sharp transition at the shock but no diffusion tail.

The consequences of our model are explicated by making the additional approximation of expanding the velocity about some constant mean value in each of the regions of the shock transition and linearizing the expression for the derivative $\frac{du}{d\tau}$. Ahead of the shock, zone 1, expand about u_1 ; just behind the shock, zone 2, expand about $\bar{u} = \frac{1}{2}(u_1 + u_2)$, further behind the shock, zones 3 and 4, expand about u_2. Zones 1 and 4 are radiative diffusion regions and zones 2 and 3 are the optically-thin shock layers.

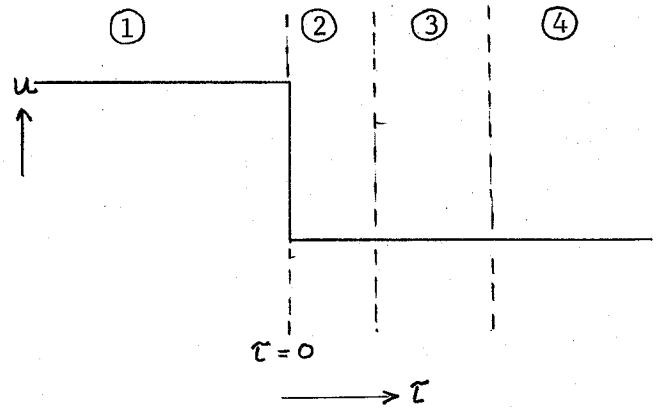

Zone 1, ahead of the shock:

Use the Eddington approximation and expand

$$u = u_1 + u^*, \quad u^* < 0$$

so

$$\frac{du^*}{d\tau''} = \frac{u^*}{A_1}$$

where

$$A_1 = \frac{u_1^3 (1-u_1)^3 (2u_1 - 1)}{u_1 - u_2}$$

$$\leq \frac{1}{64} \frac{1}{u_1 - u_2}$$

The asymptotic velocities satisfy the conditions

$$\frac{u_1}{c_1} = \left(1 + \frac{1}{\gamma M_1^2}\right)^{-1} \geq \frac{\gamma}{\gamma+1} \geq \frac{1}{2}$$

$$\frac{u_2}{c_1} = \frac{\gamma}{\gamma+1}\left[\frac{(\gamma-1)M_1^2+2}{\gamma M_1^2+1}\right] \leq \frac{1}{2} \quad \text{for } M_1^2 \geq \frac{3\gamma-1}{\gamma(3-\gamma)}$$

Thus ahead of the shock

$$\frac{du^*}{d\tau''} < 0$$

$$u = u_1 - \alpha' e^{-3\tau/16 K^* A_1}$$

and the temperature distribution is

$$\frac{dT}{d\tau''} = (1 - 2u_1 + 2|u^*|)\frac{du}{d\tau''} > 0$$

$$T = u_1(1-u_1) + \alpha'(2u_1 - 1)e^{-3\tau/16 K^* A_1}$$

Zone 2, just behind the shock face:

Use the optically-thin approximation and expand

$$u = \bar{u} + u^*, \quad \bar{u} = \tfrac{1}{2}(u_1 + u_2), \quad u^* < 0$$

so

$$\frac{du^*}{d\tau'} = \frac{A_2 - B_2 u^*}{u^*}$$

where

$$A_2 = \bar{u}^4(1-\bar{u})^4$$

$$B_2 = 4\bar{u}^3(1-\bar{u})^3(2u-1)$$

and

$$\frac{\bar{u}}{c_1} = \frac{1}{\gamma+1}\left(\frac{\gamma + \frac{1}{M_1^2}}{1 + \frac{1}{\gamma M_1^2}}\right) = \frac{\gamma}{\gamma+1} \geq \frac{1}{2}$$

Thus just behind the shock

$$\frac{du^*}{d\tau'} < 0$$

$$\frac{dT}{d\tau'} = (1 - 2\bar{u} + 2|u^*|)\frac{du^*}{d\tau'} > 0$$

$$\tau' + \alpha'' = \frac{1}{4K^* B_2^2}\left[A_2 - B_2 u^* - A_2 \ln(A_2 - B_2 u^*)\right]$$

Zone 3, behind the shock:

Use the optically-thin approximation and expand

$$u = u_2 + u^*, \quad u^* > 0$$

so

$$\frac{du^*}{d\tau'} = -\left(A_3 + B_3 u^*\right)$$

where

$$A_3 = \frac{u_2^4 (1-u_2)^4}{u_1 - u_2} > 0$$

$$B_3 = \frac{u_2^3 (1-u_2)^3}{(u_1-u_2)^2}\left[4u_1(1-2u_2) - 3u_2\left(1-\tfrac{7}{3}u_2\right)\right] > 0$$

since $B_3 > 0$ for $4u_1(1-2u_2) - 3u_2\left(1-\frac{7}{3}u_2\right) > 0$

or

$$\frac{u_2}{c_1} = \frac{\gamma}{\gamma+1}\left[\frac{(\gamma-1)M_1^2+2}{\gamma M_1^2+1}\right] < \left[\frac{\gamma+7-6/M_1^2}{\gamma+15-14/M_1^2}\right]$$

which is always satisfied for $M_1^2 \geq 1$ and $1 \leq \gamma \leq \frac{5}{3}$.

Thus behind the shock, for u near u_2

$$\frac{du^*}{d\tau'} < 0$$

$$u = u_2 + \frac{\alpha^3}{B_3} e^{-\tau' 4K^* B_3} - \frac{A_3}{B_3}$$

and the temperature distribution is

$$\frac{dT}{d\tau'} = (1-2u_2-2u^*)\frac{du^*}{d\tau'} \gtrless 0 \text{ for } M_1^2 \lesssim \frac{3\gamma-1}{\gamma(3-\gamma)}$$

$$T = T_2 + (1-2u_2)\left(\frac{\alpha^3}{B_3} e^{-\tau' 4K^* B_3} - \frac{A_3}{B_3}\right).$$

Note, u and T cross their asymptotic values u_2 and T_2 at some finite depth τ'. This result is due to the neglect of absorption in Zone 3.

Zone 4, far behind the shock:

Here use the Eddington approximation again and expand

$$u = u_2 + u^*, \quad u^* > 0$$

so
$$\frac{du^*}{d\tau''} = \frac{u^*}{A_4}$$

where
$$A_4 = \frac{u_2^3 (1-u_2)^3 (1-2u_2)}{u_1 - u_2}$$

Thus
$$\frac{du^*}{d\tau''} \lesseqgtr 0 \quad \text{for} \quad M_1^2 \lesseqgtr \frac{3\gamma-1}{\gamma(3-\gamma)}$$

$$\frac{dT}{d\tau''} = (1-2u_2-2u^*)\frac{du^*}{d\tau''} > 0$$

and
$$u = u_2 + \alpha^4 e^{+3\tau/16} K^* A_4$$

$$T = T_2 + (1-2u_2)\alpha^4 e^{+3\tau/16} K^* A_4$$

Therefore there exists a radiation diffusion region behind a shock only for weak shock where $A_4 < 0$ or $M_1^2 < \frac{3\gamma-1}{\gamma(3-\gamma)}$.

We now determine the integration constants $\alpha^1, \alpha^2, \alpha^3, \alpha^4$ by applying the Ranhine-Hugoniot relations at the shock face. The radiative flux is continuous across the shock face and so drops out. Then

$$M_s^2 = \frac{u_-^2}{c_-^2} = \frac{u_-^2}{\gamma R T_-} = \frac{u_-}{\gamma(1-u_-)}$$

$$u_- = u_- - \alpha^1 \quad \text{and} \quad T_- = T_1 + (2u_1 - 1)\alpha^1$$

$$u_+ = \frac{\gamma-1}{\gamma+1} u_- + \frac{2\gamma}{\gamma+1}(1-u_-) = \frac{2\gamma}{\gamma+1} - u_-$$

$$T_+ = T_- + \frac{2(\gamma-1)}{(\gamma+1)^2}(u_-(\gamma+1) - \gamma)$$

where the subscripts s, $-$, $+$ signify value at, just ahead, and just behind the shock face. First we determine α^1, which sets the scale for the whole structure. For strong shocks Zone 3 reaches to the shock face and for discontinuous weak shocks Zone 4 reaches to the shock face. In both cases

$$T_+ = T_2 + (1-2u_2)(u_+ - u_2)$$

$$u_+ = \frac{2\gamma}{\gamma+1} - u_1 + \alpha'$$

so we have the condition

$$T_2 + (1-2u_2)\left(\frac{2\gamma}{\gamma+1} - u_1 - u_2 + \alpha'\right)$$

$$= T_1 + (2u_1 - 1)\alpha' + \frac{2(\gamma-1)}{(\gamma+1)^2}\left((\gamma+1)(u_1-\alpha') - \gamma\right)$$

This reduces to

$$2\alpha_1\left[u_1 + u_2 - \frac{2\gamma}{\gamma+1}\right] = \left[u_1 + u_2 - \frac{2\gamma}{\gamma+1}\right]^2$$

But, $\bar{u} = \frac{u_1+u_2}{2} = \frac{\gamma}{\gamma+1}$, thus α' is undetermined. This indeterminacy is the specific realization of the non-uniqueness of the solutions of our model due to the arbitrariness in joining solutions from different regions.

For continuous weak shocks, $M_s \leq 1$, so $T_- = T_+$ and $u_- = u_+$, we have

$$T_+ = T_2 + (1-2u_2)(u_1 - \alpha' - u_2) = T_-$$

$$= T_1 + (2u_1 - 1)\alpha'$$

so

$$\alpha' = \frac{u_1 - u_2}{2}$$

Here α' is determinate since the Eddington regions join onto each other smoothly at the shock face.

If we choose an α' we can get u_- and therefore u_+ and so determine u_0^j , where u_0^j is the velocity at the front of Zone j . For Zone 2 we have

$$\alpha^2 = \frac{1}{4K^* B_2^2}\left[A_2 - B_2 u_0^* - A_2 \ln\left(A_2 - B_2 u_0^*\right)\right]$$

so $$\tau = \frac{1}{4K^* B_2^2}\left[B_2(u_0^* - u^*) - A_2 \ln\left(\frac{A_2 - B_2 u^*}{A_2 - B_2 u_0^*}\right)\right]$$

For Zone 3 we have

$$u_0 = u_2 + \frac{\alpha^3 - A_3}{B_3}$$

so

$$\alpha_3 = (u_0 - u_2) B_3 + A_3$$

so

$$u = \left(u_2 - u_0 - \frac{A_3}{B_3}\right)\left(1 - e^{-4K^* B_3 \tau}\right) + u_0 .$$

And, for Zone 4 we have

$$u_0 = u_2 + \alpha^4$$

so

$$u = (u_2 - u_0)\left(1 - e^{-3\tau/16 K^* A_4}\right) + u_0$$

Thus the solution of our linearized model is:

Zone 1

$$u = u_1 - \alpha' e^{-3\tau/16 K^* A_1}$$

$$T = T_1 + (2u_1 - 1)\alpha' e^{-3\tau/16 K^* A_1}$$

Zone 2

$$\tau = \frac{1}{4K^* B_2^2}\left[B_2(u_0^* - u^*) - A_2 \ln\left(\frac{A_2 - B_2 u^*}{A_2 - B_2 u_0^*}\right)\right]$$

where $u^* = u - \bar{u}$ and $T = u(1-u)$

Zone 3

$$u = u_0 + \left(u_2 - u_0 - \frac{A_3}{B_3}\right)\left(1 - e^{-4K^* B_3 \tau}\right)$$

$$T = T_2 + (1 - 2u_2)\left\{\left(u_0 - u_2 + \frac{A_3}{B_3}\right) e^{-4K^* B_3 \tau} - \frac{A_3}{B_3}\right\}$$

Zone 4

$$u = u_0 + (u_2 - u_0)\left(1 - e^{3\tau/16 K^* A_4}\right)$$

$$T = T_2 + (1 - 2u_2)(u_0 - u_2) e^{3\tau/16 K^* A_4}$$

This linearized model indicates the basic features of radiative shock structure. First, the magnitude of the radiative effects is determined by the parameter

$$K^* = 2.7 \times 10^{-37} \left(\frac{\gamma-1}{\gamma+1}\right) \frac{(\gamma M_1^2+1)^6}{(\gamma M_1^2)^3} \frac{T_1^3}{\rho_1 u_1}.$$

Second, for strong shocks there is a temperature peak behind the shock which is caused by the radiative pre-heating of the gas in front of the shock. For weak shocks, $M_1^2 < (3\gamma-1)/\gamma(3-\gamma)$, the radiation smooths out the discontinuity and for weak enough shocks reduces the velocity in front of the shock to subsonic values, thus making the structure continuous. Third, the structure ahead and behind a shock is asymmetric for strong radiation since the radiation diffuses out ahead of the shock while the temperature peak, being optically thin, is rapidly cooled by radiation. Fourth, as the shock strength increases, for given radiation strength, the shock structure becomes narrower since A_1 decreases.

A numerical integration of the basic conservation law $(u-u_1)(u-u_2) = k F_r$ has been done, (using an approximation for the E_2 -functions), by Heaslet and Baldwin, Phys. of Fluids, 6, 781, (1963). Their results are given on p.136.

We observe that the exact radiative structure is qualitatively the same as that given by the perturbation expansion for weak radiative effects and our crude model for strong radiative effects.

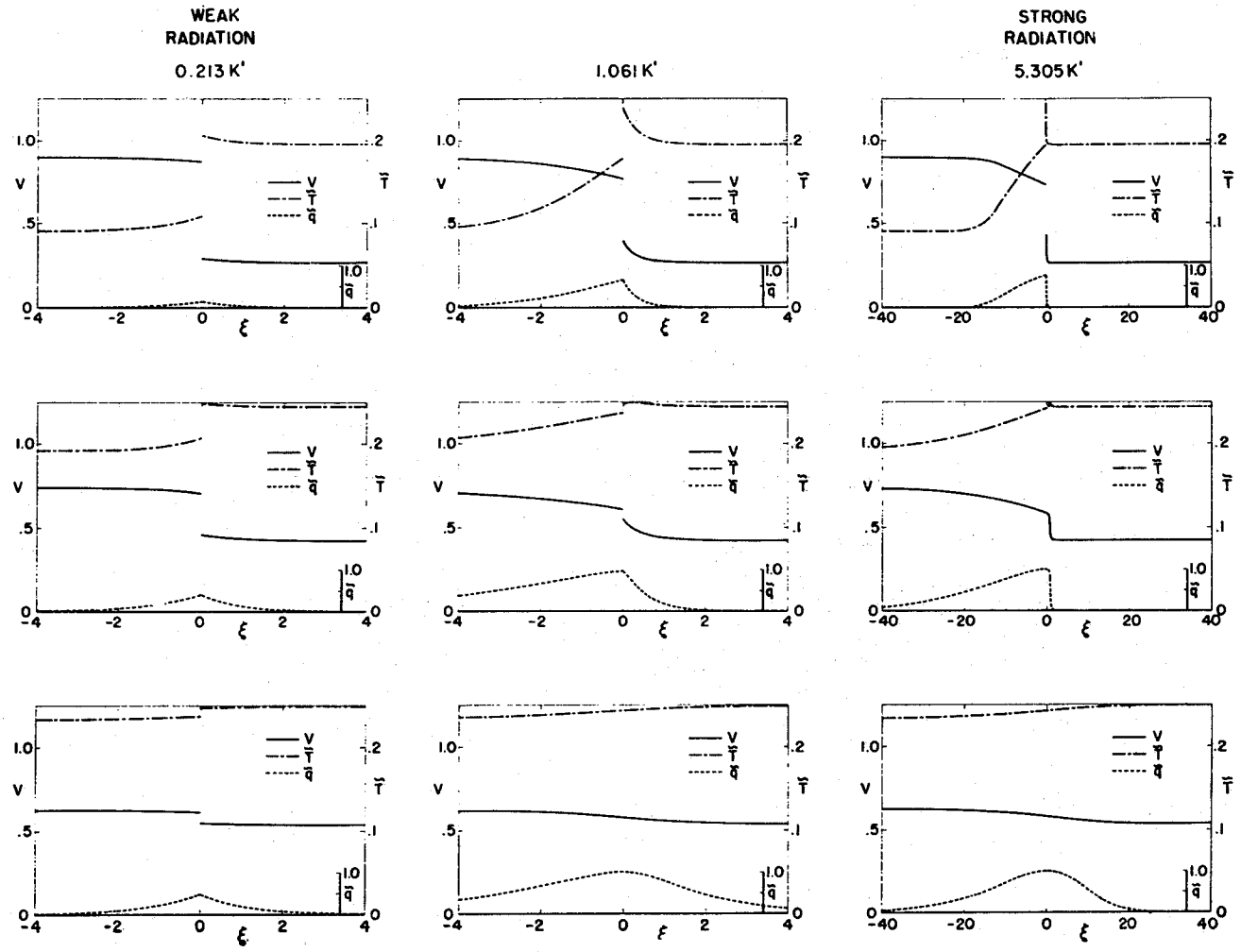

Fig. 2. Profiles of dimensionless velocity $\tilde{V}$, temperature $\tilde{T}$, and heat flux $\tilde{q}$.

$$\tilde{V} = \frac{u}{C_1}, \quad \tilde{T} = \frac{R}{C_1^2} T, \quad \tilde{q} = -\frac{4K}{(u_1 - u_2)^2} Fr$$

C. Optically Thin Systems

If the system through which a shock front moves is optically thin, then the radiation from the hot gas behind the shock is not absorbed by the gas ahead of the shock, the unshocked gas will not be preheated and the temperature behind the shock will fall below the value it would have without radiation. In order for the pressure behind the shock to support the momentum of the inrushing gas the density must increase as the temperature falls and by conservation of mass the velocity will fall. In this case the radiation acts as a heat sink and can be included in the energy conservation equation in terms of the total rate of energy loss $\int Q_r \, dx$ rather than in terms of the flux. (Ionization and dissociation act in the same way. Here thermal energy is converted into potential energy of the separation of charges and $\int Q_i \, dx = u n_i \chi$, where n_i is the number density of electrons or ions and χ is the ionization potential.)

For a strongly radiating shock in an optically thin medium, the temperature behind the shock will fall to its value ahead of the shock, (isothermal shock), and the main effect of the radiating shock will be to greatly increase the density. For a strong shock the conservation laws become approximately

$$\rho_2 u_2 \approx \rho_1 u_1$$

$$P_2 \approx \rho_1 u_1^2$$

and $$T_2 = T_1 = \frac{P_1}{\rho_1} = \frac{P_2}{\rho_2}$$

Thus $\rho_2 = \rho_1 \frac{P_2}{P_1} = \gamma \frac{P_1}{c_1^2} = \rho_1 \gamma \left(\frac{u_1}{c_1}\right)^2 = \rho_1 \gamma M_1^2$

which can get very large for high Mach number. (ref. W.Sargent, thesis Univ. of Manchester, 1959.)

To consider an optically thin medium, (which is equivalent to a system with a heat sink), we write the conservation laws in the form

$$\rho u = \rho_1 u_1$$

$$\rho u^2 + P = \rho_1 u_1^2 + P_1$$

$$\rho u \left(\frac{\gamma}{\gamma-1} RT + \frac{1}{2} u^2\right) + \int Q\,dx = \rho_1 u_1 \left(\frac{\gamma}{\gamma-1} RT + \frac{1}{2} u_1^2\right)$$

---

where Q is the rate of energy loss from the medium per unit volume, and

$$\int \frac{Q}{\rho u}\,dx = \int \frac{Q}{\rho} \frac{1}{u} \frac{dx}{dt}\,dt = \int \frac{Q}{\rho}\,dt$$

is the energy loss from the medium per gram.

To find the relation between the asymptotic states far ahead and behind the shock front, non-dimensionalize the conservation laws in terms of the values ahead of the shock:

$$v = \frac{u}{u_1} = \frac{\rho_1}{\rho}, \quad \theta = T/T_1, \quad \delta = \mu/\mu_1$$

so

$$\rho u^2 + \rho \frac{R}{\mu} T = \rho_1 \frac{R}{\mu_1} T_1 + \rho_1 u_1^2$$

$$\frac{\gamma}{\gamma-1} \frac{R}{\mu} T + \frac{1}{2} u^2 + \frac{\int Q\,dx}{\rho u} = \frac{\gamma}{\gamma-1} \frac{R}{\mu_1} T_1 + \frac{1}{2} u_1^2$$

become

$$\rho_1 u_1^2 v + \frac{\rho_1 R T_1}{\delta \mu_1} \frac{\theta}{v} = \rho_1 u_1^2 + \rho_1 \frac{R}{\mu_1} T_1$$

$$\frac{\gamma}{\gamma-1} \frac{R T_1}{\delta \mu_1} \theta + \frac{1}{2} u_1^2 v^2 + \frac{\int Q\,dx}{\rho_1 u_1} = \frac{\gamma}{\gamma-1} \frac{R}{\mu_1} T_1 + \frac{1}{2} u_1^2$$

Dividing the first by $\rho_1 u_1^2$ and the second by u_1^2 gives

$$U + \frac{\Theta}{U}\frac{1}{\gamma\delta M_1^2} = 1 + \frac{1}{\gamma M_1^2}$$

$$\frac{\Theta}{\delta(\gamma-1)M_1^2} + \frac{1}{2}U^2 + \frac{\int Q\,dx}{\rho_1 u_1^3} = \frac{1}{(\gamma-1)M_1^2} + \frac{1}{2}$$

so $$\Theta = \delta U\left(1 + \gamma M_1^2 - \gamma M_1^2 U\right)$$

and

$$-\frac{1}{2}\frac{\gamma+1}{\gamma-1}U^2 + \frac{\gamma}{\gamma-1}\left(1+\frac{1}{\gamma M_1^2}\right)U - \left(\frac{1}{2} + \frac{1}{(\gamma-1)M_1^2} - \int\tilde{Q}\,dx\right) = 0$$

so

$$U = \frac{\gamma}{\gamma+1}\left(1+\frac{1}{\gamma M_1^2}\right) \pm \frac{1}{\gamma+1}\left[\gamma^2\left(1+\frac{1}{\gamma M_1^2}\right)^2 - 2\left(\gamma^2-1\right)\left(\frac{1}{2} + \frac{1}{(\gamma-1)M_1^2} - \int\tilde{Q}\,dx\right)\right]^{1/2}$$

and

$$\left[\quad\right] = \left[\left(1-\frac{1}{M_1^2}\right)^2 + 2\left(\gamma^2-1\right)\int\tilde{Q}\,dx\right]$$

Thus

$$\boxed{U = \frac{1}{\gamma+1}\left[\gamma + \frac{1}{M_1^2} \pm \left(1-\frac{1}{M_1^2}\right)\sqrt{1 + \frac{2M_1^4(\gamma^2-1)\int\tilde{Q}\,dx}{(M_1^2-1)^2}}\right]} \qquad (4.14)$$

where $\int\tilde{Q}\,dx = \int(Q/\rho_1 u_1^3)\,dx = \frac{1}{\rho_1 u_1^2}\int Q\,dt$ is the rate of energy loss from the medium, scaled by the rate of kinetic energy input. The (-) sign corresponds to states behind the shock and the (+) sign to states in front. Thus a heat source $(-Q)$ causes the velocity to decrease in front of the shock and a heat sink (Q) causes the velocity to decrease behind the shock.

The pressure is

$$P = \frac{P_2}{P_1} = \Theta/U = \delta\left(1 + \gamma M_1^2 - \gamma M_1^2 U\right)$$

Thus $$\boxed{\underline{P} = \frac{\delta}{\gamma+1}\left[1+\gamma M_1^2 + \gamma(M_1^2-1)\eta\right]} \tag{4.15}$$

where $\eta = \sqrt{1 + \frac{2M_1^4(\gamma^2-1)\int\tilde{Q}\,dx}{(M_1^2-1)^2}}$. And, the temperature is

$$\Theta = \delta U\left(1+\gamma M_1^2 - \gamma M_1^2 U\right) = \underline{P}\,U$$

so

$$\Theta = \frac{\delta}{(\gamma+1)^2}\left[\left(\gamma+\frac{1}{M_1^2}\right)\left(\gamma M_1^2+1\right) - \gamma\left(1-\frac{1}{M_1^2}\right)\left(M_1^2-1\right)\right.$$

$$\left. + (\gamma-1)\left(M_1^2-1\right)\left(\gamma+\frac{1}{M_1^2}\right)\eta - 2\gamma(\gamma^2-1)M_1^2\int\tilde{Q}\,dx\right]$$

which equals

$$\boxed{\Theta = \delta\left[1+\frac{\gamma-1}{(\gamma+1)^2}\left(M_1^2-1\right)\left(\gamma+\frac{1}{M_1^2}\right)\left(1+\eta\right) - \frac{2\gamma(\gamma-1)}{\gamma+1}M_1^2\int\tilde{Q}\,dx\right]} \tag{4.16}$$

We thus observe that the effect of a heat sink behind a shock is to increase the density and pressure and to decrease the velocity and temperature from the values they would have had without the energy loss.

For a strong shock

$$U = \frac{1}{\gamma+1}\left[\gamma-\eta\right]$$

$$\underline{P} = \frac{\gamma\delta M_1^2}{\gamma+1}\left(1+\eta\right) \tag{4.17}$$

$$\Theta = \delta + \frac{\delta M_1^2\gamma(\gamma-1)}{\gamma+1}\left(\frac{1}{\gamma+1} + \frac{1}{\gamma+1}\eta - 2\varepsilon'\right)$$

where

$$\eta = \left(1+2(\gamma^2-1)\varepsilon'\right)^{1/2}, \quad \varepsilon' = \int\tilde{Q}\,dx$$

since

$$U > 0$$

$$\eta < \gamma \text{ or } 1+2(\gamma^2-1)\varepsilon' < \gamma^2$$

so $\varepsilon' < \frac{1}{2}$

Thus the maximum rate of energy loss for strong shock is

$$\int Q\,dx < \tfrac{1}{2}\rho_1 u_1^3$$

that is, the kinetic energy of mean flow. The extra increase in pressure is $\leq \frac{\gamma+1}{2}$, which is small. The extra increase in density is unlimited and the temperature can decrease to its value ahead of the shock.

D. Radiation Pressure

Consider now the effect of radiation pressure on the shock structure. The radiation pressure is $P_r = \frac{1}{3}\alpha T^4$ and so will be especially significant in the temperature peak just behind the shock. The takeover by radiation pressure of part of the support of the gas means that the gas pressure $P_g = \rho R T$ will decrease and so the temperature and density will be lower.

The conservation laws without heat sources or sinks are

$$\rho u = \rho_1 u_1$$

$$\rho u^2 + P = \rho_1 u_1^2 + P_1$$

$$C_p T + \tfrac{1}{2}u^2 + \frac{F_r}{\rho_1 u_1} = C_p T_1 + \tfrac{1}{2}u_1^2$$

and $P = P_g + P_r = \rho R T + \frac{1}{3}\alpha T^4$. Eliminating the pressure gives

$$\rho u = \rho_1 u_1$$

$$\rho u^2 + \rho RT + \tfrac{1}{3} a T^4 = \rho_1 u_1^2 + \rho_1 R T_1 + \tfrac{1}{3} a T_1^4$$

$$C_p T + \tfrac{1}{2} u^2 + \frac{F_r}{\rho_1 u_1} = C_p T_1 + \tfrac{1}{2} u_1^2$$

Put in non-dimensional form

$$\rho_1 u_1^2 U + \rho_1 R T_1 \frac{\Theta}{U} + \tfrac{1}{3} a T_1^4 \Theta^4 = \rho_1 u_1^2 + \rho_1 R T_1 + \tfrac{1}{3} a T_1^4$$

$$\frac{\gamma}{\gamma-1} R T_1 \Theta + \tfrac{1}{2} u_1^2 U^2 + \frac{F_r}{\rho_1 u_1} = \frac{\gamma}{\gamma-1} R T_1 + \tfrac{1}{2} u_1^2$$

or

$$U + \frac{1}{\gamma M_1^2} \frac{\Theta}{U} + \frac{\frac{1}{3} a T_1^4}{\rho_1 u_1^2} \Theta^4 = 1 + \frac{1}{\gamma M_1^2} + \frac{\frac{1}{3} a T_1^4}{\rho_1 u_1^2}$$

$$\frac{\Theta}{(\gamma-1) M_1^2} + \tfrac{1}{2} U^2 + \frac{F_r}{\rho_1 u_1^3} = \frac{1}{(\gamma-1) M_1^2} + \tfrac{1}{2}$$

The significance of radiation pressure depends on

$$\beta_1 \Theta^4 = \frac{\frac{1}{3} a T_1^4}{\rho_1 u_1^2} \Theta^4 = \tfrac{1}{3} \frac{a}{R^4} \left(\frac{1}{\gamma M_1^2}\right)^4 \frac{u_1^6}{\rho_1} \Theta^4$$

For strong shocks this becomes

$$\frac{2^4}{3} \frac{a}{R^4} \frac{(\gamma-1)^4}{(\gamma+1)^8} \frac{u_1^6}{\rho_1}$$

The shock structure is therefore determined by the set of equations

$$\boxed{\begin{aligned} &U + \frac{\Theta}{U} \frac{1}{\gamma M_1^2} + \beta_1 \Theta^4 = 1 + \frac{1}{\gamma M_1^2} + \beta_1 \\ &\frac{\Theta}{(\gamma-1) M_1^2} + \tfrac{1}{2} U^2 + \frac{F_r}{\rho_1 u_1^3} = \tfrac{1}{2} + \frac{1}{(\gamma-1) M_1^2} \\ &F_r = 2\sigma T_1^4 \left[\int_{-\infty}^{\tau} \Theta^4(\tau') E_2(\tau - \tau') d\tau' - \int_{\tau}^{\infty} \Theta^4(\tau') E_2(\tau' - \tau) d\tau' \right] \end{aligned}} \qquad (4.18)$$

where $\beta_1 = \frac{\frac{1}{3} a T_1^4}{\rho_1 u_1^2} = \frac{1}{3} \frac{a}{R^4} \left(\frac{1}{\gamma M_1^2}\right)^2 \frac{u_1^6}{\rho_1}$.

These can be integrated numerically.

E. Local Thermodynamic Equilibrium

We have assumed that the gas passing through the shock is in local thermodynamic equilibrium, (LTE), everywhere, so that the rate of emission of radiation is proportional to T^4. However, close behind a strong shock this is not valid. The gas passes through the shock with the occupation of its various energy states corresponding to equilibrium at the temperature T_s just ahead of the shock. The temperature just behind a strong shock is much higher, so that the low-energy states will be overpopulated and the high-energy states underpopulated relative to L.T.E.

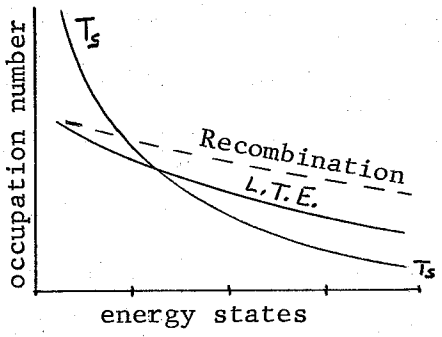

number of particles occupying various energy states just behind a shock.

The system is not in equilibrium because time is necessary for the atomic processes to redistribute the particles among the energy states. For high flow velocities the gas travels a large distance away from the shock front in the time necessary for relaxation.

The actual physical process is as follows: The gas comes through the shock face and is excited and ionized. This occurs by inelastic collisions with already present free electrons or by absorption of photons. Thus heat is absorbed from the electrons in

the inelastic collisions. For ionization $e + a \longrightarrow i + e + e$, the initial electron loses the ionization energy and the two final electrons have substantially less energy per particle. Similarly, in photoexcitation, the photons absorbed come predominantly from cooler regions and so have less than the local equilibrium energy. For ionization $\gamma + a \longrightarrow i + e$, the emitted electron has the low-photon energy further diminished by the ionization energy. Thus the temperature of the electrons is decreased below that of the atoms and ions. Elastic collisions between electrons, atoms and ions then bring down the atom and ion temperatures. Deexcitation and photorecombination then take place. The recombination rate is proportional $1/n$, while the equilibrium distribution is proportional e^{1/n^2}, where n is the principal quantum number of an energy level $\epsilon_n = -2\pi_m^2 z^2 e^4 / h^2 n^2$, therefore in the radiative region the upper levels will be overpopulated. Final equilibrium is reached through collisional deexcitation.

An accurate treatment of the radiative shock structure must therefore use the transport equation with the rates for the various important processes. (For a detailed treatment see Skalafuris, thesis Brandeis Univ. 1963 and W.Sargent, thesis, Univ. of Manchester, 1959.)

F. Discussion and Applications

Shock waves occur in stellar atmospheres of pulsating stars. The gas ahead of the shock, predominantly hydrogen, is opaque to Lyman radiation, (corresponding to the transition between the ground and

the first excited state of the hydrogen atom). Thus the gas ahead of the shock will be heated and ionized. This results in a substantial increase in temperature just behind the shock and this high temperature region will be optically thick in the first few Balmer lines but optically thin elsewhere. The gas behind the shock will thus be cooled by the lower energy photons. The main observable feature of a shock in the atmosphere of a star will be, therefore, Lyman emission from in front of the shock and Balmer emission from the back. For a detailed discussion see Shalafuris and Whitney, Ap.J. Aug. 1963.

The interstellar gas is composed mainly of hydrogen at a low temperature of about 100°K. Therefore it will be practically transparent to radiation of frequency $\nu < \nu_0$, (except for the Lyman α line), and will absorb radiation of frequency $\nu > \nu_0$, where $h\nu_0$ = 13.7 e.v. the ionization potential of hydrogen. However the opacity of hydrogen in the ground state falls off as $1/\nu^3$ for $\nu > \nu_0$, so the photon mean free path will increase with frequency. The collision of two clouds of interstellar gas will form shock fronts and heat up the gas. The greater the relative speed of collision, the higher the temperature will be and so the higher will be a typical frequency of the emitted radiation, $\nu \sim \frac{\kappa T}{h}$. The photon mean free paths in the interstellar medium for various shock speeds are,

SPEED (Km/sec)	T_{max} (°K)	λ_r (cm)
100	10^5	10^{17}
500	5×10^6	10^{21}
1000	2×10^7	10^{23}

(ref. W.Sargent, Thesis, Univ. of Manchester, 1959.)

The radius of the galactic disk is about 10^{21}cm so the galaxy is optically thin to radiation from strong shocks.

Thus if two clouds of interstellar gas collide with a relative speed greater than a few km/sec they will form a nearly isothermal shock and the main result will be a great increase in the density of the gas. This is one possible mechanism for the formation of star condensations.

A typical cloud has a radius of about 7 parsecs (1pc=3×10^{18}cm) and a mass of about 400 solar masses. The density of clouds is about 5×10^{-5} per cubic parsec and the interval between collisions is about 10^7 years. The root mean square cloud velocity is about 14 hm/sec and the fraction of clouds with velocities of the order of 200 km/sec is about 10^{-4}. Thus the rate of formation of condensations is

$$800\, M_\odot \times 10^{-7}\frac{1}{yr} \times 5 \times 10^{-5}\frac{1}{pc^3} \times 10^{-4}$$

$$= 4 \times 10^{-13}\frac{M_\odot}{yr\, pc^3}$$

The observed rate of star formation is $10^{-11}\frac{M_\odot}{yr\, pc^3}$, which is an order of magnitude greater.

Neutrally-buoyant Time Bombs

by

H. Tinkelenberg

Neutrally-buoyant Time Bombs

H. Tinkelenberg

Introduction

Neutrally-buoyant floats have long been useful in the mapping of ocean currents at depth. In their usual form they are called Swallow floats after their inventor J.C.Swallow (1955). Essentially they are long, thin tubes floating at a fixed depth in the ocean and emitting some sort of fixed-frequency, short-range signal by which a ship on the surface may track them.

Since it is necessary that a ship follow the float for as long as a record is required, it is obvious that the cost of this method becomes prohibitive whenever a record of long and significant duration is needed. Another drawback of the Swallow floats is that their useful life is proportional to the size of the battery pack in the float. Thus even for a track of one- to two-weeks duration the floats measure eight feet in length and would become excessive in size if longer periods were required.

A distinct advantage of Swallow's method is the beautiful detail obtained by tracking his floats continuously. See, for example, Swallow (1955) where tidal oscillations are depicted. If one is interested, however, in the deep-current transport averaged over a long period of time such detail is neither necessary nor often desired. For such applications the Swallow float and it's tracking vessel obviously form a far too costly and

demanding instrument.

This paper discusses the feasibility of using neutrally-buoyant floats to obtain a long-term averaged view of the oceanic circulation at depth without the need either for local ship-tracking or excessively large floats.

Neutrally-buoyant Floats*

Neutrally-buoyant floats owe their existence to the fact that a body less compressible than sea water gains relative buoyancy as it sinks. Ignoring such influences as temperature and salinity, the density of sea water increases with depth as successive layers become more compressed under the weight of the water above them. Now imagine a body which at the surface is slightly denser than the water, so that it may sink, but which is less compressible than the water under the hydrostatic pressure (see fig. 1). At some depth the two density curves will intersect and the body will become neutrally-buoyant.

If such a float is to be useful in oceanography certain requirements must be met. A float should have enough buoyancy so that it can carry a payload. Since the floats are made of aluminum and carry all or most of their payload inside, an increase in buoyancy can be

*The next two sections deal with the basic principles of neutrally-buoyant floats and SOFAR. They are included to provide some necessary background information. A reader familiar with these topics may omit either or both of these sections without loss of continuity.

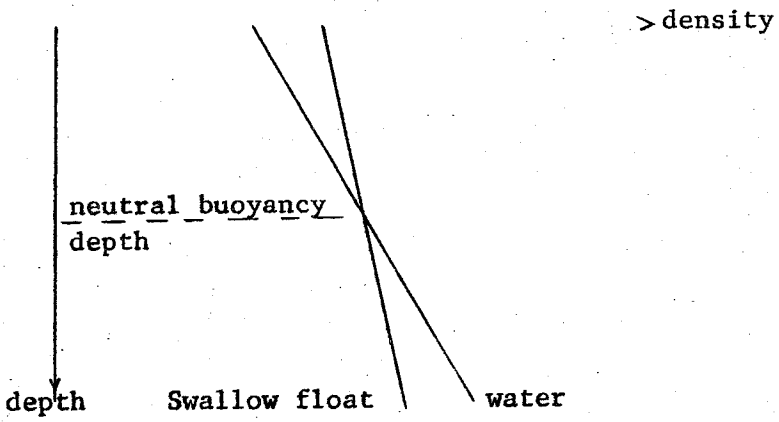

Figure 1.

achieved most easily by enlarging the volume of the tube. This, however, increases the total weight of the float still more so that another increase in volume is required for greater buoyancy. For the Swallow floats used by the Woods Hole Oceanographic Institution this vicious circle is represented by the relation:

$$\ell \simeq \frac{1}{18} P + 35,$$

where ℓ = total length of float in cm.,

P = weight of payload in grams.

An obvious requirement for Swallow floats is that they must not collapse. Nearly all floats now in use are designed to withstand even the highest pressures encountered in the world's oceans.

Last, but not least, a float should ideally maintain a constant depth. Due to variations in temperature and salinity the

isopycnal surfaces are seldom parallel to the local horizontal plane so that the path of a float will fluctuate vertically. Swallow (1955) estimates the inaccuracy in the depth to be $\pm$ 200 m. for a float adjusted to drift at 600 m. For an account of the techniques necessary to adjust a float so that it will become neutrally-buoyant at a given depth the reader is referred to Swallow and Worthington (1961).

SOFAR

SOFAR stands for Sound Fixing And Ranging and usually refers to the system for determining the location of underwater sound as far as 3000 miles from shore. In this connection one often refers to the SOFAR channel. This expression denotes the surface in the ocean where the velocity of sound has its minimum.

The velocity of sound is dependent on the density of the propagation medium. In the case of seawater the density is most sensitive to variations in temperature. For a typical location in the ocean the variation of temperature with depth and the consequent variation of sound-velocity with depth are as shown in figure 2. ($\frac{\partial^2 V}{\partial z^2}$ is not necessarily 0 everywhere).

Ignoring the seasonal and diurnal thermoclines, $\frac{\partial T}{\partial z}$ varies little at any given location and is nearly constant throughout the world's oceans. Thus $\frac{\partial V}{\partial z}$ is necessarily also quite constant throughout the oceans and the variation with depth of the points where $\frac{\partial V}{\partial z} = 0$ (i.e. where sound-velocity has its minimum) is only

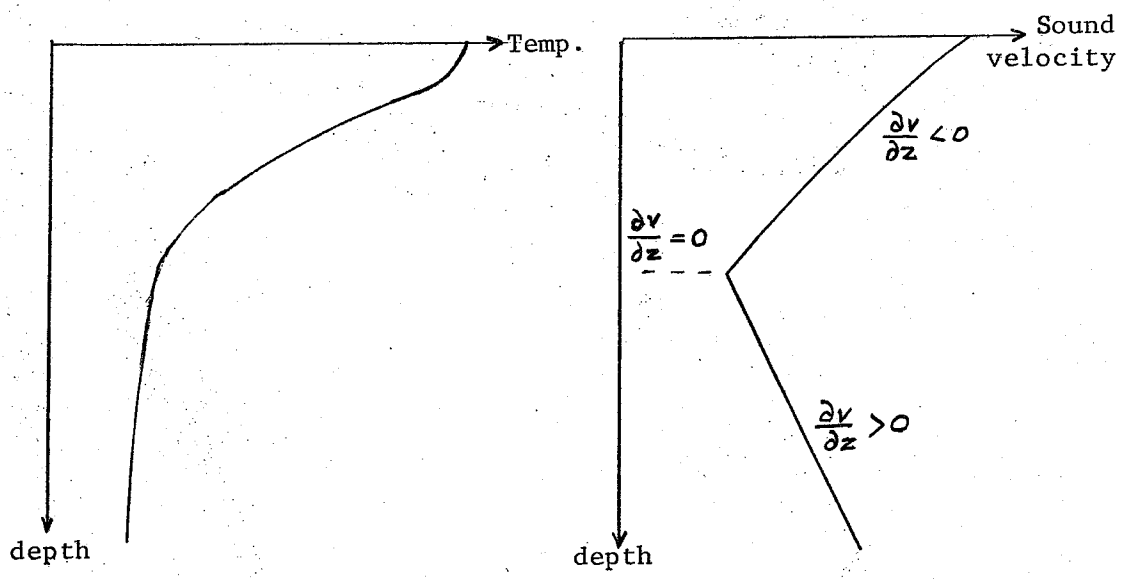

Figure 2.

slight. Hence the surface $\frac{\partial v}{\partial z} = 0$ is everywhere approximately parallel to the local horizontal plane. It is called the axis of the SOFAR channel and it's depth in the oceans varies from 1000 to 6000 feet.

If a sound is generated on the axis of the SOFAR channel the initial spreading will be three-dimensional. Due to the form of $\frac{\partial v}{\partial z}$, however, most of the sound initially travelling up or down will be refracted back towards the axis. Thus spreading becomes essentially two-dimensional as graphically depicted in figure 3. Energy is conserved so that the sound becomes audible at great distances.

Imagine a listener L at some distance from the origin of the sound. The energy paths numbered 1 in figure 3 are longer than

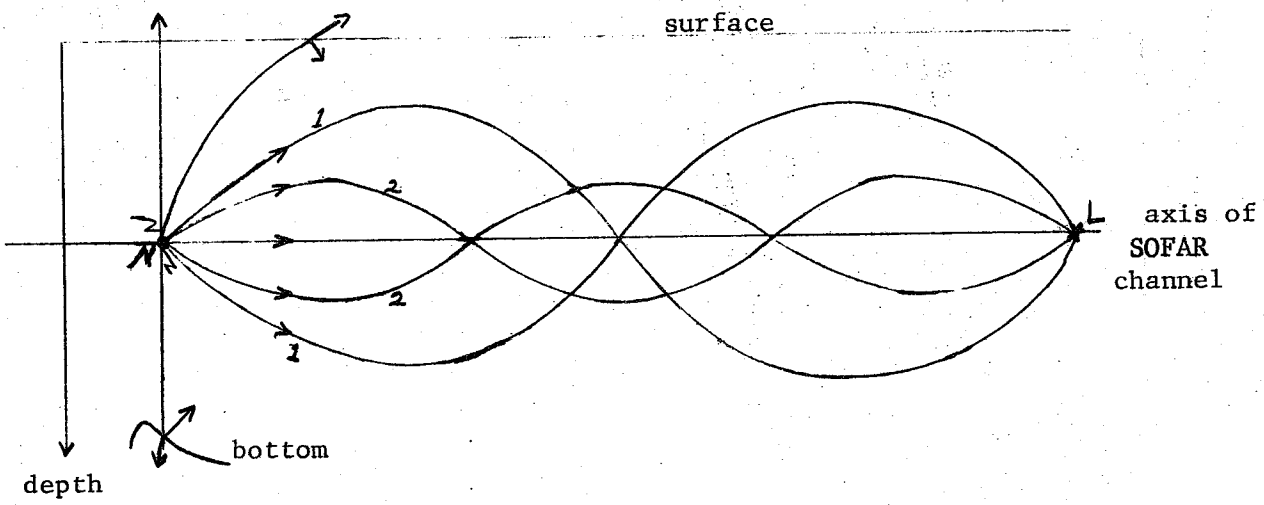

Figure 3.

those numbered 2. Since, however, along paths 1 the sound travels faster, the energy propagated along those paths will arrive first at L . Energy propagated along paths 2 will arrive later, while energy propagated along the axis will arrive last. Due to the essentially two-dimensional spreading process proportionally more energy becomes concentrated in propagation paths as those paths deviate less from the axis. Hence a SOFAR signal generated and received on the axis will appear as shown in figure 4a. If such ideal conditions cannot be established the form, duration, and intensity of the signal may all be changed (see figure 4b).

Neutrally-buoyant Time Bombs

With the above background information in mind the choice for an instrument to measure the averaged transport of deep currents seems to be clear. To remain at a fixed depth a neutrally-buoyant float

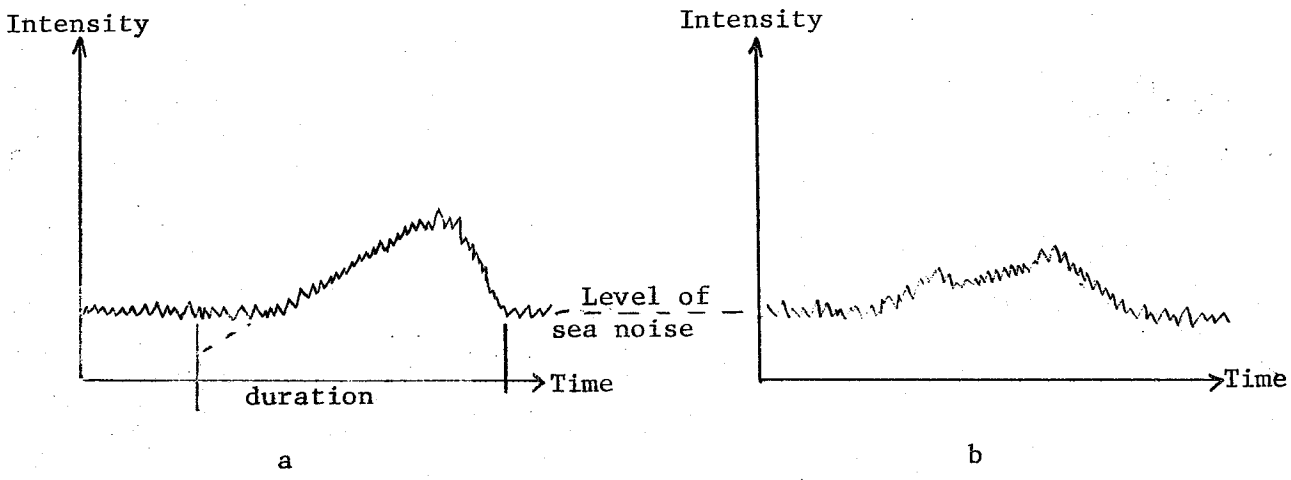

Figure 4

forms the simplest and cheapest carrier. To use existing SOFAR stations the float must carry a potential source of audible energy, such as a time bomb. Ideally the sound should be received by at least three stations so that the float's position at the time of the explosion may be accurately determined. The bombs should be activated by a clock so that the times at which different bombs explode may be previously regulated. One immediate problem which will be dealt with later is generating a loud enough noise.

The time element will be of great importance in this project. The time-lapse between the releasing of a float and it's exploding is not only an accurate measure of it's travel time but is also the only practical means of identifying one bomb among many. Indeed, for the actual time measurements the accuracy of the clocks is of no great importance. In order to avoid errors in transport measurements caused by the initial sinking time of each float we could take the first explosion time as our initial time t_1. (This also

avoids the need for precise ship navigation since the geographical position of the first explosion becomes of basic importance.) Then each consequent explosion time t_k yields an extremely accurate measure of the time lapse between explosions l and K by mere subtraction. If, for example, one wants to use 100 floats timed to explode at daily intervals an accuracy of only 1% is required to assure that the bombs will report in the proper sequence so that correct identification is possible.

To obtain an accurate estimate of the time-averaged current transport at depth the use of many floats over a significant period of time is essential. It will be neither necessary nor practical, however, to make the interval between reports much shorter than a day. In the first place, any interval shorter than six hours will yield tidal oscillations, a detail we are presumably not interested in. Secondly, Crease (1960) using Swallow floats has measured velocities of order 10 cm/sec at a depth of 2000 m. in the Atlantic off Bermuda. This means an approximate travel distance of 2 km. in 6 hours which is resolvable only if the phones and the floats are all fairly close together.

Last, but not least, it should be pointed out that the use of many one-shot floats makes minimum cost per float a desirable objective. Initially it was feared that the price of fairly accurate timing devices would prove prohibitive. There is available, however, a radio alarm-clock manufactured by Westclox which runs on 1.5 volts.

In tests these clocks ran for five weeks on one 1.5 volt penlite battery with an accuracy better than ± 5 minutes (.05%) and maintained this accuracy when placed in a refrigerator at about 4°C. The cost per clock is $11.80 and it is quite easy to adapt these clocks to our purposes. Cost can also be reduced by making the floats as small as possible. This, however, decreases the accuracy with which depth adjustment may be made. Later another reason will be presented to make the floats rather large.

Two sources of energy have been considered: explosive bombs and implosive bombs.

TNT as Energy Source

Tests with the SOFAR system have shown that four-pound blocks of TNT are easily audible at distances up to 3000 miles. This project would require the use of many floats, all loaded with a respectable amount of TNT. Since each float would essentially form a mine, the use of TNT is decidedly a dangerous venture.

If TNT is to be used, safety must be the most important initial consideration. Handling and storage are two basic problems. Since in handling human error forms the greatest danger, safety can often be assured by strict adherence to established procedure; no smoking, separation of explosives and detonators, etc. Storage on a vessel would require the same strict procedure. Here, however, the environment becomes of great and often detrimental importance.

One fortunate fact about TNT, and no doubt the reason for its popularity, is that by itself it forms a relatively inert substance. Indeed, the standard method of exploding TNT is by means of a booster, commonly tetryl. The booster is usually exploded by an electrically-activated detonator. The use of such detonators carries with it the risk of accidental discharge. To overcome this danger pressure-activated detonators were developed especially suited for underwater use. In their present form they resemble a two-inch piece of common pencil. Made of copper, they carry a crimped plug at one end. When the hydrostatic pressure upon the plug reaches a critical value it flies into the tube and explodes a blasting cap. This sets off the booster which in turn explodes the TNT. Under normal atmospheric pressure these detonators are completely harmless.

Another requirement for a TNT-loaded float is that it never return to the surface once it is set adrift; any unsuspecting finder could too easily be hurt. Thus in case the float malfunctions, it should be self-destructive. This could be achieved by exploding which, however, is hardly desirable if the float is at or near the surface. Sinking would be a more preferable method of self-destruction. This could be done by spring-loading one of the end-caps of the float. The float would be set overboard in a clamp to a depth where the force due to the hydrostatic pressure on the end-cap would exceed the force of the spring. Then the clamp would be released and the float would sink to its drifting depth. If the float ever came close

enough to the surface, the spring would open the tube which would fill with water and sink.

A possible design for a TNT-float is shown in figure 5.

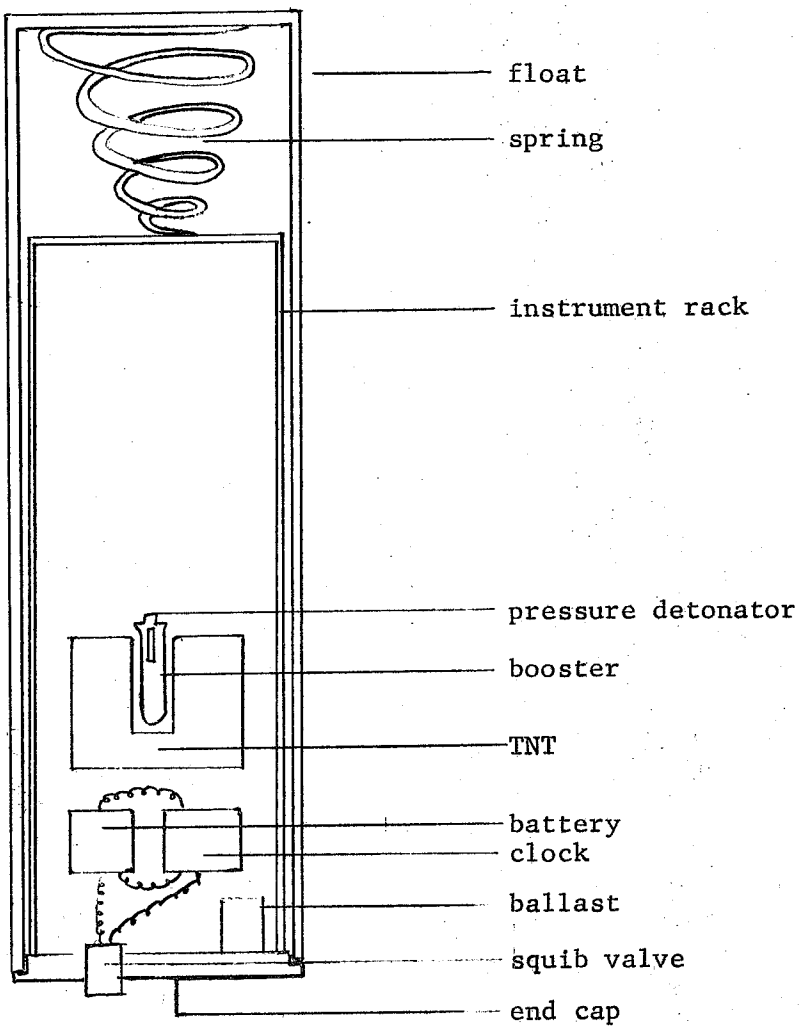

Figure 5 (not to scale)

Using 1 lb. of TNT the payload is still light enough so that the tube need not be longer than three feet. At the present time the clock activates the valve so that the float floods and begins to

sink. When the pressure inside the float becomes high enough at some depth (ideally the axis of the SOFAR channel) the pressure detonator will explode the TNT.

Implosions as Energy Source

When a hollow body collapses under excessive hydrostatic pressure energy is released as a consequence of the work done by the water. If, for example, the body is a sphere the energy is equal to the product of the spherical volume and the pressure under which collapse occurs.

For buoyancy, all Swallow floats have a rather large hollow volume. To use the potential energy represented by this volume for signal purposes is an appealing idea. Since, however, Swallow floats are designed to withstand all pressures encountered in the ocean, rupture disks would have to be used to allow an implosive energy release. Rupture disks are made of metal and appear slightly curved in shape. They are designed to collapse when subjected to a specified critical pressure. One problem on which no information is available at present is the deformation of a rupture disk under increasing pressure; this might critically alter the buoyancy of the float.

The great advantage of using implosive floats is that they are completely without danger. A basic problem, however, is to determine how much useful energy may be obtained from an implosion. It is not possible to do this in a liquid-pressurized tank of any finite volume;

as soon as the rupture disk begins to collapse the pressure in the tank will decrease substantially. A 1947 unpublished WHOI report estimated, evidently without experimental evidence, that at 1800 psi a volume of ½ cubic foot would release an amount of energy approximately equivalent to that in one pound of TNT. Even if this estimate were off by a factor of ten, it might still be better to use implosive floats than to make extensive use of TNT-loaded floats. Fortunately we were able to perform a field test on the energy of implosion bombs.

The Bermuda Experiment

During the summer of 1963 Allyn C. Vine of the Woods Hole Oceanographic Institution had in his possession several small implosion bombs set for different pressures. Their implosive volume was formed by a cylinder, 18 inches long with a 2.5-inch diameter, or a volume of .05 cubic feet approximately. We chose two bombs, both set for 1880 psi, which corresponds to the depth of the SOFAR channel around Bermuda. The bombs were placed in the R/V CRAWFORD which sailed on 1 August, 1963, from Woods Hole to Barbados, passing closely by Bermuda. In addition to the bombs two DePont Waterworks Boosters were put on board equipped with 1800 psi pressure detonators. The boosters are equivalent to 1/18 lbs. of TNT and were needed to calibrate the implosion signals.

The first booster and bomb were thrown overboard 15 minutes apart

when the CRAWFORD was 94 miles south of Bermuda. Six hours later at a distance of 176 miles the second booster and bomb were treated similarly. The signals from the two boosters and the second bomb are shown in figures 6, 7, and 8. At the time the first bomb should have imploded, a ship passed by Bermuda and increased the signal-level sufficiently to hide any implosions. In all three figures the horizontal scale is 5 divisions = 1 second; the vertical scale is 1 division = 1 decible. On all figures the bottom recording represents the time base; the other recordings represent different hydrophones.

If a and b represent voltages, then

$$\left(\frac{a}{b}\right)_{db} = 20 \log_{10}\left(\frac{a}{b}\right),$$

where $\left(\frac{a}{b}\right)_{db}$ is the difference in decibles between the signals resulting from a and b respectively. Assume that the energy flux at the hydrophones is proportional to the output voltage of the preamplifier. Then, since for the second that the difference in the db-level between the booster and the signal is 13 db, it follows that

$$13 = 20 \log_{10}\left(\frac{a}{b}\right)$$

where a represents the booster and b the signal. Then

$$\frac{a}{b} = 4.5$$

whence it follows that the implosion signal was approximately equivalent in energy to 1/80 lbs. of TNT. Considering the volume of

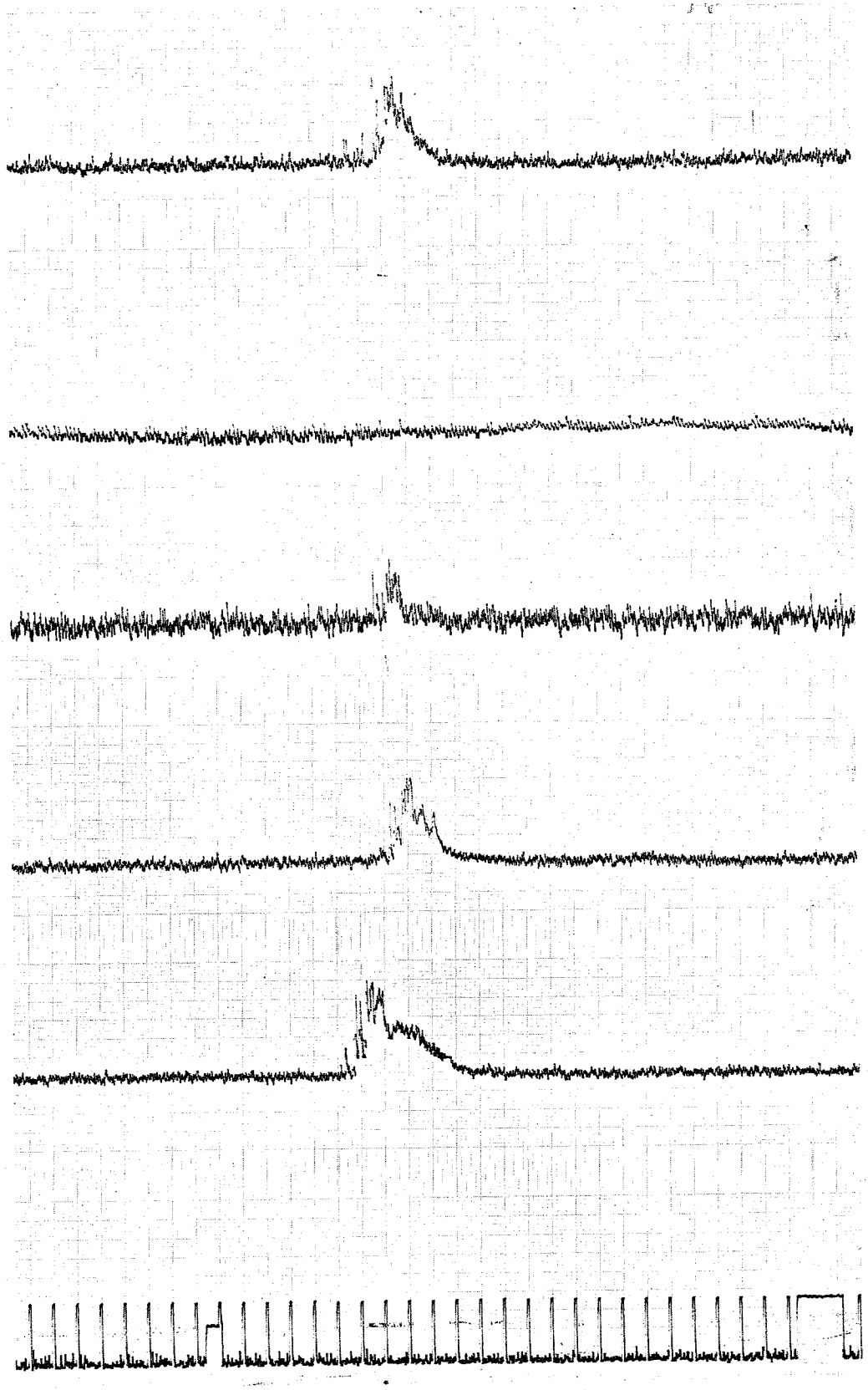

Figure 6

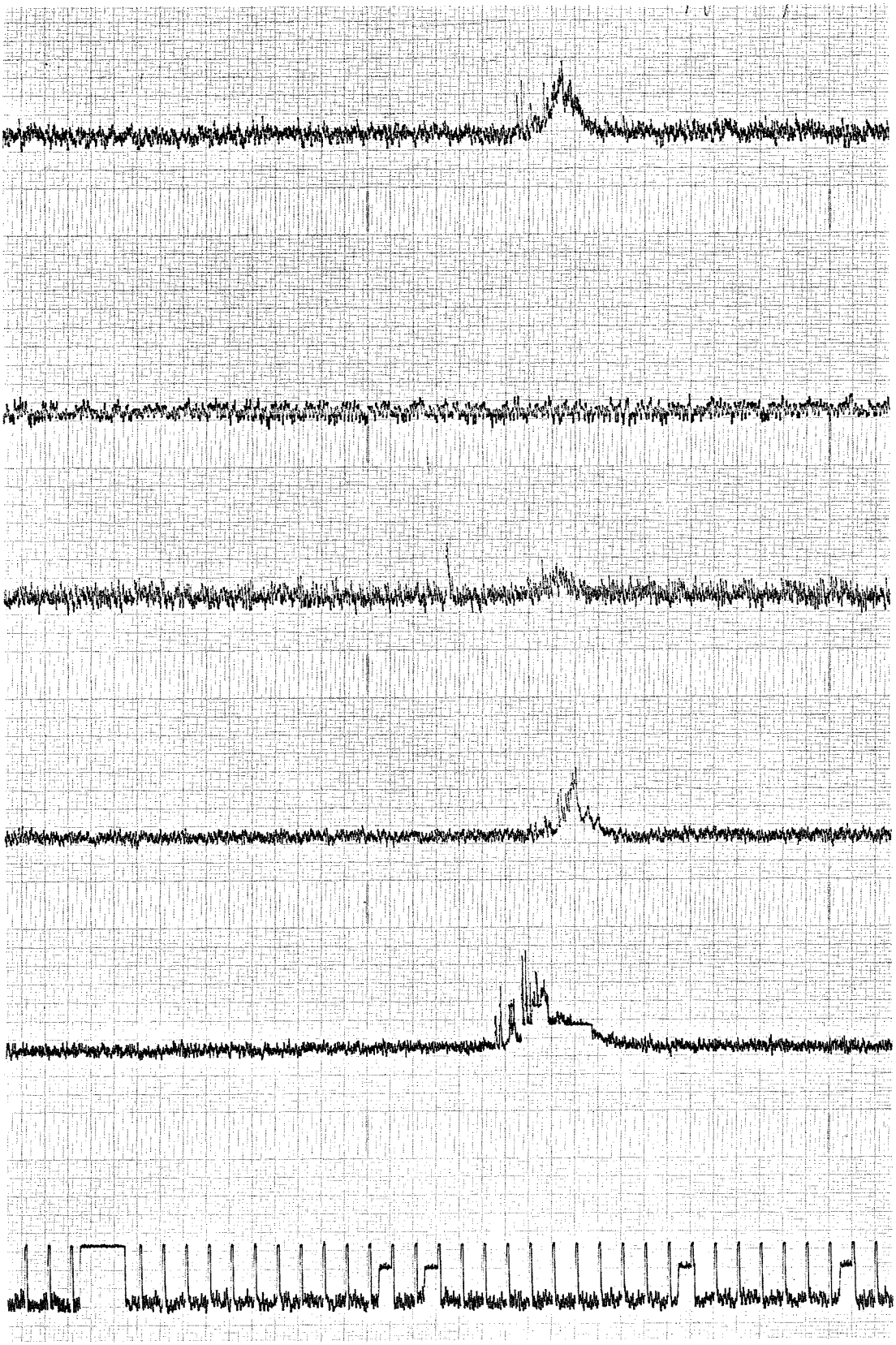

Figure 7

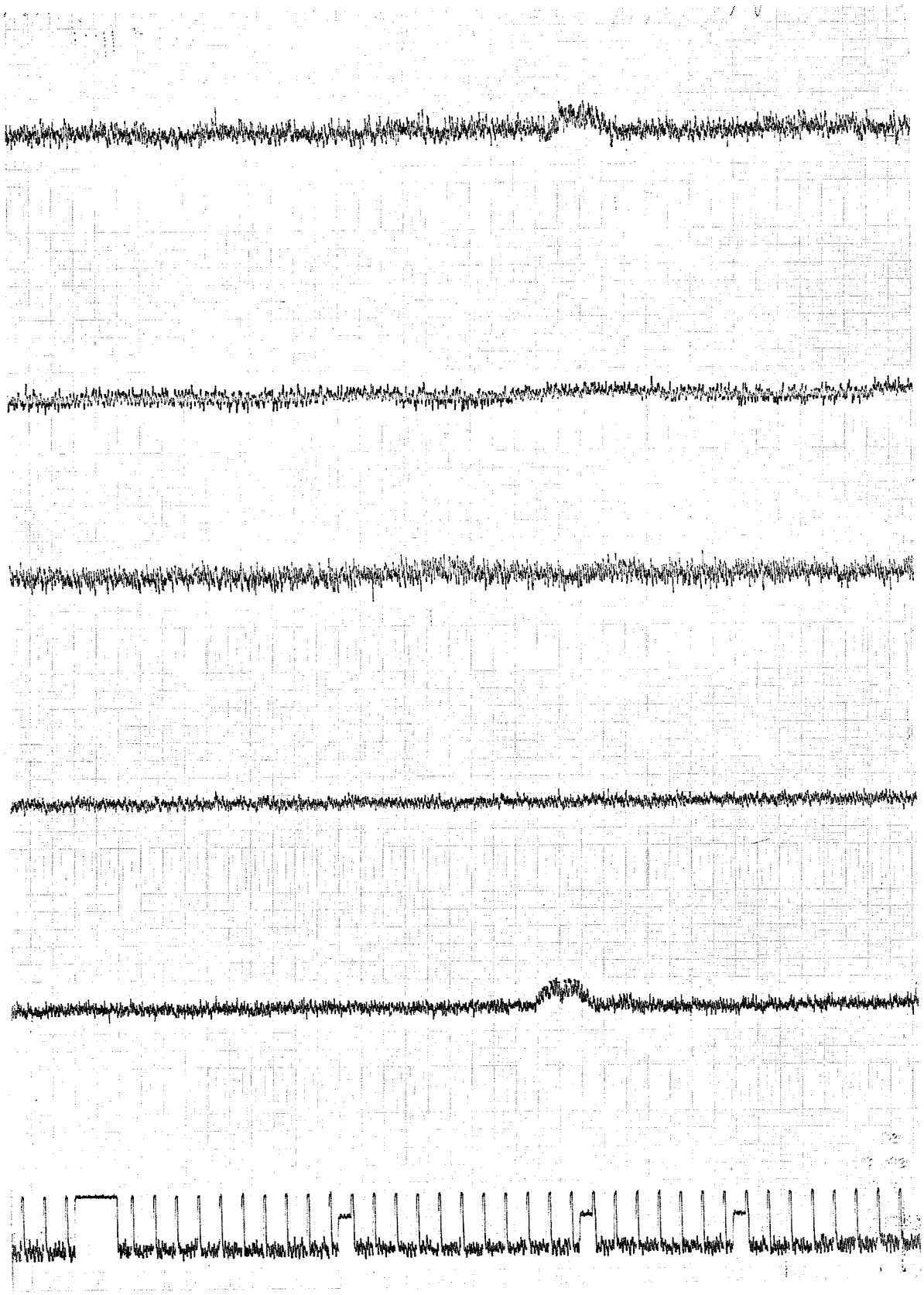

Figure 8

the bomb, it appears that at 1880 psi, a volume of four cubic feet is approximately equivalent in potential energy to one lb. of TNT.

Figure 9 shows a possible design for an implosive float using

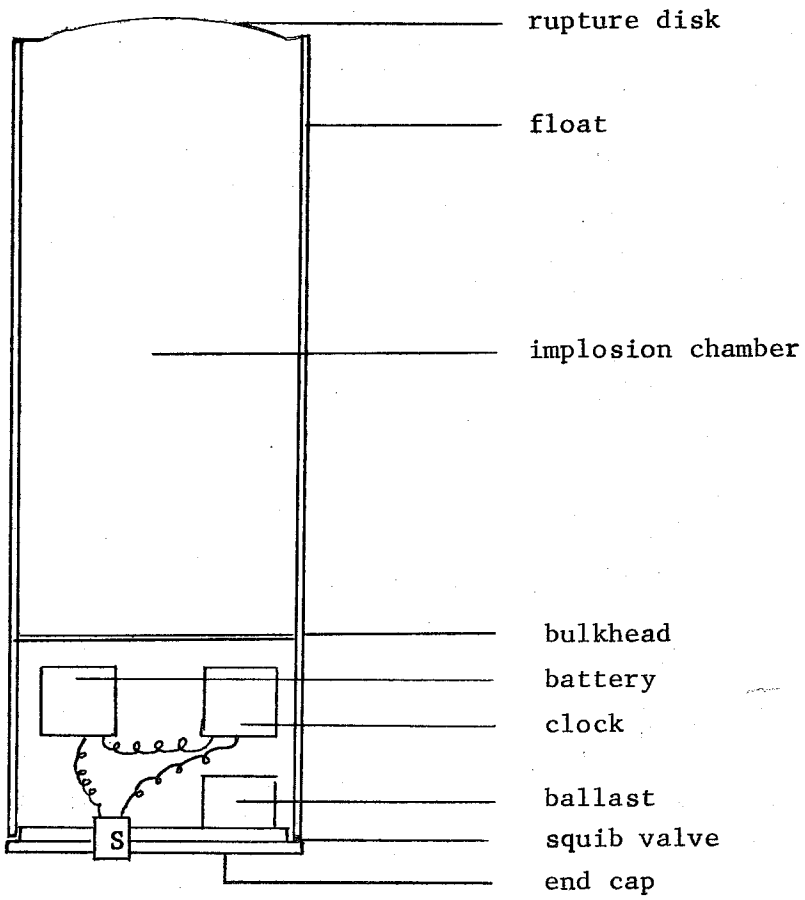

Figure 9 (not to scale)

using the ideas and results set forth above. The pressure at which the disk ruptures corresponds to the depth of the SOFAR channel. The float would drift with the currents at some depth above the channel. At the pre-set time the electrically-activated valve S

would open, water would flood the lower compartment and the float would sink to its implosion depth.

Conclusion

An implosive float producing enough energy to be audible at long distances will certainly be larger than a TNT-loaded float producing an equivalent amount of energy. However, considering not only energy but also safety it is definitely recommended that in the tracking of deep currents with neutrally-buoyant time bombs implosive floats be used.

To increase the energy, the floats could be enlarged. An increase in diameter would have to be accompanied by an increase in wall thickness to preserve strength. An increase in length would be easiest provided that storage and handling do not become too difficult. As usual, cost may place a limit on the maximum size to be used.

One future problem of great interest is the tracking of currents below the SOFAR channel since it will be quite difficult in that case to generate a signal on the axis. As implosive energy is not only proportional to volume but also to pressure, it might be possible to implode a float quite far below the SOFAR axis and, due to increased energy, still trap enough energy in the channel to obtain a signal audible at great distances. Another problem is the fouling of floats that are to drift for long periods of time.

Perhaps, however, the newly developed anti-fouling paints will provide enough protection for the periods that interest oceanographers.

Acknowledgment

The author wishes to express his gratitude and indebtedness to the many people at the Woods Hole Oceanographic Institution and the Bermuda SOFAR station without whom the above investigation would not have been possible.

References

1. Crease,J.C.,"Velocity Measurements in the Deep Water of the Western North Atlantic. - Summary", Turbulence in Geophysics, Am. Geophys. Union, 1962, pp.3173 - 3176.

2. Swallow, J.C., "A Neutral-buoyancy Float for Measuring Deep Currents", Deep-Sea Research, 1955, Vol.3, pp.74-81.

3. Swallow, J.C. and L.V.Worthington, "An Observation of a Deep Counter-current in the Western North Atlantic", Deep-Sea Research, 1961, Vol.8, pp. 1-19.

Modified Ekman Flows

by

Paul H. LeBlond

Modified Ekman Flows

Paul H. LeBlond

Introduction

This study is concerned with the influence of non-uniformities of the oceanic fluid (in the form of a velocity field and temperature gradients) on the flow field induced by surface perturbations. Stommel and Veronis (1957) investigated the effect of a vertical temperature gradient for large-scale temperature perturbations; they found that, besides the usual Elman flow, a cellular convective regime was generated, characterized by a scale depth L ($L >>$ than Ekman depth), the depth.

We will limit our attention here to phenomena restricted to a surface layer of vertical extent comparable or slightly larger than that of pure frictional influence. Boundary conditions will include surface stresses as well as surface temperature or heat flux constraints. An attempt will be made to discover the circumstances in which important modifications of the Ekman flow will arise.

The Perturbation Equations

The ocean is assumed of infinite depth: it fills the half space $z < 0$. In the absence of perturbations there exists a main field $\bar{\Theta}(x, z)$ and $V(x, z)$; the y-direction is along V. This main field is known and need not be solved for; it is postulated to have a vertical scale H between 1 and 2 km.

The perturbation variables u, v, w, θ, p will be of much smaller magnitudes than V, $\bar{\Theta}$ and the hydrostatic pressure respectively in order to make the perturbation analysis valid. Their depth scale D is smaller than 50m and their horizontal variation is assumed periodic in x and y: of the form $e^{i(\ell x + my)}$. Since $D << H$, the derivatives of the mean field velocities will be neglected as well as the second derivatives of $\bar{\Theta}$ and V, $\frac{\partial \bar{\Theta}}{\partial z}$ and $\partial\bar{\Theta}/\partial x$ will be approximated by their average values in the upper layer. The model makes use of Boussinesq's approximation; the pressure is hydrostatic and a steady state is assumed. The rotation vector is in the z-direction and is uniform in all directions. Eddy coefficients of viscosity (A) and of diffusivity (K) are used in the heat and momentum equations. A simple linear equation of state is assumed. The perturbation equations can then be written

$$V \frac{\partial u}{\partial y} - fv = -\frac{1}{\rho_0} \frac{\partial p}{\partial x} + A \frac{\partial^2 u}{\partial z^2} \qquad (1)$$

$$V \frac{\partial v}{\partial y} + fu = -\frac{1}{\rho_0} \frac{\partial p}{\partial y} + A \frac{\partial^2 v}{\partial z^2} \qquad (2)$$

$$\frac{\partial u}{\partial x} + \frac{\partial v}{\partial y} + \frac{\partial w}{\partial z} = 0 \tag{3}$$

$$\frac{\partial p}{\partial z} = -\rho g \tag{4}$$

$$V\frac{\partial \theta}{\partial y} + w\frac{\partial \theta}{\partial z} + u\frac{\partial \theta}{\partial x} = K\frac{\partial^2 \theta}{\partial z^2} \tag{5}$$

$$\rho = \rho_0 (1 - \alpha\theta) \tag{6}$$

The boundary conditions at great depth are that all perturbation variables vanish for $z \to -\infty$; at the surface, the stress condition gives

$$\left.\frac{\partial u}{\partial z}\right|_0 = \frac{\tau_x}{\Delta} \quad ; \quad \left.\frac{\partial v}{\partial z}\right|_0 = \frac{\tau_y}{\Delta}$$

and a surface temperature or surface heat flux condition imposes

$$\theta|_0 = \theta_0 \quad \text{or} \quad \left.\frac{\partial \theta}{\partial z}\right|_0 = \Phi .$$

Eliminating p, ρ and w from the set (1) to (6) yields

$$im\frac{\partial}{\partial z}(Vu) - f\frac{\partial v}{\partial z} = -il g\alpha\theta + A\frac{\partial^3 u}{\partial z^3} \tag{7}$$

$$im\frac{\partial}{\partial z}(Vv) + f\frac{\partial u}{\partial z} = -img\alpha\theta + A\frac{\partial^3 v}{\partial z^3} \tag{8}$$

$$im\frac{\partial}{\partial z}(V\theta) + \frac{\partial}{\partial z}(ub) - S[il u + imv] = K\frac{\partial^3 \theta}{\partial z^3} \tag{9}$$

$\frac{\partial \theta}{\partial z}$ and $\frac{\partial \theta}{\partial x}$ have been abbreviated as S and b respectively. As stated above, V, b and S are considered to be constants over the small depths in which perturbations will be present.

Elimination of v from (7), (8), (9) leaves us with

$$\left[-Aim\frac{\partial^3}{\partial z^3}-\frac{fb}{S}\frac{\partial^2}{\partial z^2}+(ilf-m^2V)\frac{\partial}{\partial z}\right]u=\left[-\frac{fK}{S}\frac{\partial^4}{\partial z^4}+\frac{imfV}{S}\frac{\partial^2}{\partial z^2}+g\alpha lm\right]\Theta \quad (10)$$

and

$$\left[-\frac{Ab}{S}\frac{\partial^4}{\partial z^4}+ilA\frac{\partial^3}{\partial z^3}+\frac{imbV}{S}\frac{\partial^2}{\partial z^2}+(imf+lmV)\frac{\partial}{\partial z}\right]u=$$

$$=\left[-\frac{AK}{S}\frac{\partial^6}{\partial z^6}+\frac{V}{S}(A+K)im\frac{\partial^4}{\partial z^4}+\frac{m^2V^2}{S}\frac{\partial^2}{\partial z^2}+g\alpha m^2\right]\Theta \quad (11)$$

The last step is to eliminate Θ, leading to an 8^{th} order equation in u:

$$\left\{\frac{\partial^8}{\partial z^8}-\frac{imV}{K}\left(\frac{2K+A}{A}\right)\frac{\partial^6}{\partial z^6}+\frac{f^2}{A^2}\left[1-\frac{m^2V^2}{f^2}\left(\frac{2A+K}{K}\right)\right]\frac{\partial^4}{\partial z^4}-\frac{ibg\alpha l}{KA}\frac{\partial^3}{\partial z^3}-\left[\frac{g\alpha S}{AK}(m^2+l^2)+\right.\right.$$

$$\left.\left.+\frac{imVf^2}{A^2K}\left(1-\frac{m^2V^2}{f^2}\right)\right]\frac{\partial^2}{\partial z^2}+\frac{imfg\alpha b}{A^2K}\left(1+\frac{ilV}{f}\right)\frac{\partial}{\partial z}+\frac{iSg\alpha mV}{A^2K}(m^2+l^2)\right\}u=0 \quad (12)$$

We now introduce non-dimensional variables of order unity, u_0 and ζ, defined by

$$u=Vu_0$$

$$\zeta=N\sqrt{\frac{A}{f}}\,z$$

The use of $N\sqrt{\frac{A}{f}}$ for a scale depth (N is a small rational number, $1\leq N\leq 5$) is in keeping with previous specifications on the vertical extent of the perturbations. Equation (12) now takes the form

$$\left\{\frac{\partial^8}{\partial\zeta^8}-\frac{imV}{f}\left(\frac{2K+A}{K}\right)N^2\frac{\partial^6}{\partial\zeta^6}+\left[1-\frac{m^2V^2}{f^2}\left(\frac{2A+K}{K}\right)\right]N^4\frac{\partial^4}{\partial\zeta^4}-\frac{ibg\alpha lA}{Kf^2}\sqrt{\frac{A}{f}}N^5\frac{\partial^3}{\partial\zeta^3}-\left[\frac{g\alpha SA^2}{f^3K}(m^2+l^2)+\right.\right.$$

$$\left.\left.+\frac{imVA}{fK}\left(1-\frac{m^2V^2}{f^2}\right)\right]N^6\frac{\partial^2}{\partial\zeta^2}+\frac{img^2\alpha b}{f^2}\frac{A}{K}\sqrt{\frac{A}{f}}N^7\frac{\partial}{\partial\zeta}+\frac{ig\alpha mVSA^2}{Kf^4}(m^2+l^2)N^8\right\}u_0=0 \quad (13)$$

Equation (13) will henceforth be referred to as Λu_o for brevity. The differential operator Λ can be written in a more revealing and simpler fashion if we introduce the following notation:

$$\lambda^n = \frac{\partial^n}{\partial \zeta^n} \tag{14}$$

$$E = \frac{m^2 V^2}{f} \tag{15}$$

$$F = \frac{bg\alpha m}{f^2} \frac{A}{K} \sqrt{\frac{A}{f}} \tag{16}$$

$$G = \frac{Sg\alpha A^2}{Kf^3}(m^2+l^2) \tag{17}$$

so that Λ is now

$$\Lambda = \lambda^8 - iE\left(\frac{2K+A}{K}\right)N^2\lambda^6 + \left[1 - E^2\frac{(2A+K)}{K}\right]N^4\lambda^4 - iF\frac{l}{m}N^5\lambda^3 - \left[G - \frac{iA}{K}E(1-E^2)\right]N^6\lambda^2 +$$

$$+ iF\left(1 + \frac{il}{m}E\right)N^7\lambda + iGEN^8 \tag{18}$$

Since E, G, F vary little over the depth $N\sqrt{\frac{A}{f}}$ and are approximated by their average values, (18) becomes $\Lambda = 0$, an eight-degree algebraic equation with complex coefficients, and u has solutions of the form $e^{\lambda\zeta}$.

The non-dimensional parameters E, F, G represent the influence of non-linear advection terms, horizontal and vertical temperature gradients respectively. If they are all entirely negligible one is left with the pure Ekman flow. Since the character of the flow depends ultimately on the values of E, F and G, it is useful to know their magnitude for values of their constituents

likely to be found in the oceans. This is done in table I, for $A = K = 10^2$; this value (10^2) is chosen to make the Ekamn depth $\sqrt{\frac{A}{f}}$ equal to 10 m, which seems reasonable.

Table I

$\log_{10}m \rightarrow$		-3		-4		-5		-6		-7		-8	
	$\log_{10}V$												
	-1	0	1	-1	0	-2	-1	-3	-2	-4	-3	-5	-4
$\log_{10}E$	0	1	2	0	1	-1	0	-2	-1	-3	-2	-4	-3
	+1	2	3	1	2	0	1	-1	0	-2	-1	-3	-2
	$\log_{10}b$												
	-6	1	3.5	0	2.5	-1	1.5	-2	0.5	-3	-0.5	-4	-1.5
$\log_{10}F$	-7	0	2.5	-1	1.5	-2	0.5	-3	-0.5	-4	-1.5	-5	-2.5
	-8	-1	1.5	-2	0.5	-3	-0.5	-4	-1.5	-5	-2.5	-6	-3.5
	$\log_{10}S$												
$\log_{10}G$	-4	3	6	1	4	-1	2	-3	0	-5	-2	-7	-4
	-5	2	5	0	3	-2	1	-4	-1	-6	-3	-8	-5
	$\log_{10}f \rightarrow$	-4	-5	-4	-5	-4	-5	-4	-5	-4	-5	-4	-5

Table I. Log_{10} of non-dimensional parameters E, F, G for some values of m, b, V, f, S.

$$E = \frac{mV}{f} \; ; \; F = \frac{bg\alpha mA}{f^2 K}\sqrt{\frac{A}{f}} \; ; \; G = \frac{g\alpha SA^2}{Kf^3}(m^2+l^2)$$

$$A = K = 10^2 \; ; \; g = 10^3 \; ; \; \alpha = 2.5 \times 10^{-4}$$

Examination of table I shows that in regions where $f \simeq 10^{-4}$ (left-hand side of columns of equal $\log_{10} m$) only scales of motion of wave number less than 10^{-5} will produce E, F, G with values of $O(1)$ or greater; such small-scale steady state perturbations seem unlikely to exist over the ocean. In more equatorial regions, where f is more closely approximated by 10^{-5}, larger scales of perturbation ($m \simeq 10^{-6}$) can produce appreciable values of E, F or G. In both regions however surface disturbances of oceanic scale (10^{-8}) lead to very small values of E, F, G, showing that their influence will be felt over much greater depths.

With this knowledge, we go back to (18); where $N \simeq 1$, so that $\lambda^4 N^4 \simeq \lambda^8$, the resulting flow is a modified Ekman flow, in that both Ekman terms (λ^4 and λ^8) are present as well as other terms. Table I shows that no other powers of λ are likely to be of importance unless one goes near equatorial regions.

If N is large enough so that $N^4 >> 1$ (eg. $N = 2$) the λ^8 term can be neglected with respect to the λ^4 term, and the corresponding flow is not a modified Ekman flow, but something else of slightly larger vertical extent superimposed upon the pure frictional flow. Larger values of N will of course allow smaller E, F, G to have some influence in (18).

Therefore, even though the velocity and the temperature gradients of the main field may not have any appreciable effect on the scale of the order of the Ekman depth, they might induce flows of a scale depth

only 2 or 3 times as large which, when superimposed upon the Ekman flow, may produce very different integrated effects.

Before we go on to study special cases it is useful to trace back the terms of Λ to their source terms in the perturbation equations (7), (8) and (9). Table 2 does just that and allows one to judge, on the basis of knowledge of the dominant terms in Λ, which will be the dominant terms in the momentum and heat equations.

A few words about table 2: one notices immediately that F and G control the horizontal and vertical mean gradient effects in the heat equation; that E has a general control over the non-linear advection terms in all three basic equations, and that, unless A and K differ widely, such terms stand in the same proportion to the turbulent mixing terms in the three equations, at least where $N \simeq 1$. F and G, together with their products with E, control the pressure terms in the momentum equations.

We will now study the effects of individual parameters and try and bring out special cases of interest, first in the modified Ekman flow ($N \simeq 1$), and also for less shallow flow fields ($N > 1$).

Table II

Λ (18)	Heat equation (9)	x Momentum equation (7)	y Momentum equation (8)
λ^8	MIX.	MIX	MIX
$\lambda^6(-iEN^2)(2+\frac{A}{K})$	MIX + ADV	(ADV, MIX) + MIX	(ADV, MIX) + MIX
$\lambda^4 N^4[1-E^2\frac{2A}{K}-E^2]$	MIX + ADV + MIX	COR. + (ADV, MIX) + ADV	COR. + (ADV, MIX) + ADV
$\lambda^3 N^5[-iF\frac{l}{m}]$	b	PRESS.	MIX
$\lambda^2 N^6[-G+i\frac{AE}{K}-i\frac{AE^3}{K}]$	S, + ADV + ADV	(MIX, PRESS) + COR + ADV	(PRESS, MIX) + COR + ADV
$\lambda N^7[iF-FE\frac{l}{m}]$	b, b	COR. + PRESS	PRESS + ADV
$N^8 iGE$	S	(ADV, PRESS)	(PRESS, ADV)

Table 2: Relation between terms in the operator Λ and terms in the heat and momentum equations. MIX. is an eddy viscosity or diffusivity term $\left(A\frac{\partial^3}{\partial z^3}\right)$; ADV is a non-linear advection term, $im^{-}V^{-}\frac{\partial}{\partial z}$; COR is a coriolis acceleration term and PRESS is a pressure term. b and S are the $\frac{\partial\theta}{\partial x}$ and $\frac{\partial\theta}{\partial z}$ advection terms in the heat equation. The abbreviations indicate the correspondence in equations (9) (7) and (8) to terms (and subterms) in (18); two abbreviations in a bracket mean that a given subterm in Λ comes from those two terms in the perturbation equation.

Special Cases

1. Modified Ekman flows: $N \simeq 1$. A and K are assumed to be of the same order of magnitude and E, F, G will be of $O(1)$ at the most and constants, so that (18) is an 8^{th} degree algebraic equation in λ. For the most general case, and for those cases where E, F or G vanish individually, (18) is still 7^{th} and 8^{th} degree; simpler and more tractable expressions in λ result when two of the parameters are simultaneously small. In order of increasing simplicity they are as follows:

a) $E << 1$, $G << 1$; GE and FE will also be small. Λ will still in general be of 7^{th} degree, unless we let $m = 0$, in which case Λ reduces to $\lambda^5 + \lambda - i\frac{Fl}{m} = 0$

and the perturbation equations become

$$-f\frac{\partial v}{\partial z} = -il g\alpha\theta + A\frac{\partial^3 u}{\partial z^3}$$
$$fu = A\frac{\partial^2 v}{\partial z^2}$$
$$wb = K\frac{\partial^2\theta}{\partial z^2}$$

b) For E and $F << 1$ (and consequently FE and GE also) Λ reduces to a cubic in λ^2:

$$\lambda^6 + \lambda^2 - G = 0$$

and the perturbation equations are as for the previous set except that both pressure terms are in general present and that the balance in the heat equation is between ws and $K\frac{\partial^2\theta}{\partial z^2}$.

c) The simplest case is F and $G << 1$ (and also $FE + GE << 1$). The perturbation equations are then decoupled and there is no need to solve the cubic in λ^2 which results from (18). One has

$$iEu - v = \frac{A}{f}\lambda^2 u$$

$$iEv + u = \frac{A}{f}\lambda^2 v$$

$$iE\Theta = \frac{K}{f}\lambda^2\Theta$$

so that $\lambda_\Theta^2 = i\frac{Ef}{K}$ and $\lambda_{u,v}^2 = \frac{if}{A}(E \pm 1)$; this case will be treated in more detail later.

2. When N is large enough so that $N^4 >> 1$, and E, F, G are again of $O(1)$ at most and constant, the degree of Λ drops from 8 to 6 in general and we may rewrite (18) as

$$-iE\left(\frac{2K+A}{K}\right)\lambda^6 + \lambda^4 N^2\left[1 - E^2\frac{(2A+K)}{K}\right] - iF\frac{\ell}{m}N^3\lambda^3 - \left[G - i\frac{A}{K}E(1-E^2)\right]N^4\lambda^2 +$$

$$+ iF\left(1 + i\frac{\ell}{m}E\right)N^5\lambda + iGEN^6 = 0 \qquad (19)$$

Once more we let A and K be comparable and look for simpler forms of (19).

a) If the advective effects are small so that $EN^2 << 1$, (19) degenerates into a cubic in λ :

$$\lambda^3 - i\frac{F\ell}{m}N\lambda^2 - GN^2\lambda + iFN^3 = 0$$

This includes both horizontal and vertical mean gradient effects; if $N \leq 5$ it is applicable to $G > \frac{1}{25}$ or $F > \frac{1}{125}$ or $\frac{F\ell}{m} > \frac{1}{5}$. The very special case $m = 0$, $G << \frac{1}{25}$ gives a pure imaginary λ which cannot be treated when neglecting vertical variation of the mean field parameters.

b) Another simple situation arises when all the F terms are unimportant:

$F N^5 \ll 1$, $EF \frac{l}{m} N^5 \ll 1$ and (19) reduces to a cubic in λ^2 :

$$-iE\left(\frac{2K+A}{K}\right)\lambda^6 + N^2\left\{1-E^2\left(\frac{2A+K}{K}\right)\right\}\lambda^4 - \left[G - i\frac{AE}{K}(1-E^2)\right]N^4\lambda^2 + iGEN^6 = 0$$

Within the range of N the balance in this equation will depend on the values of E and G ; if $E \simeq 1$, the vertical stratification effects can enter for $G > \frac{1}{625}$. The presence of non-linear advective terms can thus make the vertical stratification important on depth scales much smaller than the Lineykin depth, $\left[A/fG\right]^{1/2}$, which is the scale depth when only the $GN^4\lambda^2$ and the $N^2\lambda^4$ terms enter in Λ .

3. Only one of the special cases above has been worked out in detail, case 1c), in which $N \equiv 1$, F and $G \ll 1$. We repeat the basic perturbation equations

$$iEu - v = \frac{A}{f}\lambda^2 u \tag{20}$$

$$iEv + u = \frac{A}{f}\lambda^2 v \tag{21}$$

$$iE\theta = \frac{K}{f}\lambda^2\theta. \tag{22}$$

The equations are decoupled; we can solve for θ immediately, keeping only $\lambda = (1+i)\sqrt{\frac{Ef}{2K}}$ which allows θ to vanish at $z = -\infty$. The surface boundary condition can be a specified temperature $\theta_0 \cos(lx + my)$, in which case

$$\theta = \theta_0 \exp\sqrt{\frac{Ef}{2K}}\, z \cos\left(\sqrt{\frac{Ef}{2K}}\, z + lx + my\right),$$

or a heat flux condition, $\left.\frac{\partial\Theta}{\partial z}\right|_{z=0} = \Phi\cos(\ell x + my)$, which gives

$$\Theta = \frac{\Phi\cos(\ell x+my)\exp\sqrt{\frac{Ef}{2K}}z\cos\left(\ell x+my+\sqrt{\frac{Ef}{2K}}z\right)}{\sqrt{\frac{Ef}{K}}\cos(\ell x+my+\pi/4)}.$$

For the momentum equations, (20) and (21) give

$$\lambda^2 = i\frac{f}{A}(E\pm 1). \tag{23}$$

If we want to keep roots with a positive real part only (to insure vanishing values at great depths) it is clear that we have to choose different roots depending on whether E is greater than or smaller than 1.

a) When $E > 1$, the proper roots are

$$\lambda = \sqrt{\frac{f}{2A}}(1+i)(E\pm 1)^{\frac{1}{2}}$$

With surface stress boundary conditions the velocities are

$$u = \frac{|\tau|}{2\sqrt{Af}}\left\{\frac{\exp\left[\sqrt{\frac{f}{2A}}(E+A)^{\frac{1}{2}}z\right]}{(E+1)^{1/2}}\cos\left[\sqrt{\frac{f}{2A}}(E+1)^{\frac{1}{2}}z+y+\psi-\pi/4\right]+\frac{\exp\left[\sqrt{\frac{f}{2A}}(E-1)^{\frac{1}{2}}z\right]}{(E-1)^{1/2}}\cos\left[\sqrt{\frac{f}{2A}}(E-1)^{\frac{1}{2}}z+\gamma-\psi-\pi/4\right]\right\} \tag{24}$$

$$v = \frac{|\tau|}{2\sqrt{Af}}\left\{\frac{\exp\left[\sqrt{\frac{f}{2A}}(E+1)^{\frac{1}{2}}z\right]}{(E+1)^{1/2}}\sin\left[\sqrt{\frac{f}{2A}}(E+1)^{\frac{1}{2}}z+y+\psi-\pi/4\right]-\frac{\exp\left[\sqrt{\frac{f}{2A}}(E-1)^{\frac{1}{2}}z\right]}{(E-1)^{1/2}}\sin\left[\sqrt{\frac{f}{2A}}(E-1)^{\frac{1}{2}}z+\gamma-\psi-\pi/4\right]\right\} \tag{25}$$

in which $|\tau|$ is the magnitude of the surface stress $(\tau_x^2+\tau_y^2)^{1/2}$, ψ its angle with the x-axis $\left(\tan^{-1}\frac{\tau_y}{\tau_x}\right)$ and γ is the horizontal phase angle, $(\ell x+my)$. The velocity field is seen to consist of

two superimposed Ekman spirals of different scale depths coiling in opposite directions (see fig. 1); if we write u and v as the sum of two components $u_1 + u_2$ and $v_1 + v_2$, we have:

$$(u_1^2 + v_1^2)^{1/2} = \frac{|\tau| \exp\left[\sqrt{\frac{f}{2A}}\,(E+1)^{1/2} z\right]}{2\sqrt{Af}\,(E+1)^{1/2}} \tag{26}$$

$$(u_2^2 + v_2^2)^{1/2} = \frac{|\tau| \exp\left[\sqrt{\frac{f}{2A}}\,(E-1)^{1/2} z\right]}{2\sqrt{Af}\,(E-1)^{1/2}} \tag{27}$$

$$\tan^{-1}\frac{v_1}{u_1} = \sqrt{\frac{f}{2A}}\,(E+1)^{1/2} z + \gamma + \psi - \pi/4 \tag{28}$$

$$\tan^{-1}\frac{v_2}{u_2} = -\left(\sqrt{\frac{f}{2A}}\,(E-1)^{1/2} z + \gamma - \psi - \pi/4\right) \tag{29}$$

The spiral with components u_1, v_1 coils clockwise, the other one counterclockwise: the direction of the flow at any depth will then depend upon E, γ and ψ as well as on the depth z.

At the surface, the velocity vectors of the sub-spirals lie at equal angles $[\pi/4 - \gamma]$ on either side of the direction of the stress vector (ψ); the components of the counterclockwise spiral have greater amplitude, so that the surface total velocity vector traces a clockwise ellipse as γ varies from 0 to π.

Integration of the momentum equations yields expressions relating the momentum transport and the surface stresses:

$$\int_{-\infty}^{0} u\,dz = M_x = \frac{1}{(E^2-1)}\left[\frac{\tau_x}{f} E \sin\gamma - \frac{\tau_y}{f}\cos\gamma\right] \tag{30}$$

$$\int_{-\infty}^{0} v\,dz = M_y = \frac{1}{(E^2-1)}\left[\frac{\tau_x}{f}\cos\gamma + E\frac{\tau_y}{f}\sin\gamma\right] \tag{31}$$

The amplitude is modulated with twice the phase γ :

$$|M| = \frac{|\tau|}{2f(E^2-1)} \left[(E^2+1) - (E^2-1)\cos 2\gamma\right]^{1/2} \qquad (32)$$

and the direction is

$$\tan^{-1}\frac{M_y}{M_x} = \left(\frac{\tau_x^2 + E^2\tau_y^2}{\tau_y^2 + E^2\tau_x^2}\right)^{1/2} \frac{\cos\left(\gamma - \tan^{-1} E\frac{\tau_y}{\tau_x}\right)}{\cos\left(\gamma + \tan^{-1}\frac{\tau_y}{E\tau_x}\right)} . \qquad (33)$$

The hodograph of the transport (fig.2) is then an ellipse with its major axis along the direction of the applied stress; the semi-major axis and the semi-minor axis are

$$|M|_{max} = \frac{|\tau|\,E}{\sqrt{2}f(E^2-1)}$$

and

$$|M|_{min} = \frac{|\tau|}{\sqrt{2}f(E^2-1)}$$

respectively, so that the eccentricity increases with E . As γ varies from 0 to 2π the ellipse is traced counterclockwise if τ_x and τ_y have the same sign, in the opposite direction otherwise.

b) When $E < 1$, the roots which make the velocity components vanish at great depths are

$$\lambda_1 = (1+i)\sqrt{\frac{f}{2A}}\,(E+1)^{1/2}$$

and

$$\lambda_2 = (1-i)\sqrt{\frac{f}{2A}}\,(1-E)^{1/2}.$$

With the same boundary conditions as above,

$$u = \frac{|\tau|}{2\sqrt{Af}}\left\{\frac{\exp\left[\sqrt{\frac{f}{2A}}(E+1)^{\frac{1}{2}}\right]}{(E+1)^{1/2}}\cos\left[\sqrt{\frac{f}{2A}}(E+1)^{\frac{1}{2}}+\gamma+\psi-\pi/4\right]+\frac{\exp\left[\sqrt{\frac{f}{2A}}(1-E)^{\frac{1}{2}}\right]}{(1-E)^{1/2}}\cos\left[-\sqrt{\frac{f}{2A}}(1-E)^{\frac{1}{2}}+\gamma-\psi+\pi/4\right]\right\} \quad (34)$$

$$v = \frac{|\tau|}{2\sqrt{Af}}\left\{\frac{\exp\left[\sqrt{\frac{f}{2A}}(E+1)^{\frac{1}{2}}\right]}{(E+1)^{1/2}}\sin\left[\sqrt{\frac{f}{2A}}(E+1)^{\frac{1}{2}}+\gamma+\psi-\pi/4\right]-\frac{\exp\left[\sqrt{\frac{f}{2A}}(1-E)^{\frac{1}{2}}\right]}{(1-E)^{1/2}}\sin\left[-\sqrt{\frac{f}{2A}}(1-E)^{\frac{1}{2}}+\gamma-\psi+\pi/4\right]\right\}. \quad (35)$$

We recognize again a superposition of two spiralling flows (fig.1), but in this case they coil in the same direction (counterclockwise). The resultants of the two spirals are separated by an angle 2γ at the surface, the direction of the applied stress lying half way between them; the total surface vector again describes a clockwise ellipse as γ varies.

The transport formulae (30) to (33) still apply; the ellipse in the hodograph plane (fig. 2) is now oriented with its major axis 90^{o} to the right of the stress; the ratio of the axes is now $\frac{1}{E}$. As E tends to zero, the flow looks more and more like the pure Ekman regime. The direction of rotation of the transport vector depends on the sign of τ_x/τ_y in the same manner as in the previous case.

The case $E = 1$ has not been examined in detail yet. We have however enough information about the cases $E > 1$ and $E < 1$ to conclude that whenever E is large enough to matter the direction of the integrated transport can be very different from that of the pure Ekman transport.

We plan to study in similar detail one other simple case extracted from (18) and then, with knowledge of the effects of individual

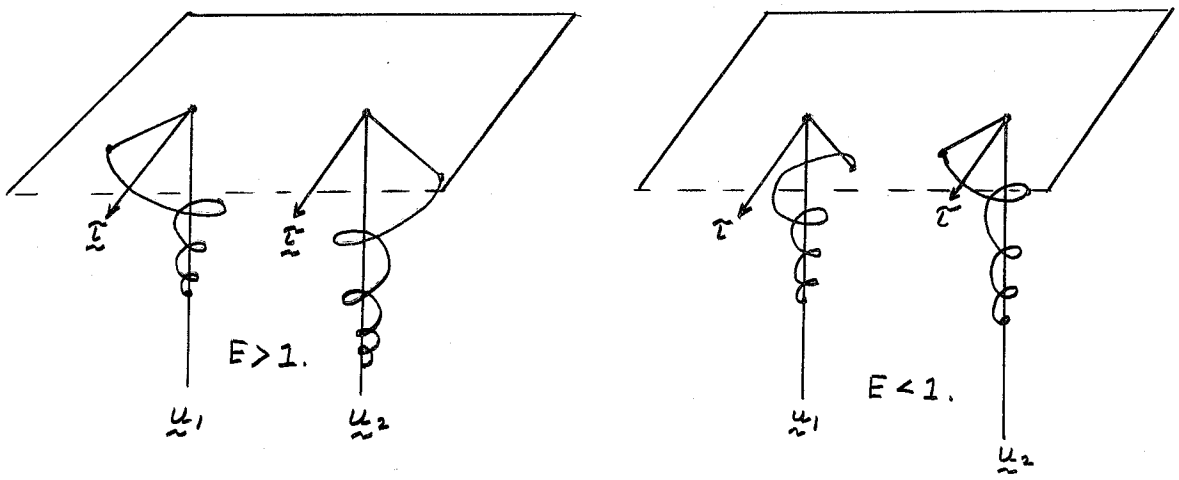

Fig. 1. Sub-spirals of the velocity in cases $E>1$ and $E<1$; in both cases, the pitch of the spirals of $\underset{\sim}{u}_1$ and $\underset{\sim}{u}_2$ differ, and for $E>1$, their direction of coiling is opposite.

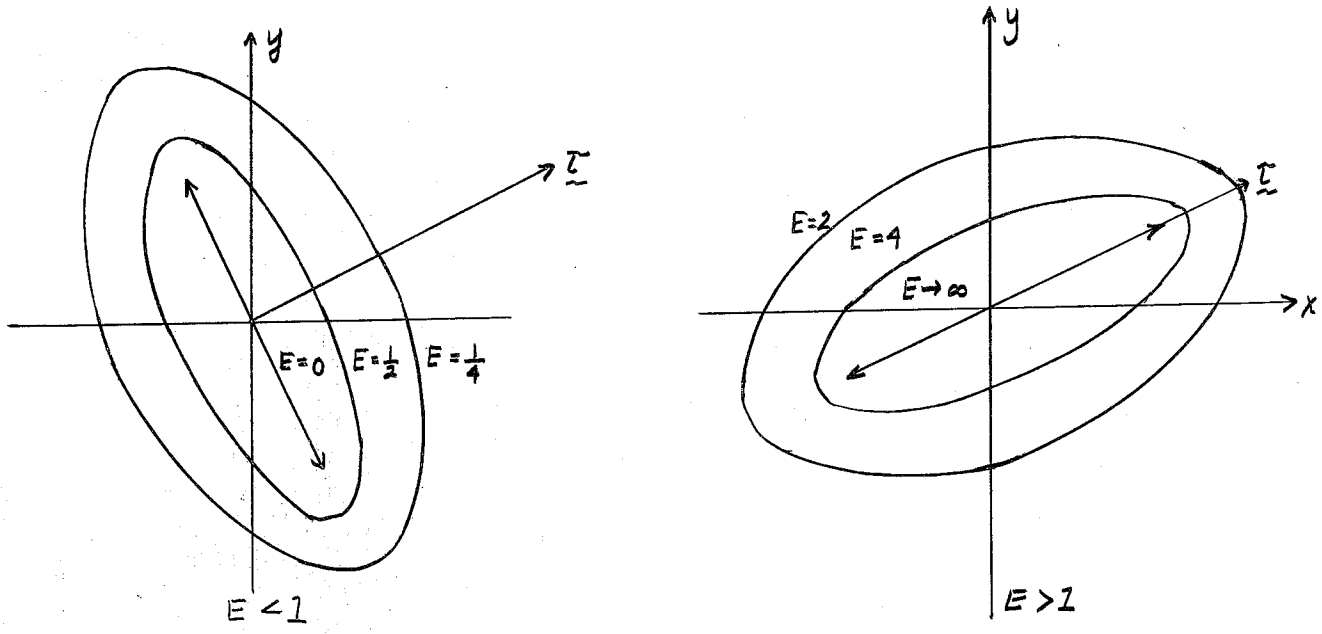

Fig. 2. Hodographs of the momentum transports for the cases $E>1$ and $E<1$; the direction and amplitude vary with $(\ell x+my)=\gamma$.

parameters E, F or G, attempt to apply this analysis to a situation arising in the North Equatorial current in the Atlantic. Prof. Stommel has pointed out that in a wide region the isopycnals at 200 m lie along the direction of the mean current, which is geostrophic, whereas at the surface they are tilted with respect to the direction of the current by an angle of about 60^{o}. (METEOR Atlas).

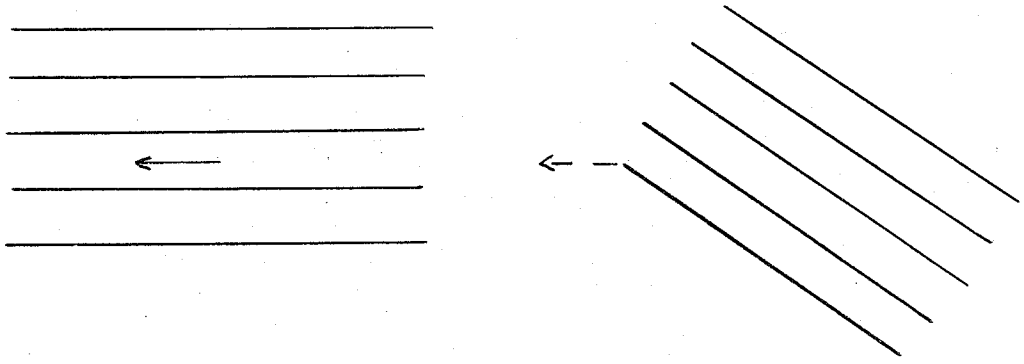

Fig. 3. Isopycnals at 200 m and at the surface in the North Equatorial Atlantic current.

References

H. Stommel and G. Veronis, 1957. Steady convective motion in a horizontal layer of fluid heated uniformly from above and cooled non-uniformly from below. Tellus, 1957.

METEOR Atlas: vol. V, table 50, or 5.
vol. V, table 77 or 47.